REPORT NO.
UCB/EERC-78/24
NOVEMBER 1978

EARTHQUAKE ENGINEERING RESEARCH CENTER

INVESTIGATION OF THE ELASTIC CHARACTERISTICS OF A THREE STORY STEEL FRAME USING SYSTEM IDENTIFICATION

by
IZAK KAYA
and
HUGH D. McNIVEN

Report to the National Science Foundation

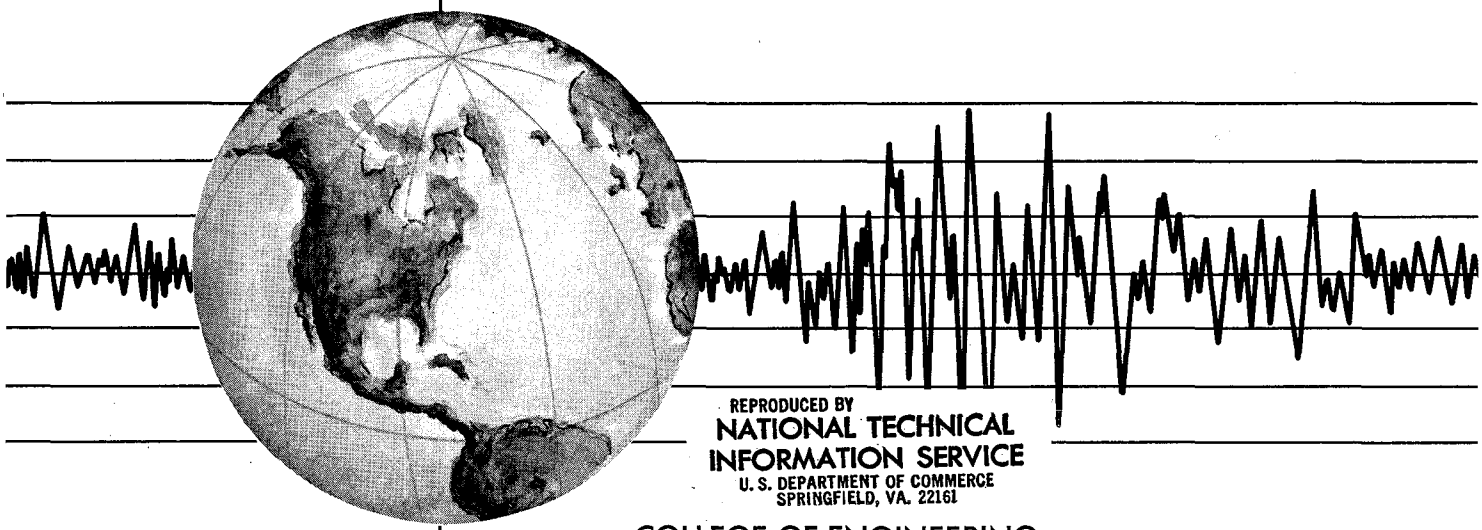

COLLEGE OF ENGINEERING

UNIVERSITY OF CALIFORNIA · Berkeley, California

BIBLIOGRAPHIC DATA SHEET	1. Report No. NSF/RA-780577	2.	3. Recipient's Accession No. PB296225

4. Title and Subtitle Investigation of the Elastic Characteristics of a Three Story Steel Frame Using System Identification	5. Report Date November 1978 6.
7. Author(s) Izak Kaya and Hugh D. McNiven	8. Performing Organization Rept. No. UCB/EERC-78/24
9. Performing Organization Name and Address Earthquake Engineering Research Center University of California, Richmond Field Station 47th and Hoffman Blvd. Richmond, California 94804	10. Project/Task/Work Unit No. 11. Contract/Grant No. ENV76-04262-A02
12. Sponsoring Organization Name and Address National Science Foundation 1800 G. Street, N.W. Washington, D. C. 20550	13. Type of Report & Period Covered 14.

15. Supplementary Notes

16. Abstracts

In this report, three different models in increasing order of complexity have been used to identify the seismic behavior of a three story steel frame subjected to arbitrary forcing functions all of which excite responses within the elastic range.

In the first model, five parameters have been used to identify the frame. Treating the system as a shear building, one stiffness coefficient is assigned to each floor and Rayleigh type damping is introduced with two additional parameters. The mass, assumed to be concentrated at a floor level, is kept constant throughout the study. The parameters are established using a modified Gauss-Newton algorithm. The match between measured and predicted quantities is satisfactory when these quantities are restricted to floor acceleration or displacement.

To remove the constraint imposed by assuming the frame deforms as a shear building, a second model with eight parameters is introduced, allowing rotations of the joints as independent degrees of freedom. Six of the eight parameters are related to the stiffness characteristics of the structural members while the remaining two are related to damping as before.

An integral squared error function is used to evaluate the discrepancy between the model's response and the structure's response when both are subjected to the same excitation. Different quantities such as displacements, accelerations, rotations, etc., are used in different combinations in forming the error function, in an effort to determine the best set of measurements that need to be made to identify the structure properly. The final eight parameter model is the last of three. The discoveries that were made between the first and third models are significant.

The match between measured and predicted quantities for the final model is excellent. The set of parameters derived from the minimum squared error gives a model that shows very good correlation using information on the full duration of the pulse or only a portion of it. Also the same correlation exists between the coefficients obtained from different excitations.

17c. COSATI Field/Group

18. Availability Statement Release Unlimited	19. Security Class (This Report) UNCLASSIFIED	21. No. of Pages 116
	20. Security Class (This Page) UNCLASSIFIED	22. Price A06-A01

BIBLIOGRAPHIC DATA SHEET	1. Report No.	2.	3. Recipient's Accession No.
4. Title and Subtitle			5. Report Date
			6.
7. Author(s)			8. Performing Organization Rept. No.
9. Performing Organization Name and Address			10. Project/Task/Work Unit No.
			11. Contract/Grant No.
12. Sponsoring Organization Name and Address			13. Type of Report & Period Covered
			14.
15. Supplementary Notes			

16. Abstracts

In an effort to explain the values of the parameters associated with the girders, an additional degree of freedom, namely the pitching motion of the shaking table is considered as an additional degree of freedom. The stiffness of the symmetrical springs at the base of the table is introduced as a ninth parameter in the model.

The match between measured and predicted response is improved, if slightly, over the eight parameter model. The value of the nine parameter model is not primarily due to this improvement, but because from it we gain physical insight into the values that the parameters converge to during optimization.

Comparison of the quality of predictions from the eight and nine parameter models convinces us that higher order models would further improve the quality of the model little if any.

It is gratifying to have mathematical models that predict the response of a structure accurately to a variety of excitations, but we feel that such an achievement is not enough in itself. We feel that it is important to gain from the model insight into its physical behavior. The models that we have established in this study, particularly the nine parameter model, have been unusually useful to this end. The insight we have gained is described in the report.

17c. COSATI Field/Group

18. Availability Statement	19. Security Class (This Report)	21. No. of Pages
Release Unlimited	UNCLASSIFIED	116
	20. Security Class (This Page) UNCLASSIFIED	22. Price

INVESTIGATION OF THE ELASTIC CHARACTERISTICS OF A THREE STORY STEEL FRAME USING SYSTEM IDENTIFICATION

by

IZAK KAYA

and

HUGH D. McNIVEN

Report to the

National Science Foundation

Report No. UCB/EERC-78/24

Earthquake Engineering Research Center
College of Engineering
University of California
Berkeley, California
November 1978

ACKNOWLEDGEMENT

The research described in this report was supported by the National Science Foundation under Grant No. ENV76-04262-A02. This support is gratefully acknowledged.

ABSTRACT

In this report, three different models in increasing order of complexity have been used to identify the seismic behavior of a three story steel frame subjected to arbitrary forcing functions all of which excite responses within the elastic range.

In the first model, five parameters have been used to identify the frame. Treating the system as a shear building, one stiffness coefficient is assigned to each floor and Rayleigh type damping is introduced with two additional parameters. The mass, assumed to be concentrated at a floor level, is kept constant throughout the study. The parameters are established using a modified Gauss-Newton algorithm. The match between measured and predicted quantities is satisfactory when these quantities are restricted to floor acceleration or displacement.

To remove the constraint imposed by assuming the frame deforms as a shear building, a second model with eight parameters is introduced, allowing rotations of the joints as independent degrees of freedom. Six of the eight parameters are related to the stiffness characteristics of the structural members while the remaining two are related to damping as before.

An integral squared error function is used to evaluate the discrepancy between the model's response and the structure's response when both are subjected to the same excitation. Different quantities such as displacements, accelerations, rotations, etc., are used in different combinations in forming the error function, in an effort to determine the best set of measurements that need to be made to identify the structure properly. The final eight parameter model is the last of three. The discoveries that were made between the first and third models are significant.

The match between measured and predicted quantities for the final

model is excellent. The set of parameters derived from the minimum squared error gives a model that shows very good correlation using information on the full duration of the pulse or only a portion of it. Also the same correlation exists between the coefficients obtained from different excitations.

In an effort to explain the values of the parameters associated with the girders, an additional degree of freedom, namely the pitching motion of the shaking table is considered as an additional degree of freedom. The stiffness of the symmetrical springs at the base of the table is introduced as a ninth parameter in the model.

The match between measured and predicted response is improved, if slightly, over the eight parameter model. The value of the nine parameter model is not primarily due to this improvement, but because from it we gain physical insight into the values that the parameters converge to during optimization.

Comparison of the quality of predictions from the eight and nine parameter models convinces us that higher order models would further improve the quality of the model little if any.

It is gratifying to have mathematical models that predict the response of a structure accurately to a variety of excitations, but we feel that such an achievement is not enough in itself. We feel that it is important to gain from the model insight into its physical behavior. The models that we have established in this study, particularly the nine parameter model, have been unusually useful to this end. The insight we have gained is described in the report.

ACKNOWLEDGMENTS

The research reported here was sponsored by the National Science Foundation under Grant No. ENV76-04262. The computing and plotting facilities were provided by the University of California Computer Center at Berkeley.

Al Klash and his associates are responsible for the drafting and Judith Sanders typed the manuscript.

TABLE OF CONTENTS

LIST OF TABLES

LIST OF TABLES (cont.)

LIST OF FIGURES

LIST OF FIGURES (cont.)

NOTE

In all of the Figures in which comparison is made between measured and computed responses, the solid line represents the measured response, the dotted line the computed.

CHAPTER I INTRODUCTION

We are sure that there are many who, having read the title of this report, will conclude that the study is surely a waste of effort and certainly not worthy of the application of system identification. They probably feel that when the complete geometry of the three story frame is specified along with the sizes of all of the members, the model for the linear behavior of the frame is well known and the predictions of seismic responses using the model will be accurate. We show in this report that this is not so.

In earlier studies using system identification for constructing mathematical models to predict seismic response, such as McNiven and Matzen [1], we have argued that the major value of system identification is derived from the fact that using it enables one to appraise the form of the model. This is not its value here. In this study we have accepted the usual form for a set of simultaneous, linear differential equations. System identification has been invaluable, however, in arriving at sets of parameters which, when introduced into the set of equations, give models that predict accurately the seismic response of the frame.

There is no such thing as a single mathematical model for a physical frame. There are large numbers of models of different orders of complexity. The job of the person constructing the models is to ensure that each model of a particular order is the best possible of all models of that order.

The order of a model, reflected in the number of parameters involved, derives from the number of degrees of freedom which the model accommodates. We construct, in this report, three separate models: a five parameter for a frame with three degrees of freedom, an eight for a frame with six degrees of freedom and finally a nine in which an additional degree of freedom is introduced to account for probable pitching of the shaking table during excitation.

In choosing which of these models is appropriate for a particular analysis, one must be aware that there is always a trade off. The higher the order of a model, the more accurate it is, but the more costly to use.

When one sets about to construct a mathematical model to represent a physical entity, he or she has ideally three purposes. The first is to construct a model that will predict as accurately as possible the actual behavior of the physical entity, in this case the frame. The second is to learn from the model something of the physics or engineering of the prototype and finally, to extend the knowledge of the mathematical technique one uses, in this case system identification. This study has been particularly satisfying in that all three objectives have been realized.

The eight and nine parameter models predict response quantities that match all of the experimental responses with exceptional accuracy. We learn in constructing the models what it is about the engineering of the frame that must be understood in formulating the models. Finally, we have learned that some response quantities are not independent of others. We have learned what constitutes complete data for a model of a particular order, and that each response quantity in that data must impose a constraint on the structure independent of all of the others. We have also learned a great deal about incomplete data which we leave for a later report.

System identification needs experimental response data. We are fortunate in having an excellent set of data from experiments performed in 1975 on the shaking table at the Earthquake Engineering Research Center of the University of California, Berkeley, and reported by Clough and Tang [2]. The frame, the experiments performed on it, and the test results are described in detail in the report. The report supplies data for both linear and nonlinear responses. A nonlinear model constructed using the nonlinear response data will be reported in a subsequent report.

This study is the third that we know of which uses the data from the Clough and Tang experiments to construct mathematical models. The first was conducted by Tang himself [3] in 1975. Tang used the same model form as we do. He formulated his best model using physical intuition and trial and error and arrived at a very credible model. Distefano and Peña-Pardo [4] used system identification but introduced a new form for the equations. Their model is fairly successful.

From our point of view, one of the interesting aspects of this study is that we learned as much from our "mistakes" as from our successes. For this reason we have chosen to present the work in chronological order as we proceeded step by step. In the discussion of the eight parameter model we describe the development of an ineffective model, how and why we backtracked to a different model, and how this in turn needed to be modified. It was from the physical interpretation of this final eight parameter model that we decided on a nine parameter model.

In Chapter II, the general formulation using system identification is described and a summary of the modified Gauss-Newton optimization algorithm is presented. Chapter III deals with the features of the computer program and the results of working with simulated data to test the validity

of the program. The flexibility of the program enables one to introduce additional parameters or change the way in which they are used without having to change its framework. Chapters IV, V and VI are devoted to the construction, in successively increasing order, of the three models. In Chapter VII we present a set of conclusions.

CHAPTER II DESCRIPTION OF SYSTEM IDENTIFICATION AS USED IN THIS STUDY

In this chapter, the equations which form the basis of the identification process as applied to this work will be developed. Although much of the treatment is classical, for the sake of completeness, a moderately detailed treatment will be given.

II.1 Form of the Model

For an n story structure subjected to rigid base motion the following set of linear second order differential equations with constant coefficients is used:

$$[M]\{\ddot{u}\} + [C]\{\dot{u}\} + [K]\{u\} = -[M]\{I\}\ddot{u}_g \qquad (1)$$

$$\{\dot{u}\}_o = \{u\}_o = \{0\}$$

where [M] is the mass matrix and [C] and [K] are the damping and stiffness matrices for the structure. {I} is a unit vector; $\ddot{u}_g$ is the base acceleration and {u}, {u} and {ü} are vectors for relative nodal displacement, velocity and acceleration, respectively.

The mass of the structure is assumed to be lumped at the nodal points and therefore [M] will be a diagonal matrix and taken as constant throughout this work. The total stiffness matrix which is obtained from the individual element stiffnesses is condensed to an n x n translational stiffness matrix [K] to be used in Eq. (1). The damping matrix [C] is assumed to be linearly dependent on both the mass and stiffness matrices

and is taken of the form

$$[C] = a_0[M] + a_1[K] \tag{2}$$

The coefficients a_0 and a_1 can be related to the damping ratios provided the frequencies of the system are known:

$$\lambda_n = \frac{1}{2}\left(\frac{a_0}{\omega_n} + a_1 \omega_n\right) \tag{3}$$

where ω_n are the frequencies and λ_n the corresponding damping ratios.

Eq. (1) can be expressed in incremental form as

$$[M]\{\Delta\ddot{u}\} + [C]\{\Delta\dot{u}\} + [K]\{\Delta u\} = -[M]\{I\}\Delta\ddot{u}_g \tag{4}$$

where the changes $\{\Delta\ddot{u}\}$, $\{\Delta\dot{u}\}$ and $\{\Delta u\}$ occur between times t and $t+\Delta t$.

If the acceleration for each degree of freedom is assumed to vary linearly within the time increment Δt, a direct integration over the increment indicates that the change in acceleration is

$$\{\Delta\ddot{u}\} = \frac{6}{(\Delta t)^2}\{\Delta u\} + \{A\} \tag{5}$$

where

$$\{A\} = -\frac{6}{\Delta t}\{\dot{u}\}_t - 3\{\ddot{u}\}_t$$

and the change in velocity is

$$\{\Delta\dot{u}\} = \frac{3}{\Delta t}\{\Delta u\} + \{B\} \tag{6}$$

where

$$\{B\} = -3\{\dot{u}\}_t - \frac{\Delta t}{2}\{\ddot{u}\}_t$$

In addition, as the damping matrix is assumed to be the form in Eq. (2), Eq. (1) can be put in the form

$$[\bar{K}]\{\Delta u\} = \{\Delta\bar{R}\} \tag{7}$$

where

$$[\bar{K}] = \left[[K] + \left(\frac{6}{\Delta t^2} + \frac{3a_o}{\Delta t}\right) [M] + \frac{3}{\Delta t} a_1 [K] \right]$$

and

$$[\Delta\bar{R}] = \left[- [M]\{I\} \Delta\ddot{u}_g - [M] [\{A\} + a_o\{B\}] - a_1 [K]\{B\} \right]$$

Eq. (7) can be solved for the incremental displacements $\{\Delta u\}$, from which the total displacements, velocities and accelerations can be calculated from the following equations:

$$\begin{aligned} \{u\}_{t+\Delta t} &= \{u\}_t + \{\Delta u\} \\ \{\dot{u}\}_{t+\Delta t} &= \{\dot{u}\}_t + \{\Delta \dot{u}\} \\ \{\ddot{u}\}_{t+\Delta t} &= \{\ddot{u}\}_t + \{\Delta \ddot{u}\} \end{aligned} \tag{8}$$

In Eqs. (8), $\{\Delta\dot{u}\}$ and $\{\Delta\ddot{u}\}$ are obtained from Eqs. (5) and (6).

Thus, given the time history of the base motion $\ddot{u}_g(t)$ and defining the proper [M], [C] and [K] matrices, Eq. (1) yields the displacement, velocity and acceleration time history at each floor level.

II.2 The Error Function

An error or criterion function is introduced to indicate how well the assumed model, with its defined characteristics, predicts the response of the structure. The criterion function used here is an integral squared error function that includes errors in some set of quantities measured at a number of floors, which will be defined in more detail in the following chapters. At this stage we shall call those measured quantities (which could be displacements, accelerations, rotations or any other related quantities) $\{y_j(t)\}_m$ and their predicted counterparts by $\{x_j(t)\}_m$ such that

$$m = 1, 2, \ldots, \ell \quad \text{and} \quad 1 < j < n$$

where ℓ will denote the maximum number of quantities used at any one floor in constructing the error function and j identifies the floor number, n being the total number of floors.

Since the predicted quantities depend on a set of parameters which will be denoted by $\{\beta\}$ or $\bar{\beta}$ and defined later, the error function can now be expressed as

$$J(\bar{\beta}, T) = \sum_{j=1}^{n} \sum_{m=1}^{\ell} \int_{o}^{T} \{k_j \times [x_j(\bar{\beta}, t) - y_j(t)]_m^2\} dt \qquad (9)$$

where T is the full duration of the excitation or any portion of it, the lower limit of the integral being always zero and corresponding to zero initial conditions. $\{k_j\}$ is a vector containing terms which are either 1 or 0, depending on whether measurements at all floor levels or at only some floors are being used.

The model response to a specified ground acceleration is found by giving values to the parameters and integrating the mathematical model step-by-step through time using a linear distribution of acceleration as described already. The integration of the model yields, for each set of parameters $\bar{\beta}$, acceleration velocity and displacement at all floor levels as functions of time, from which local response quantities such as moments, rotations can be obtained directly. Those measured quantities when introduced into the error function, compared to their measured counterparts and integrated over the period of time T, completely define $J(\bar{\beta}, T)$.

II.3 Estimation of Parameters

The next step is the selection of an algorithm to adjust the parameters in the mathematical model systematically until the error function is minimized. If the number of parameters used is q, it is convenient to think of the error function as describing a q dimensional surface imbedded

in a $q+1$ dimensional space. The problem then consists in finding the coordinates of the global minimum point on the surface.

Defining by $\bar{\beta}_i$ the vector of parameters, $\bar{\beta}_{i+1}$ will denote an improved set of parameters which gives a smaller value for J. The fundamental equation will be taken as

$$\bar{\beta}_{i+1} = \bar{\beta}_i + \alpha \bar{d}_i \tag{10}$$

where $\bar{d}_i$ is a direction vector and α a step size. After a study of several optimization methods, a modified Gauss-Newton method was chosen for this problem.

The Gauss-Newton method is derived by expanding the error function in a Taylor series about the previous point $\bar{\beta}_i$ and retaining only the first three terms:

$$J(\bar{\beta}_{i+1}, T) = J(\bar{\beta}_i, T) + \bar{\nabla}J^T(\bar{\beta}_i, T).(\bar{\beta}_{i+1} - \bar{\beta}_i)_+ \tag{11}$$

$$+ \frac{1}{2}(\bar{\beta}_{i+1} - \bar{\beta}_i)^T \bar{\bar{\nabla}}^2 J(\bar{\beta}_i, T)\,(\bar{\beta}_{i+1} - \bar{\beta}_i)$$

where $\bar{\nabla}J(\bar{\beta}_i, T)$ is the column gradient vector and $\bar{\bar{\nabla}}^2 J(\bar{\beta}_i, T)$ is the Hessian matrix. To minimize $J(\bar{\beta}_{i+1}, T)$, its gradient with respect to $\bar{\beta}_{i+1}$ is set equal to the zero vector

$$\bar{\nabla}J(\bar{\beta}_i, T) + \bar{\bar{\nabla}}^2 J(\bar{\beta}_i, T)\,(\bar{\beta}_{i+1} - \bar{\beta}_i) = 0 \tag{12}$$

or, if the Hessian can be inverted,

$$\bar{\beta}_{i+1} = \bar{\beta}_i - [\bar{\bar{\nabla}}^2 J(\bar{\beta}_i, T)]^{-1}\, \bar{\nabla}J(\bar{\beta}_i, T) \tag{13}$$

If the error surface is not quadratic, Eq. (13) may lead to an increased value of the error function by going beyond the valley and up the other side. To insure that the error is decreased in each iteration

a positive scalar, α, is inserted so that the step size can be adjusted separately. The resulting equation is

$$\bar{\beta}_{i+1} = \bar{\beta}_i - \alpha [\bar{\bar{\nabla}}^2 J(\bar{\beta}_i, T)]^{-1} \bar{\nabla} J(\bar{\beta}_i, T) \tag{14}$$

The components of the gradient vector and Hessian matrix are found by taking the appropriate derivatives of the error function. The $p^{\underline{th}}$ component of the gradient is

$$\frac{\partial}{\partial \beta_p} J(\bar{\beta}, T) = 2 \sum_{j=1}^{n} \sum_{m=1}^{\ell} \int_0^T k_j \{[x_j(\bar{\beta},t) - y_j(t)]_m \left(\frac{\partial x_j(\bar{\beta},t)}{\partial \beta_p}\right)_m\} dt \tag{15}$$

The $ps^{\underline{th}}$ component of the Hessian is

$$\frac{\partial^2}{\partial \beta_p \partial \beta_s} J(\bar{\beta}, T) = 2 \sum_{j=1}^{n} \sum_{m=1}^{\ell} \left[\int_0^T k_j \left(\frac{\partial x_j(\bar{\beta},t)}{\partial \beta_p}\right)_m \left(\frac{\partial x_j(\bar{\beta},t)}{\partial \beta_s}\right)_m dt + \right. \tag{16}$$

$$\left. + \int_0^T k_j [x_j(\bar{\beta}, t) - y_j(t)]_m \left(\frac{\partial^2 x_j(\bar{\beta},t)}{\partial \beta_p \partial \beta_s}\right)_m dt \right]$$

In the modified Gauss-Newton method, the second integral in the right hand side of Eq. (16) is neglected. Assuming, as the iterative process proceeds, that the errors go to zero and the second partial derivatives do not increase faster than the errors are decreasing, the approximation for the Hessian matrix would be justified. Experience has shown that the approximation is almost always justified, and the complicated work finding the elements involving second derivatives in the second term of the Hessian is avoided. The Gauss-Newton method, now called modified, is defined as

$$\bar{\beta}_{i+1} = \bar{\beta}_i - \alpha [\bar{\bar{AH}}(\bar{\beta}_i, T)]^{-1} \bar{\nabla} J(\bar{\beta}_i, T) \tag{17}$$

where

$$\bar{\bar{AH}}_{ps}(\bar{\beta}, T) = \frac{\partial^2}{\partial\beta_p \partial\beta_s} \bar{\bar{AH}}(\bar{\beta}, T) =$$

$$= 2 \sum_{j=1}^{n} \sum_{m=1}^{\ell} \left[\int_0^T k_j \left(\frac{\partial x_j(\bar{\beta},t)}{\partial\beta_p}\right)_m \left(\frac{\partial x_j(\bar{\beta},t)}{\partial\beta_s}\right)_m dt \right]$$

Comparing Eqs. (17) and (10) it is seen that the direction vector $\bar{d}_i$ is defined as

$$\bar{d}_i \doteq -[\bar{\bar{AH}}(\bar{\beta}_i, T)]^{-1} \bar{\nabla J}(\bar{\beta}_i, T) \tag{18}$$

To obtain the approximate Hessian as well as the gradient vector, it is necessary to evaluate the first partial derivatives of the response quantities with respect to each parameter. These quantities, called sensitivity coefficients, can be obtained in two different ways. The first solution is obtained by partially differentiating Eq. (1) with respect to each parameter. The resulting equation has the form:

$$[M]\{\frac{\partial \ddot{u}}{\partial\beta_s}\} + [C]\{\frac{\partial \dot{u}}{\partial\beta_s}\} + [K]\{\frac{\partial u}{\partial\beta_s}\} = -[\frac{\partial M}{\partial\beta_s}]\{\ddot{u}\} - [\frac{\partial C}{\partial\beta_s}]\{\dot{u}\} - [\frac{\partial K}{\partial\beta_s}]\{u\} \tag{19}$$

Assuming the [M] matrix to be constant and independent of $\bar{\beta}$, the first term on the right hand side drops out and the resulting equation is

$$[M]\{\frac{\partial \ddot{u}}{\partial\beta_s}\} + [C]\{\frac{\partial \dot{u}}{\partial\beta_s}\} + [K]\{\frac{\partial u}{\partial\beta_s}\} = -[\frac{\partial C}{\partial\beta_s}]\{\dot{u}\} - [\frac{\partial K}{\partial\beta_s}]\{u\} \tag{20}$$

The time histories of the sensitivity coefficients for the displacements, velocities and accelerations are obtained from the solution of Eq. (20). This equation has the same form as Eq. (1) and we note that the forcing function on the right hand side of Eq. (20) is well known after the solution to Eq. (1) has been obtained.

The second solution uses finite differences for the evaluation of the sensitivity coefficients. This second approach seems to be much more versatile than the first and yields very consistent solutions when compared to the first which, however, is the more rigorous.

The procedure is to solve Eq. (1) twice, first with the given set of parameters $\bar{\beta}$ and then with all $\bar{\beta}$ parameters kept constant except for β_p which is increased by $\Delta\beta_p$. Thus, the time history of the sensitivity coefficient for an arbitrary parameter β_p will be evaluated by writing

$$\frac{\Delta x_j(\bar{\beta},t)}{\Delta\beta_p} = \frac{x_j(\bar{\beta},t)\Big|_{\beta_p+\Delta\beta_p} - x_j(\bar{\beta},t)\Big|_{\beta_p}}{\Delta\beta_p} \tag{21}$$

Both methods have been used in different parts of the present work and the agreement is very good.

Having obtained the terms in the gradient vector and the approximate Hessian from the solution of Eq. (20) or Eq. (21), the direction vector is obtained from Eq. (18).

To obtain an improved version of the $\bar{\beta}$ parameters in Eq. (17) a satisfactory step size α must be determined.

The step size α is established by systematically searching the error surface in the direction given by the direction vector until a point is found on this profile where the slope is sufficiently small.

To evaluate the slope of the error surface along the profile, the error function is written in terms of α, as

$$J(\bar{\beta}_{i+1}, T) = J[\bar{\beta}_i - \alpha[\bar{\bar{A}}\bar{\bar{H}}(\beta_i, T)]^{-1}\bar{\nabla}\bar{J}(\beta_i, T)] \tag{22}$$

and then differentiated with respect to α

$$\frac{\partial}{\partial\alpha} J(\bar{\beta}_{i+1}, T) = -\bar{\nabla}\bar{J}^T(\bar{\beta}_{i+1}, T)[\bar{\bar{A}}\bar{\bar{H}}(\bar{\beta}_i, T)]^{-1}\bar{\nabla}\bar{J}(\bar{\beta}_i, T) \tag{23}$$

We are now looking for the value of α which sets the right hand side of Eq. (23) to zero, or, more practically, to a sufficiently small value.

The search begins by using values of the error function and its slope that are already known at the current point $\alpha = 0$. The first point selected in the line search is $\alpha = 1$. The error and slope are evaluated at this point and the slope is compared with a specified line stopping tolerance. If the slope is too large and is positive a second and improved point is found on the profile using cubic interpolation. A cubic polynomial is constructed so as to match the error and slope of the profile at both $\alpha = 0$ and $\alpha = 1$. The stationary point of the constructed curve locates a new value for α between $\alpha = 0$ and $\alpha = 1$. The stationary point of the constructed curve will not be the stationary point of the profile. The error and slope are evaluated at this second point and the slope is again compared with the specified tolerance. If this slope is also too large, another point is located on the profile using two of the previous points located on opposite sides of the minimum and repeating the curve fitting procedure between those two points.

If the slope at $\alpha = 1$ is too large and negative, then quadratic extrapolation using the slopes at $\alpha = 0$ and $\alpha = 1$ locates a new point beyond $\alpha = 1$.

The procedure continues using cubic interpolation or quadratic extrapolation until a value for α is found at which the slope of the error profile is less than the specified tolerance. The resulting value of α is used in Eq. (17) to establish the parameters for the next cycle of the iterative process.

After completing one full cycle to locate α_{min} on the error profile

(this will be referred to as a line search), the iterative process to establish $\overline{\beta}$ continues for a number of cycles of directions and line searches until a point is found on the error surface at which the slope is less than a specified tolerance. This tolerance which will be called the program stopping tolerance can be chosen to be as small as possible so that the $\overline{\beta}$ coefficients are accurately located.

This completes the mathematical treatment of the identification process to be used in this work. To summarize, it can be stated that we are looking for the solution of Eq. (1) using the Newmark method with a given set of parameters $\overline{\beta}$ such that the error function defined in Eq. (9) is minimized. The minimizing set of parameters $\overline{\beta}^*$ are obtained from an initial crude guess $\overline{\beta}_1$ which is improved through successive applications of Eq. (10), in which the direction vector $\overline{d}_i$ is defined in Eq. (18). The final step for an iteration is to find the minimum point on the profile of the surface along this direction vector. Its location establishes the step size α. The technique for finding α is to fit a simple curve to the profile and find the minimum point of the curve.

The next step is the development of computer programs to solve the equations and to accommodate the iterative schemes developed in this chapter.

CHAPTER III DEVELOPMENT OF A COMPUTER PROGRAM AND USE OF SIMULATED DATA

III.1 The Computer Program

To set up the iterative scheme presented in Chapter II, a computer program is developed the details of which are given below and a flow chart presented.

The program consists of the main program OPTIM and eleven subroutines. Control always returns to OPTIM in which the numerous checks are performed and decisions made as to whether to continue or stop the process.

Subroutine ONE reads in all of the input data, which consists of the ground acceleration time history $\ddot{u}_g(t)$, the nodal masses, the measured quantities which enter into the error function and which have been denoted by $\{y_j(t)\}_m$, the initial set of parameters $\overline{\beta}_1$, the duration of the excitation or a portion of it denoted by T, the maximum number of iterations in a given line search, k_{max}, the maximum number of cycles allowed in the program, i_{max}, the $\{k_j\}$ vector identifying the measurements of those floors which are to constitute the error function, the line search tolerance (LST) and the program stopping tolerance (PST).

Subroutine TWO sets up the n x n translational stiffness matrix [K] (see Appendix A) and forms the damping matrix [C].

Subroutine THREE consists of the solution of Eq. (1), for a given set of parameters by linear acceleration, summarized in Chapter II, and yields the $\{x_j(t)\}_m$ predicted quantities corresponding to the $\{y_j(t)\}_m$

measured quantities.

FOUR evaluates the error function $J(\bar{\beta}_i, T)$ while subroutines FIVE and SIX evaluate the terms in the gradient vector $\bar{\nabla J}(\bar{\beta}_i, T)$ and the approximate Hessian matrix $\bar{\bar{AH}}(\bar{\beta}_i, T)$, respectively. The terms in $\bar{\nabla J}(\bar{\beta}_i, T)$ and $\bar{\bar{AH}}(\bar{\beta}_i, T)$ are evaluated either by differentiating Eq. (1) and solving it using subroutine THREE or by finite differences again using the same routine.

Subroutine SEVEN evaluates the inverse of the approximate Hessian $[\bar{\bar{AH}}(\bar{\beta}_i, T)]^{-1}$, while EIGHT evaluates the direction vector

$$\bar{d}_i = -[\bar{\bar{AH}}(\bar{\beta}_i, T)]^{-1} \bar{\nabla J}(\bar{\beta}_i, T)$$

and the initial slope

$$J'(\alpha, T)\Big|_{\alpha=0} = \bar{\nabla J}^T(\beta_i, T)\, \bar{d}_i$$

At this stage OPTIM checks the value of $J'(\alpha, T)\Big|_{\alpha=0}$ against the program stopping tolerance. If the slope is too large, routine NINE is called in to perform the line search. With $k = 1$ and $\alpha_k = 1$ it evaluates

$$\bar{\beta}_{i+1} = \bar{\beta}_i + \alpha_k \bar{d}_i$$

and calls subroutines TWO through FIVE to evaluate $J(\bar{\beta}_{i+1}, T)$ and $\bar{\nabla J}(\bar{\beta}_{i+1}, T)$ and computes

$$J'(\alpha, T)\Big|_{\alpha=\alpha_k} = \bar{\nabla J}^T(\bar{\beta}_{i+1}, T)\, \bar{d}_i$$

At this stage OPTIM checks the value of $J'(\alpha, T)\Big|_{\alpha=\alpha_k}$ against the line stopping tolerance. If the requirement is satisfied control returns to subroutine TWO with the new values for $\bar{\beta}_{i+1}$. Otherwise a new value for α_k is obtained within routine TEN by cubic interpolation or quadratic

extrapolation and the process is repeated until a new value for α_k is found such that

$$J'(\alpha, T)\Big|_{\alpha=\alpha_k} < \text{line stopping tolerance}$$

This completes one complete cycle of iteration and the process is repeated for a number of cycles until within OPTIM the requirement

$$J'(\alpha, T)\Big|_{\alpha=0} < \text{program stopping tolerance}$$

is met.

Subroutine ELEVEN is called in at that time to print as output the final value of the error, the final set of coefficients $\bar{\beta}^*$, the elements of the stiffness matrix [K] and the final predicted $\{x_j(\bar{\beta}^*, T)\}_m$ and related quantities required and also the input values $\{y_j(t)\}_m$ for comparison purposes.

A flow chart of the identification program is given in Fig. 1.

During a run of the program the following conditions might arise:

Stop 1 is self explanatory and indicates perfect convergence. If the initial guess for the parameters $\bar{\beta}_1$ is a poor one, the program may fail to converge. To avoid wasting computer time the following precautions are taken:

Initially the maximum number of iterations i_{max} is taken to be a small number. Usually a value of $i_{max} = 3$ gives a good indication of the performance for a given set of initial values. If during those first few iterations the error and the slope $J(\bar{\beta}_i, T)$ and $J'(\alpha, T)\Big|_{\alpha=0}$ are continuously being reduced and the final value of α_k in each of the line searches is increasing and tending towards one, the procedure is obviously converging and the run may be restarted with the final values obtained for the $\bar{\beta}_i$'s and a much larger value for i_{max}. The maximum number of iterations for a

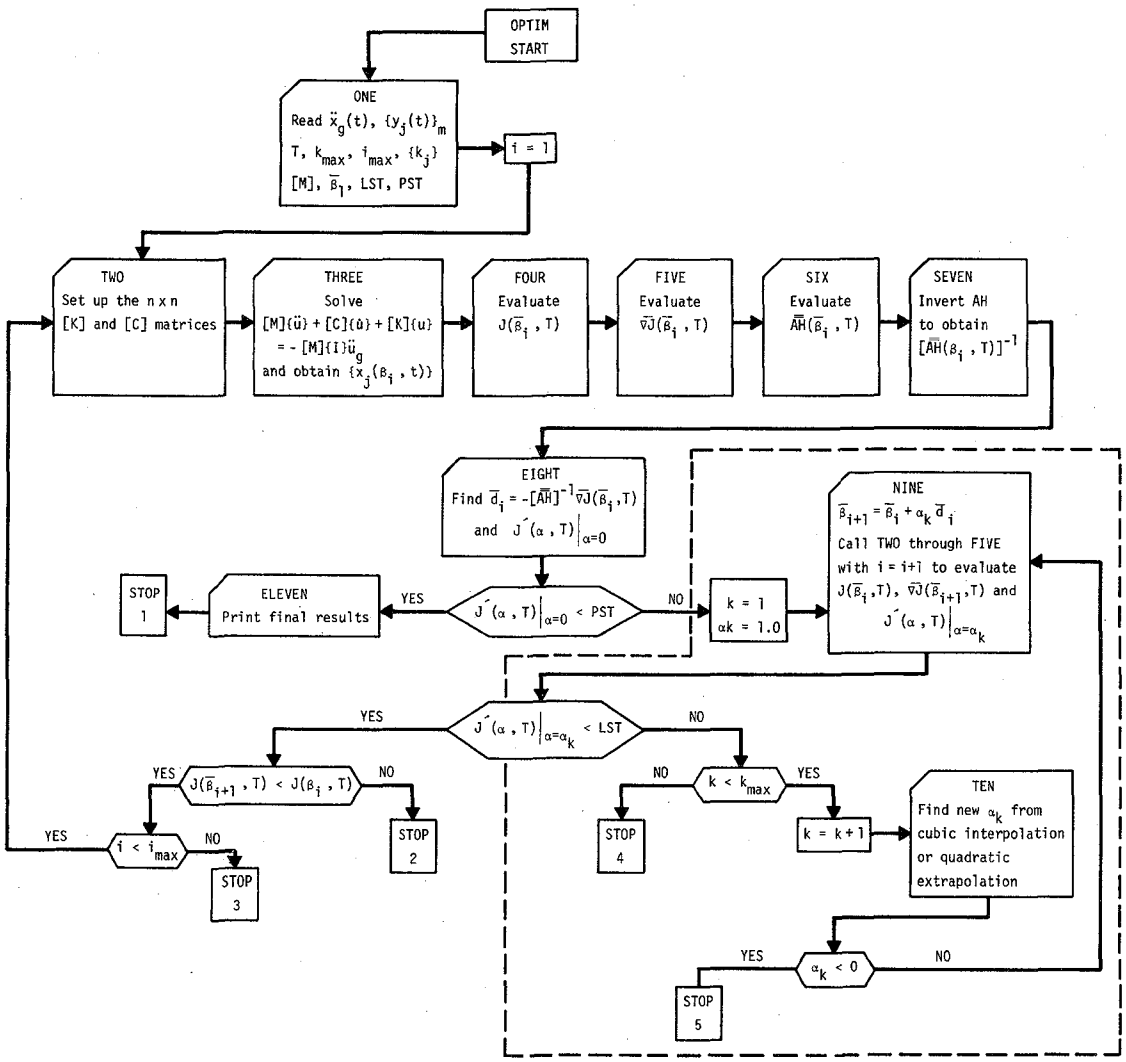

FIGURE 1 FLOW CHART FOR THE IDENTIFICATION PROGRAM

good convergence has never exceeded 10 to 12. Thus, $i_{max} = 20$ was a safe guess. Thus stop 3 is provided for an early detection of a diverging run.

A particular line search usually required four to six iterations and k_{max} is set equal to 10. If within a line search 10 iterations are not sufficient for finding a proper α_k, either the line search tolerance is increased or the initial $\overline{\beta}_1$ values are modified. Usually for the first few iterations on i, k would reach rather high values of the order of 6 to 8, but as i increases, i.e., as the iterative process progresses and we get closer and closer to the minimum, the number of iterations within a line search would go down to 2 or 3 and α_k would tend to 1, indicating that the error surface is becoming more and more quadratic. Thus stop 4 is provided for the detection of an unsuccessful line search.

Stop 2 is a typical indication of divergence and the initial guess on $\overline{\beta}_1$ had to somehow be modified and improved. Rarely did this condition arise throughout the work, mostly being the indication of a programming error within parts of the program or indication of a wild guess relating to the initial set of parameters $\overline{\beta}_1$.

During the first few iterations, depending on the initial values chosen for $\overline{\beta}_1$, it may very well be that α_k is of the order 0.2. If this is the case a choice of an initial step size equal to 1 may take us to a point on the error surface with a very large error and a very large positive value for the slope. Therefore a cubic interpolation based on $\alpha = 0$ and $\alpha = 1.0$ may be far from furnishing the true stationary point of the error profile within a reasonable number of steps and α_k may even turn out to be smaller than 0. The program stops at stop 5 and usually this condition is remedied by choosing an initial smaller step size of the order of 0.5 for the first few cycles. As the process keeps improving,

i.e., as α_k continues to grow larger, the value of the initial step size may be taken equal to one, and the process continued.

In subroutine NINE an additional check is provided to meet any physical constraints on the parameters. The only constraint for the linear problem we are dealing with would be that none of the parameters $\overline{\beta}_i$ be negative. That also would cause a stop of the program and is a faster way of detecting a divergence than stop 2. Very seldom did this condition occur and was taken as an indication of a rapidly diverging run. Again a new and more logical guess for $\overline{\beta}_i$ would prevent this condition from occurring.

III.2 Use of Simulated Data

Before being subjected to actual test data, the identification program was tested with simulated data to ensure that the algorithms it contains are correct and also to get a feel for the process. For this purpose, a three story frame as depicted in Fig. 2 is chosen and the frame is subjected to a sinusoidal excitation for which closed form solutions can be obtained for the displacements and accelerations of each floor. With this solution introduced as real data and a set of $\overline{\beta}_1$ coefficients which are different from the correct $\overline{\beta}^*$ values of the system by as much as 20 ~ 30%, the validity of the program at its most elementary stage is tested.

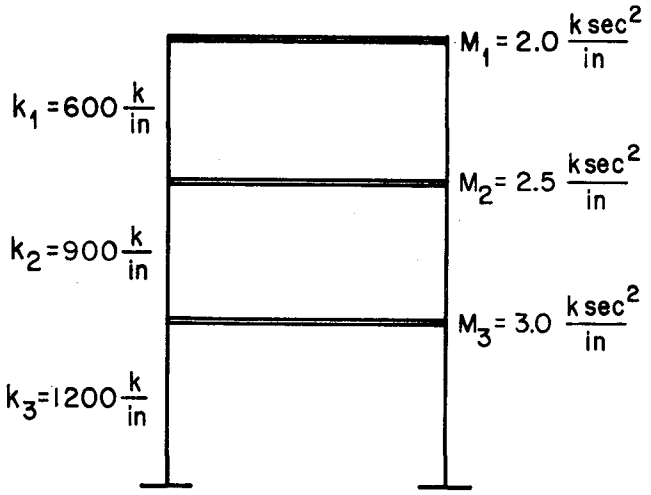

FIGURE 2. FRAME USED FOR SIMULATED DATA

For the given system

$$[M] = \begin{bmatrix} 2.0 & 0 & 0 \\ 0 & 2.5 & 0 \\ 0 & 0 & 3.0 \end{bmatrix}$$

$$[K] = \begin{bmatrix} k_1 & k_1 & 0 \\ -k_1 & k_1 + k_2 & -k_2 \\ 0 & -k_2 & k_2 + k_3 \end{bmatrix} = \begin{bmatrix} 2 & -2 & 0 \\ -2 & 5 & -3 \\ 0 & -3 & 7 \end{bmatrix} \times 300 \text{ k/in}$$

and

$$[C] = a_0 [M] + a_1 [K]$$

The mode shapes and frequencies of the system are evaluated to be

$$[\phi] = \begin{bmatrix} 1.000 & 1.000 & 1.000 \\ 0.711 & -0.630 & -2.410 \\ 0.346 & -0.870 & 2.210 \end{bmatrix}$$

and

$$\{\omega\} = \begin{Bmatrix} 9.3 \\ 21.9 \\ 32.0 \end{Bmatrix} \quad \text{rad/sec}$$

First assuming no damping, for which case a closed form solution is available, assuming an initial set of $\bar{\beta}_1$ as shown in Table 1, the method converged in three cycles to the final values given in the same table.

TABLE 1 USE OF SIMULATED DATA (UNDAMPED CASE)

	INITIAL $\bar{\beta}_1$	FINAL $\bar{\beta}^*$	TRUE β^*
k_1	700.	600.43	600.
k_2	1000.	906.84	900.
k_3	1100.	1204.59	1200.
a_0	0.2	0.01	0.
a_1	0.001	0.0001	0.

Then, for the same system with damping, for which a closed form solution is not available, but an approximate solution is obtained for acceleration from displacements by differentiation using central differences, the method converged again within three cycles to the solution vector, the results of which are summarized in Table 2.

The rather large differences between the $\bar{\beta}^*$ obtained from the program and the true $\bar{\beta}^*$ values in this case compared to the nondamped system is mainly due to the fact that the first solution used as observed measurements is an exact one while in the second case it is not. The differences

nonetheless do not exceed 6%.

TABLE 2 USE OF SIMULATED DATA (DAMPED CASE)

	INITIAL $\bar{\beta}_1$	$\bar{\beta}_2$	$\bar{\beta}_3$	$\bar{\beta}^*$	TRUE $\bar{\beta}^*$	% DIFF.
k_1	720.	612.78	598.04	596.46	600.	0.59%
k_2	800.	890.24	891.08	892.17	900	0.87%
k_3	1000.	1214.26	1219.38	1220.56	1200.	1.71%
a_o	2.6	1.487	1.284	1.271	1.2	5.91%
a_1	0.012	0.0092	0.0073	0.0068	0.007	2.86%
ERROR	1248.6	125.2	111.3	107.5		

A third check was performed by introducing a certain amount of noise into the solution. The convergence was as good as before and the $\bar{\beta}^*$ parameters very closely matched the true $\bar{\beta}^*$ values.

The validity of the optimization technique and the correctness of the developed program being tested in this form, we can now proceed to work with a real structure and real measurements.

CHAPTER IV FORMULATION OF THE MATHEMATICAL MODELS

This section consists of two parts. In the first the physical structure is described in detail. It is a three story steel frame in which the beams and columns are joined by welding.

The second part is devoted to a discussion of possible mathematical models. The models will differ from one another in the orders of the models, reflecting the degrees of freedom allowed the model. The order of a model, in turn, is identified by the number of parameters appearing in the model to be established.

When constructing a model there is always a trade-off between the accuracy and complexity of the model. In this section we review a number of models of different order, starting with the simplest and proceeding in increasing order of complexity.

When a particular model is completed, response to the experimental earthquake input is calculated and compared to the physical response to the same excitation, thus assessing the accuracy of the model.

IV.1 The Test Structure

The real frame which was tested in the EERC laboratory in Richmond and for which very detailed information is furnished in the work by Clough and Tang (1975) and the continuation of the same work by Tang (1975) is briefly described below.

The test structure shown on the shaking table in Fig. 3 is fabricated from rolled shapes of ASTM A-36 grade steel. Typical floor plans as well as front and side elevations of the structure are shown in Fig. 4. The two frames designated A and B are separated by a distance of 6'-0". They are connected at floor levels by removable cross beams and bracing angles. Thus the effect of a floor diaphragm rigid in its own plane is obtained.

The total height of the structure is 17'-4"; the story heights are 6'-8", 5'-4" and 5'-4". The bay width is 12'-0". Sections W5-16 and W6-12 are used for column and girder numbers, respectively.

The fully penetrated welded girder to column connections are used for the test structure. Figures 5 and 6 depict the details of these connections; the panel zone thickness is 1/4" (i.e. the column web thickness) for Phase I of the experiments, and 1" (column web reinforced by 3/8" doubler plates on both sides) for Phase II. Because of the different strengths of these two types of connections, the test structure is expected to yield primarily in the panel zone in Phase I study and exclusively in the girder and column ends in Phase II tests.

Blocks of concrete weighing about 8000 lbs. per floor are added to the structure to provide a period of vibration in the range appropriate to actual steel buildings and to apply a gravity load to the girders. The use of this particular weight at each floor gives a rather small gravity load stress in the structure, so that the test structure exhibits unusually high capacity in resisting lateral loads.

Table 3 lists the nominal section properties and force capacities of the structure while Table 4 summarizes the estimated weights of the structure.

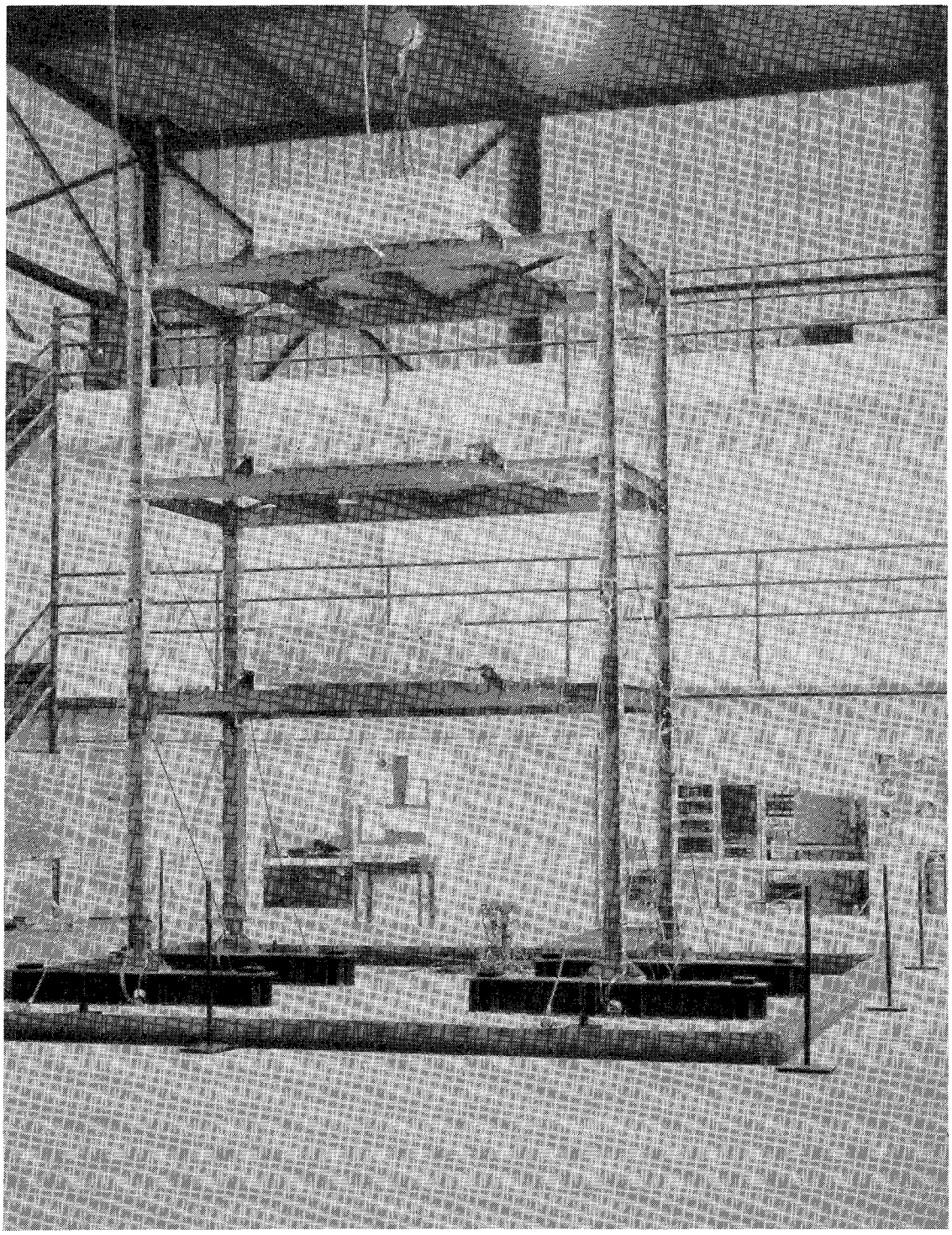

FIGURE 3 TEST STRUCTURE ON THE SHAKING TABLE

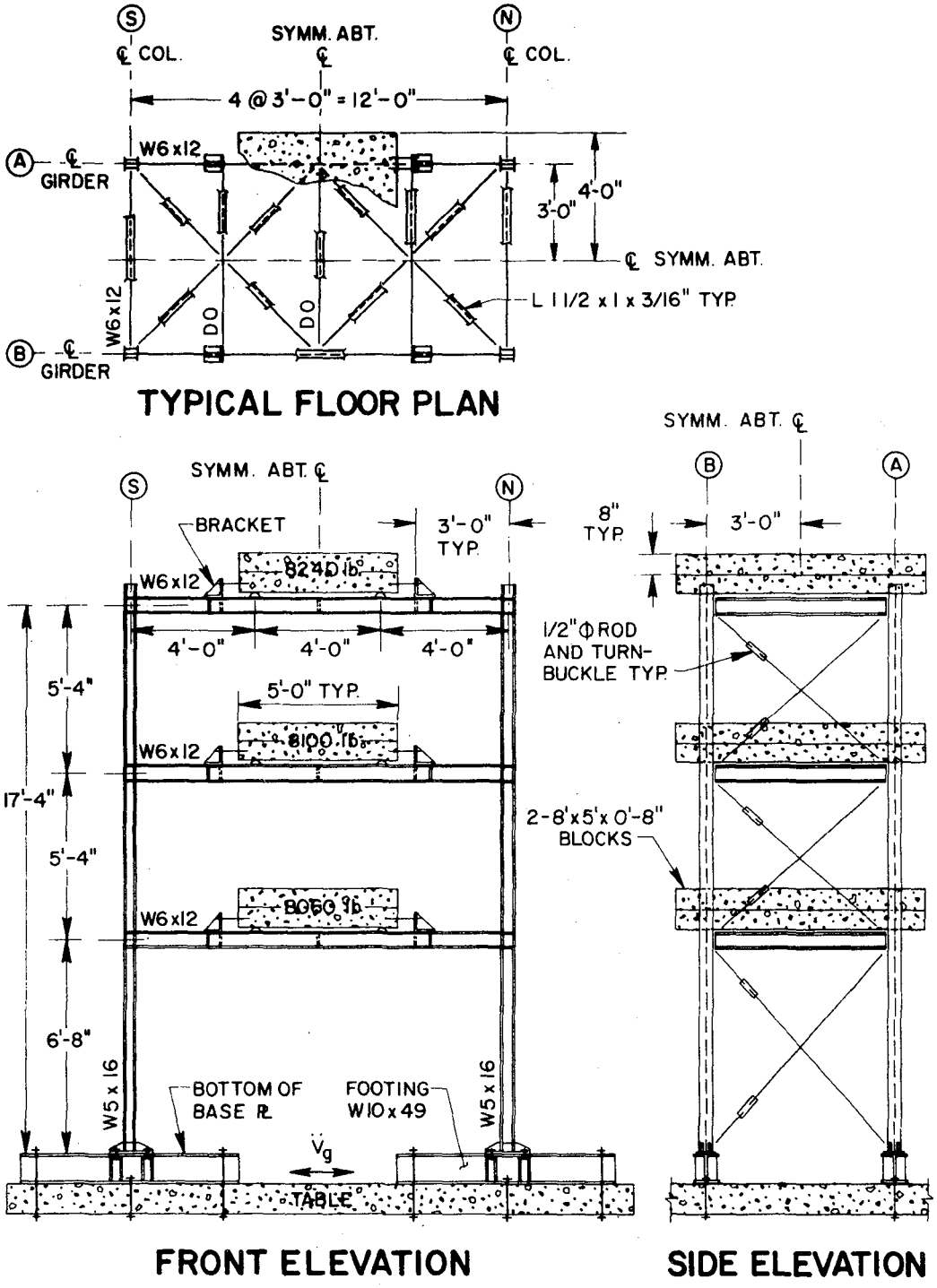

FIGURE 4 PLAN AND ELEVATIONS OF THE TEST STRUCTURE

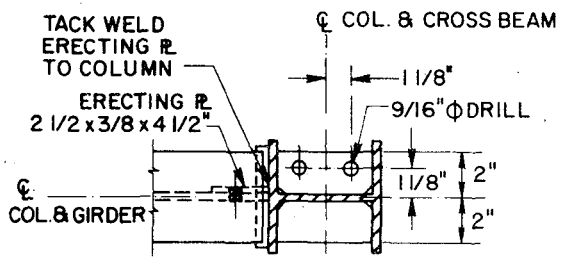

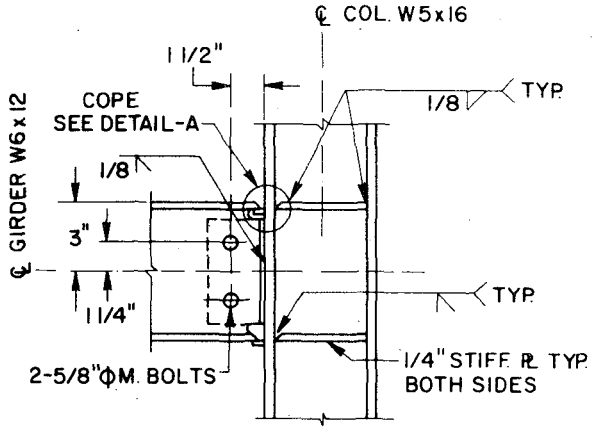

TYPICAL CONNECTION AS BUILT

FIGURE 5 DETAILS OF GIRDER-TO-COLUMN CONNECTION - UNDER-DESIGNED (PHASE I)

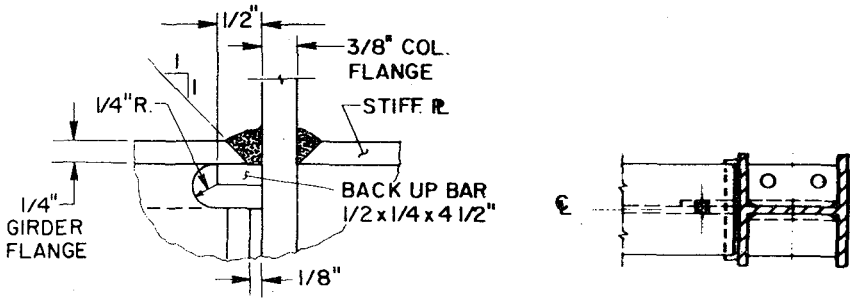

DETAIL-A

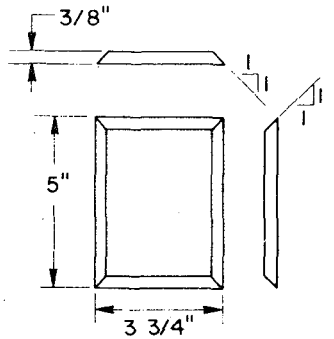

DETAIL-B

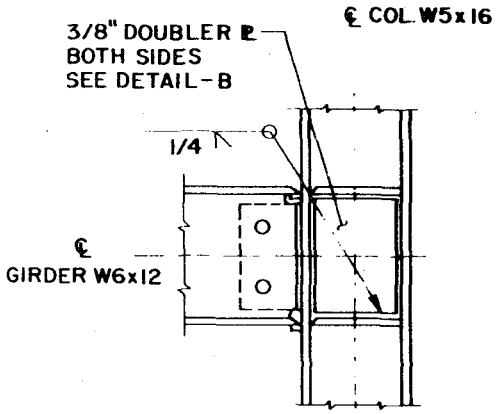

TYPICAL CONNECTION REINFORCED

FIGURE 6 DETAILS OF GIRDER-TO-COLUMN CONNECTION - REINFORCED (PHASE II)

TABLE 3 SECTION AND MATERIAL PROPERTIES

	Girder W6x12	Column W5x16
	Nominal*	Nominal*
b(in)	4.00	5.00
d(in)	6.00	5.00
t_w(in)	0.230	0.240
t_f(in)	0.279	0.360
A (in^2)	3.54	4.70
I_x (in^4)	21.7	21.3
S_x (in^3)	7.25	8.53
Z_x (in^3)	8.23	9.61
σ_y (ksi)	45.9	45.9
τ_y (ksi)	26.5	26.5
P_y (kip)	126	216
M_y (kip-in)	333	392
M_p (kip-in)	378	441

*Material properties are based on mill test report

TABLE 4 WEIGHT OF STRUCTURAL COMPONENTS AND CONCRETE BLOCKS*

	Conc. Blocks**	Column↑	Girder	Cross Beams	Brac'gs	Misc.	Total
3rd Floor (lb)	8240	214	274	402	50	120	9300
2nd Floor (lb)	8100	342	274	402	50	120	9288
1st Floor (lb)	8060	384	274	402	50	120	9290

* Frame A and Frame B

** Center of gravity at 9 1/4" above girder top flange

↑ Half column heights

It should be noted that the models developed in this study deal primarily with Phase II of the study in Clough and Tang's work (1975) although for comparison purposes some excitations from the Phase I study have been used with the same models.

IV.2 The Five Parameter Model

At the initial phase of the work, the simplest possible model is chosen which consists of three stiffness parameters, one related to each story, and two damping parameters. Thus the frame is treated as a shear building with a stiffness matrix of the form

$$[K] = \begin{bmatrix} k_1 & -k_1 & 0 \\ -k_1 & k_1+k_2 & -k_2 \\ 0 & -k_2 & k_2+k_3 \end{bmatrix}$$

and a damping matrix

$$[C] = a_o [M] + a_1 [K]$$

The $\bar{\beta}$ vector consists of

$$\bar{\beta} = < k_1 \; k_2 \; k_3 \; a_o \; a_1 >$$

In this model, the initial values used for the terms in the stiffness matrix are obtained using the usual center-to-center distances. The initial stiffness matrix accordingly is (making use of the proper values from Table 3):

$$[K] = \begin{bmatrix} \frac{24EI_1}{L_1^3} & -\frac{24EI_1}{L_1^3} & 0 \\ -\frac{24EI_1}{L_1^3} & \frac{24EI_1}{L_1^3} + \frac{24EI_2}{L_2^3} & -\frac{24EI_2}{L_2^3} \\ 0 & \frac{24EI_2}{L_2^3} & \frac{24EI_2}{L_2^3} + \frac{24EI_3}{L_3^3} \end{bmatrix} = \begin{bmatrix} 57.72 & -57.72 & 0 \\ -57.72 & 115.14 & -57.72 \\ 0 & -57.72 & 87.27 \end{bmatrix} \text{ k/in}$$

and the mass matrix, using Table 4, is taken to be:

$$[M] = \begin{bmatrix} 0.01204 & 0 & 0 \\ 0 & 0.01204 & 0 \\ 0 & 0 & 0.01204 \end{bmatrix} \text{ k-sec}^2/\text{in}$$

and kept constant throughout. The initial values for a_0 and a_1 in the damping matrix are taken as:

$$a_0 = 0.2340 \quad \text{and} \quad a_1 = 0.0003$$

approximately corresponding to damping ratios

$$\lambda_n = \begin{Bmatrix} 1.0\% \\ 1.0\% \\ 1.77\% \end{Bmatrix}$$

assuming the vibrating frequencies of the system to be

$$\omega_n = \begin{Bmatrix} 2.40 \\ 8.35 \\ 17.75 \end{Bmatrix} \text{ cps.}$$

Thus the initial $\overline{\beta}_1$ vector is taken as

$$\overline{\beta}_1 = < 57.72 \quad 57.72 \quad 29.55 \quad 0.2340 \quad 0.003 > \tag{24}$$

This initial phase of the work was rather disappointing, since no convergence was obtained for a large number of trials. A number of modifications were introduced into the program with little success. All other possibilities being removed, it was finally decided that the model is inadequate and the initial values are far from any reasonable set necessary for convergence. A large number of different starting values were used with no success.

Having a fairly good idea about the vibrating frequencies of the system, we checked on the determinant

$$|| [K] - \omega^2 [M] ||$$

and found that with the above assumed $\overline{\beta}_1$ values, the determinant was far from being zero. We then proceeded to look for the values of k_1, k_2 and k_3 which would make the determinant zero. This required the solution of a third order polynomial and only by trial and error were we able to spot a set of k values that would closely satisfy the frequency equation. Those values which were

$$< \sim 37. \quad \sim 23. \quad \sim 12. \quad >$$

and which have no physical significance and no bearing whatsoever to the initial values that were previously chosen as starting values, were the first set of initial values that started to yield convergence.

Working with the EC 400-II data reported in Clough and Tang (1975), which resulted in a linear response in Phase II of the study, forming the error function by taking m = 1 to be displacements and m = 2 to be acceleration,

and using information at all floor levels, i.e.

$$< k_j > = < 1 \quad 1 \quad 1 >$$

the method starting yielding some reasonable matching between measured versus predicted response. Figure 7 shows some typical examples of the types of match that were obtained with the simplest model using displacements and accelerations at different floors. Table 5 lists the values obtained for the coefficients.

Judging from Fig. 7, the agreement is considered to be satisfactory keeping in mind the crudeness of the model. The importance of this phase of the work essentially amounts to the experience and insight gained while working with real data rather than any of the final results obtained for the parameters or the agreement between measured versus predicted response. Problems in the future phases of the work could much more easily be detected because of the experience and enough confidence was gained to handle more complex models.

An important conclusion that can be derived from this initial phase is that the present model is in no way satisfactory to represent the given frame. A shear building type behavior seems to be totally inadequate to duplicate the real behavior of a steel frame. The fact that some reasonable response was obtained does not mean much since no physical significance can be attached to the values obtained for the stiffness coefficients except for the fact that they were a set of numbers which artificially match the frequencies of the system.

To improve on the predicted quantities the logical next step is to develop a new, more realistic model to accommodate rotations at the joints as additional degrees of freedom and work with an eight parameter

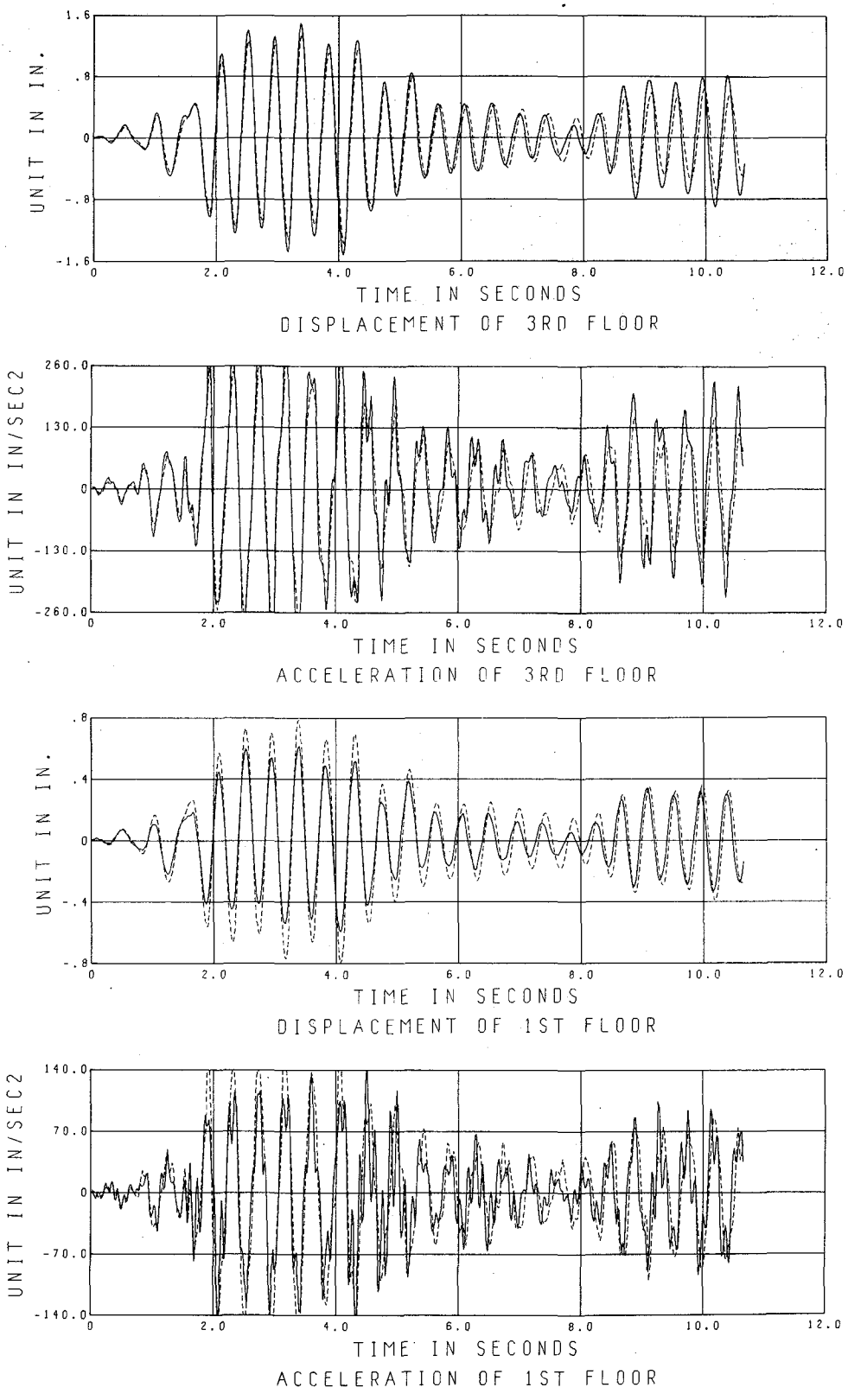

FIGURE 7 EC 400-II COMPARISON OF MEASURED AND COMPUTED RESPONSE TIME HISTORIES (FIVE PARAMETER MODEL - PARAMETERS OPTIMIZED)

TABLE 5 EC 400-II VALUES OF COEFFICIENTS AND ERROR FUNCTION FOR DIFFERENT VALUES OF T (FIVE PARAMETER MODEL)

	Parameters from 24	Initial Values for Parameters	Final Values for Parameters T = 2 sec.	Final Values for Parameters T = 4 sec.
	57.72	37.0	34.06	31.58
	57.72	23.0	17.64	19.93
	29.55	12.0	10.75	10.89
	0.2340	0.2340	0.3191	0.2751
Error ↓	0.0003	0.0003	0.0001	0.0002
T = 2 sec	23068	7248	1242	--
T = 4 sec	--	21324	--	9460
T = 12 sec	--	102524	--	42094*

*Extrapolated Error using coefficients at the end of 4 sec. of data

model. The program appeared to require only simple modifications and significant improvements were expected.

IV.3 The Eight Parameter Model

In this second phase of the work, we treat the frame as a six-degree-of-freedom system (taking advantage of symmetry), three translational degrees of freedom and three rotational. It is expected that this model will be more realistic and a better approximation to the real frame. The 3 x 3 translational stiffness matrix is obtained by writing the complete 6 x 6 stiffness matrix and condensing it to a 3 x 3 by eliminating the rotations of the joints. Thus

$$\begin{Bmatrix} \overline{M} \\ \overline{P} \end{Bmatrix} = \begin{bmatrix} [K_{11}] & [K_{12}] \\ [K_{21}] & [K_{22}] \end{bmatrix} \begin{Bmatrix} \overline{\omega} \\ \overline{\Delta} \end{Bmatrix} \tag{25}$$

where $\overline{M}$ and $\overline{P}$ are the external joint moments and forces while $\overline{\omega}$ and $\overline{\Delta}$ are the rotations and displacements of the joints. The relationship between force and displacements is obtained in the classical way, i.e., by introducing the degrees of freedom one at a time, which yields the corresponding columns in the [K] matrix.

Assuming

$$\{\overline{M}\} = \{\overline{0}\}$$

the condensation procedure yields,

$$\{\overline{\omega}\} = -[K_{11}]^{-1}[K_{12}]\{\overline{\Delta}\}$$

$$\{\overline{P}\} = [-[K_{21}][K_{11}]^{-1}[K_{12}] + [K_{22}]]\{\overline{\Delta}\}$$

or

$$\{\overline{P}\} = [\overline{K}]\{\overline{\Delta}\}$$

Given the geometry of the system, [K] is initially assumed to be

$$[K] = \begin{bmatrix} 23.15 & -33.10 & 11.52 \\ -33.10 & 71.89 & -49.64 \\ 11.52 & -49.64 & 69.48 \end{bmatrix}$$

and a_0 and a_1 are taken as before

$$a_0 = 0.2340 \quad \text{and} \quad a_1 = 0.0003$$

A slight modification is introduced at this stage to make all $\bar{\beta}_i$ coefficients of the same order of magnitude and to get a direct feel for the percentage of each parameter in the identification process. This is accomplished by defining the stiffness matrix as

$$[K] = \begin{bmatrix} \beta_1 \times 23.15 & -\beta_2 \times 33.10 & \beta_3 \times 11.52 \\ -\beta_2 \times 33.10 & \beta_4 \times 71.89 & -\beta_5 \times 49.64 \\ \beta_3 \times 11.52 & -\beta_5 \times 49.64 & \beta_6 \times 69.48 \end{bmatrix}$$

and

$$a_0 = \beta_7 \times 0.2340 \quad \text{and} \quad a_1 = \beta_8 \times 0.0003$$

The initial guess for the newly defined $\bar{\beta}_i$ coefficients consists of a series of 1.

$$\bar{\beta}_1 = < 1 \quad 1 \quad 1 \quad 1 \quad 1 \quad 1 \quad 1 \quad 1 >$$

To be able to display the power of the identification process, a number of plots have been drawn comparing the measured versus the predicted

response time histories with this initial guess for $\bar{\beta}_1$, which would be an indication of the type of response that one might hope to get with the model described above before optimization (Fig. 8). As this initial set of parameters roughly represents current practice in analysis, the shortcomings of current analysis are apparent.

Figures 9 and 10 summarize in graphic form a typical run of the optimization program. The decay of the error and the reduction of the slope of the error surface as we approach the minimum are displayed. Table 6 yields similar information in numerical form. In this table the number of cycles required for convergence, the number of iterations within each cycle to obtain a proper step size, and the value of the step size α at the end of each cycle are given. Also the component of the direction vector related to a particular β coefficient, namely β_2, is given at the end of each cycle and the variation of β_2 during one complete run is displayed as a typical example. Similar information is displayed in Table 7 for T = 6 sec. to indicate the variation in the same typical coefficient as more data is used to identify it. Note the rapid convergence of the process during the first few cycles. As the minimum is approached, the rate of convergence is reduced and if the tolerances are set to be very small the number of cycles and consequently the computer time required increases. A line stopping tolerance of the order of 1.0 and a program stopping tolerance of 0.1 are found to be reasonable.

Figure 11 compares the measured versus predicted displacements and acceleration response time histories of two floors for the EC 400-II base motion.

The time used as the upper limit T in the integral squared error function affects the computer time required significantly. Usually this

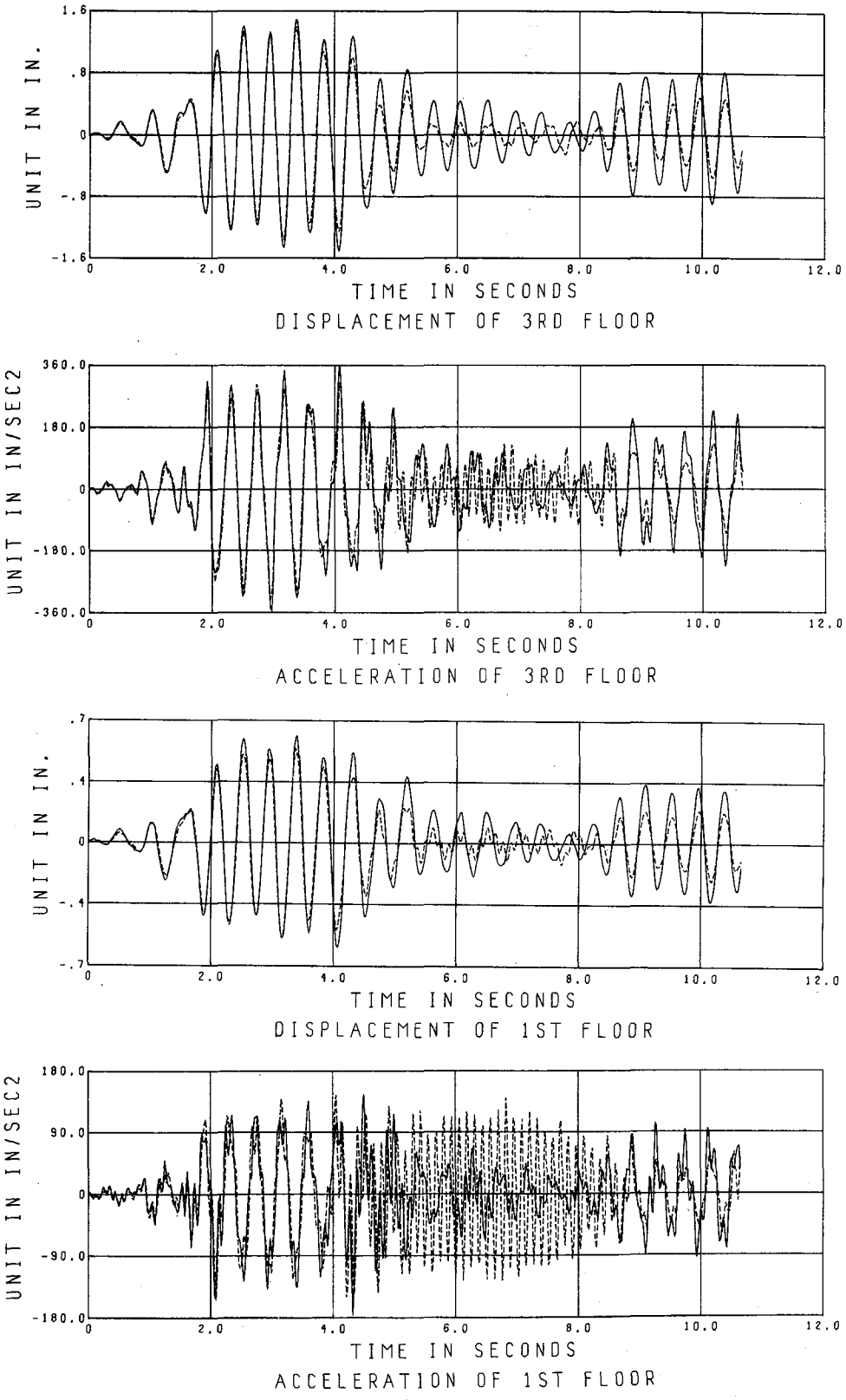

FIGURE 8 EC 400-II COMPARISON OF MEASURED AND COMPUTED RESPONSE TIME HISTORIES (FIRST EIGHT PARAMETER MODEL - BEFORE OPTIMIZATION OF PARAMETERS)

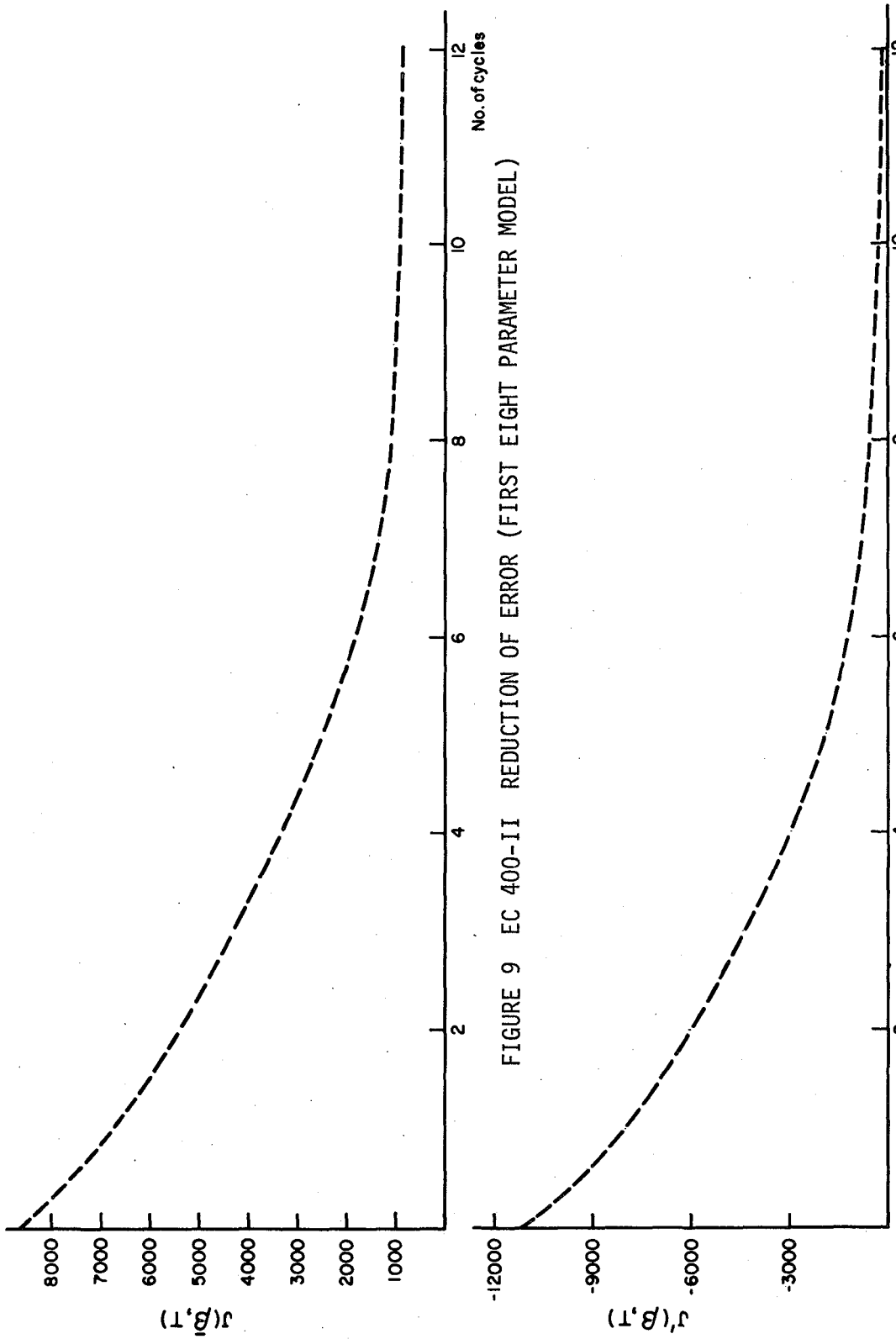

FIGURE 9 EC 400-II REDUCTION OF ERROR (FIRST EIGHT PARAMETER MODEL)

FIGURE 10 EC 400-II REDUCTION OF SLOPE OF ERROR SURFACE (FIRST EIGHT PARAMETER MODEL)

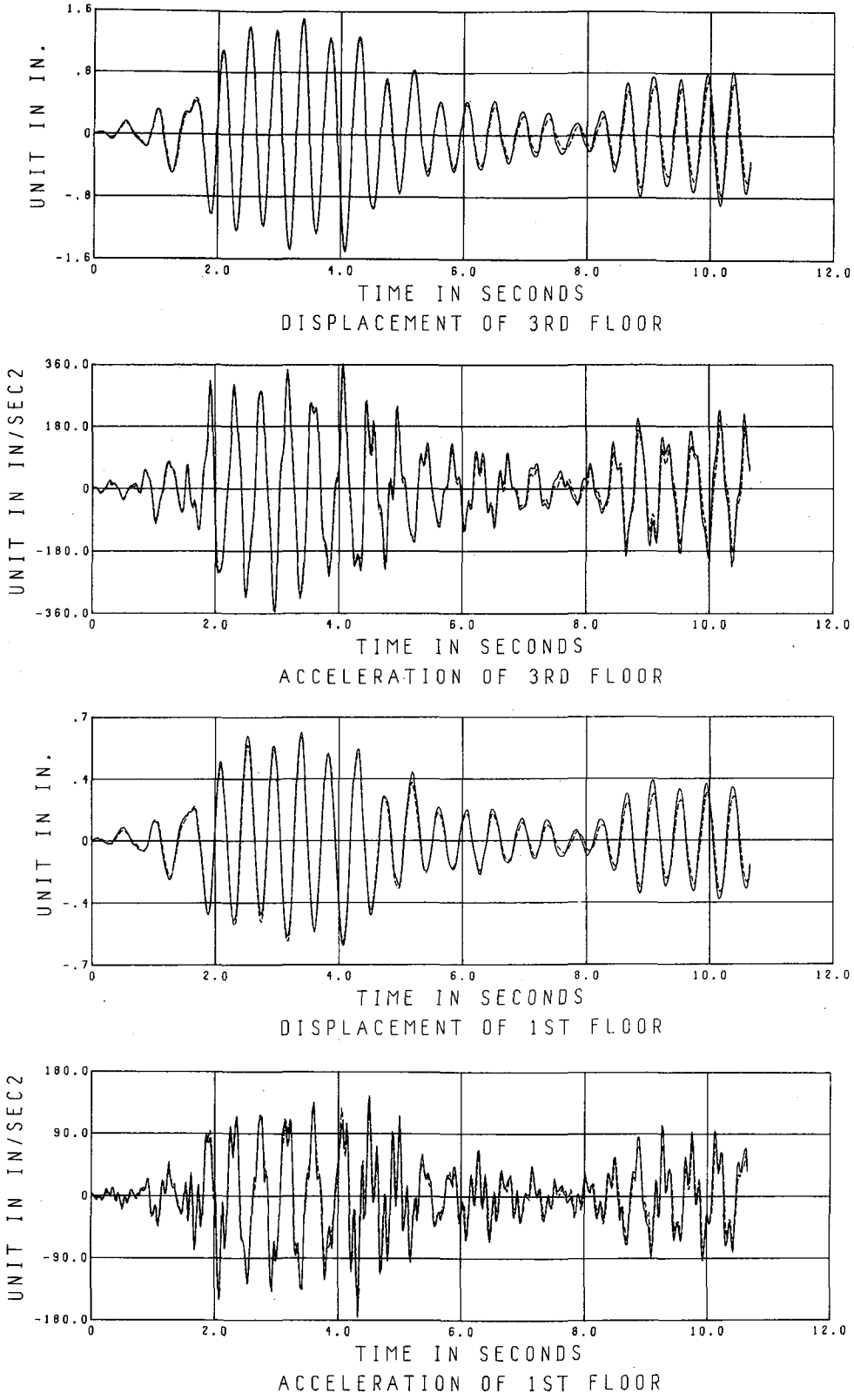

FIGURE 11 EC 400-II COMPARISON OF MEASURED AND COMPUTED RESPONSE TIME HISTORIES (FIRST EIGHT PARAMETER MODEL - PARAMETERS OPTIMIZED)

TABLE 6 EC 400-II TYPICAL RUN IN NUMERICAL FORM (T = 4 sec)

No. of Cycles	No. of iter. per Cycle	Error	Value of α	Value of d_2	$\Delta\beta_2$	β_2
		8657				1.000
1st	6		0.102	0.139	0.014	
		6796				1.014
2	5		0.127	0.118	0.015	
		5457				1.029
3	4		0.247	0.090	0.023	
		4320				1.052
4	4		0.352	0.075	0.026	
		3347				1.078
5	3		0.421	0.068	0.029	
		2493				1.107
6	4		0.551	0.047	0.026	
		1878				1.133
7	3		0.640	0.038	0.024	
		1352				1.157
8	2		0.763	0.027	0.021	
		1105				1.178
9	2		0.894	0.020	0.018	
		1002				1.196
10	2		0.971	0.010	0.010	
		937				1.206
11	1		1.000	0.003	0.003	
		875				1.209
12	1		1.000	0.002	0.002	
		862				1.211

$\sum = 0.211$

TABLE 7 EC 400-II TYPICAL RUN IN NUMERICAL FORM (T = 6 sec)

No. of Cycles	No. of iter. per Cycle	Error	Value of α	Value of d_2	$\Delta\beta_2$	β_2
		2813				1.211
1st	3		0.9068	-0.0372	-0.034	
		1938				1.177
2	3		1.2047	0.0000	0.000	
		1844				1.177
3	2		0.8816	0.0011	0.001	
		1831				1.178
4	1		1.0000	-0.0030	-0.0030	
		1830				1.175
5	1		1.0000	0.0004	0.0004	
		1830				1.175
6	1		1.0000	-0.0004	-0.0004	
		1830				1.175

$\sum = -0.036$

is restricted to the first four to six seconds of data which includes the most significant part of the signal. The output is usually extrapolated to 12 sec. using the parameters obtained with 6 sec. of data. The agreement between measured versus predicted response which is excellent for those first six seconds is also very good for the extrapolated last six seconds.

Table 8 is a comparison of the final parameters obtained using four and six seconds of data in the error function. It is seen that the variation in the final values of the stiffness parameters for the two T's is of the order of 3% on the average while the difference between the initial and final values of the same parameters is of the order of 20%. For the damping parameters the percentages are even higher. The rapid convergence of the parameters to their final values with an initial quess which is off by an order of magnitude of 20% is a good indication of the power of the process and of system identification in general. Table 9 compares the initial and final stiffness matrices and damping coefficients.

Most of the work is done with two base motions reported in Clough and Tang's work. Those are the EC 400-II and EC 100-I excitations. With either one of these two signals the structure remains within the linear range and thus suits our needs best. The symbols I and II refer to Phase I and Phase II of the work mentioned above where in Phase II the panel zones were reinforced. Thus, though the geometry of the frame is the same, it is logical to expect that the parameters estimated for the two phases will be slightly different. Also since the model which has been used does not take any panel zone distortion into account, the results from excitations in Phase II should be better and more accurate than the results obtained from excitations in Phase I. Also the MEC 600-II base motion is used to show that the present model can be considered as an

TABLE 8 EC 400-II COMPARISON OF INITIAL VERSUS FINAL VALUES OF PARAMETERS

	Starting Values of Parameters	Values of Parameters using 4 sec. of data	Values of Parameters using 6 sec. of data
β_1	1.00	1.188	1.147
β_2	1.00	1.211	1.175
β_3	1.00	1.072	1.080
β_4	1.00	1.143	1.131
β_5	1.00	0.991	1.024
β_6	1.00	0.947	0.998
β_7	1.00	0.651	0.575
β_8	1.00	0.396	0.607

TABLE 9 EC 400-II COMPARISON OF INITIAL VERSUS FINAL VALUES OF STIFFNESS MATRICES AND DAMPING COEFFICIENTS

	Initial Stiffness and Damping Parameters	Final Stiffness and Damping Parameters T = 4	Final Stiffness and Damping Parameters T = 6
	$\begin{bmatrix} 23.15 & -33.10 & 11.52 \\ -33.10 & 71.89 & -49.64 \\ 11.52 & -49.64 & 69.48 \end{bmatrix}$	$\begin{bmatrix} 27.49 & -40.11 & 12.35 \\ -40.11 & 82.16 & -49.17 \\ 12.35 & -49.17 & 65.77 \end{bmatrix}$	$\begin{bmatrix} 26.55 & -38.94 & 12.44 \\ -38.94 & 81.33 & -50.82 \\ 12.44 & -50.82 & 69.36 \end{bmatrix}$
a_o	0.2340	0.1521	0.1345
a_1	0.003	0.00012	0.00018
λ_1	1%	0.59%	0.58%
λ_2	1%	0.46%	0.60%
λ_3	1.77%	0.73%	1.07%

equivalent linear model while the frame experiences mild nonlinearities. With excitation in the highly nonlinear range, the system failed to converge indicating the need for a more refined model to take into account the energy dissipation of the system. Figures 12 and 13 compare the displacement and acceleration time histories of some typical floors for the MEC 600-II base motion before and after optimization of the parameters.

We note that in all cases the match between measured and predicted quantities is extremely good for the first six seconds of data since only that much of the data is usually used in determining final values for the parameters. From six seconds on, the comparison is mainly on measured versus extrapolated output from parameters based on the first six seconds of data. Tables 10, 11 and 12 summarize the values of the parameters obtained for the MEC 600-II base motion. Note that to avoid wasting computer time, larger tolerances have been used (LST = 100 and PST = 100). Also, final coefficient values obtained for EC 400-II have been used to reduce the number of cycles required to obtain final values of the parameters.

Speaking in the chronological context of this research, at this stage we had two mathematical models, one with five parameters and another with eight. The eight parameter model, particularly, predicted very accurate time history responses both in acceleration and displacement at all floors. This might very well have concluded the study of linear modeling, but we were very curious why the stiffness of each member based on the usual EI/L needed to be adjusted during optimization by up to 25% to predict the experimental responses. We did not understand the physics or engineering of the problem.

We decided to tackle the eight parameter model differently in an attempt to understand the physical problem. This proved to be the

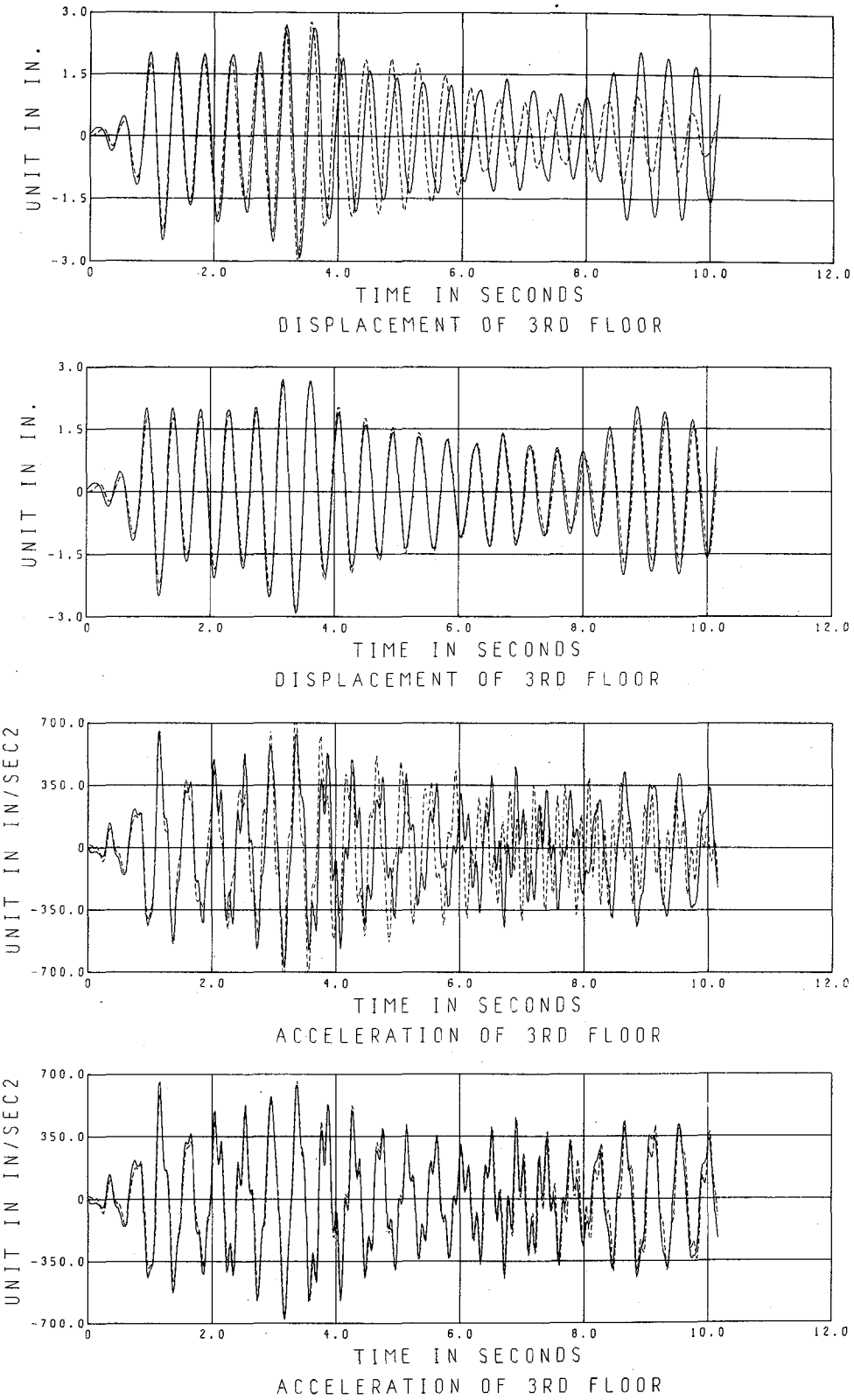

FIGURE 12 MEC 600-II COMPARISON OF MEASURED AND COMPUTED RESPONSE TIME HISTORIES BEFORE AND AFTER OPTIMIZATION OF PARAMETERS (FIRST EIGHT PARAMETER MODEL)

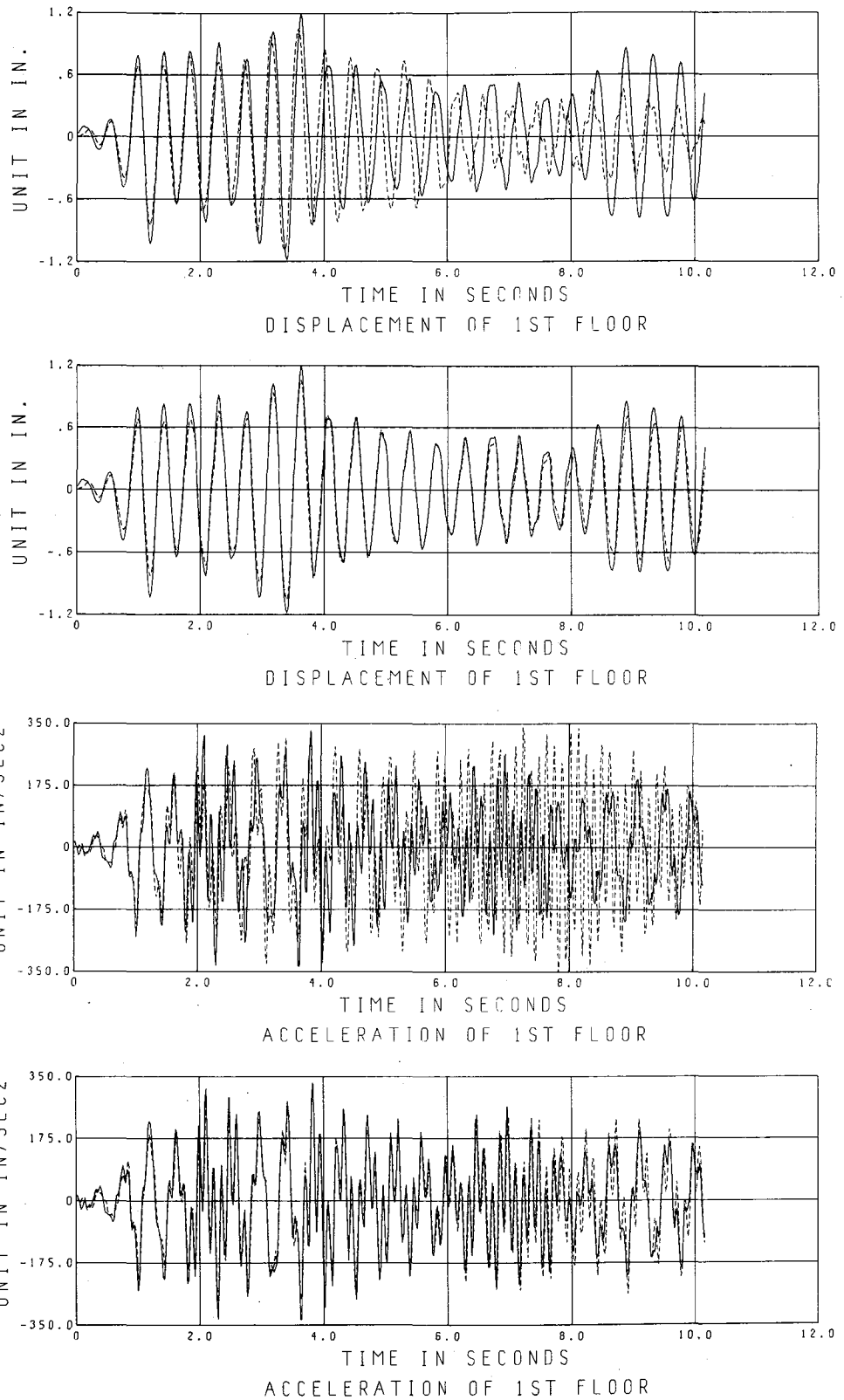

FIGURE 13 MEC 600-II COMPARISON OF MEASURED AND COMPUTED RESPONSE TIME HISTORIES BEFORE AND AFTER OPTIMIZATION OF PARAMETERS (FIRST EIGHT PARAMETER MODEL)

TABLE 10 MEC 600-II SUMMARY OF COMPUTER RUN T = 4 sec.

No. of Cycles	No. of iter. per Cycle	Error	Slope
1st	5	103156	-172030
2	4	23338	-11803
3	4	17480	-718
		17063	-92

TABLE 11 MEC 600-II SUMMARY OF COMPUTER RUN T = 6 sec.

No. of Cycles	No. of iter. per Cycle	Error	Slope
1st	2	31862	-14493
2	2	26418	-2410
3	3	24871	-1056
4	2	24414	-341
		24212	-82

TABLE 12 MEC 600-II COMPARISON OF INITIAL AND FINAL PARAMETERS

	Initial Coeff.	Final Coeff. T = 4 sec.	Final Coeff. T = 6 sec.
k_{11}	23.15	20.28	20.25
k_{12}	-33.10	-28.37	-28.72
k_{13}	11.52	7.87	8.08
k_{22}	71.89	66.66	67.92
k_{23}	-49.64	-49.43	-49.83
k_{33}	69.48	77.79	77.16
a_o	0.2340	0.372	0.415
a_1	0.0003	0.00013	0.0001

significant point of the research because in this new study we gained not only an understanding of the engineering of the structure, but a great deal about system identification.

CHAPTER V A DIFFERENT APPROACH FOR THE CONSTRUCTION OF THE MODEL

At this stage of the research we felt that it was necessary to study the significance of a change of 25% in the elements of the stiffness matrix during optimization so that the model predicts the response data accurately. We felt it necessary to gain insight into the quantities assumed for the individual stiffnesses of each of the members.

With the previous eight parameter model there is no way of making any assessments of the individual element stiffnesses. As is well known, though the 3 x 3 translational stiffness matrix is obtained from the complete 6 x 6 matrix by a condensation procedure, there is no way of proceeding backwards and trying to determine what change in the stiffness characteristics of the members would be responsible in explaining the differences in the final and initial sets of the $\overline{\beta}_i$ coefficients.

Thus the procedure had to be modified by going one step backwards and determining a new set of parameters such that the final results could be interpreted in terms of the stiffnesses of the individual members.

V.1 Another Eight Parameter Model with Different Parameters

To solve the problem of interpreting the final results in a more sensible manner, a new set of parameters was defined within the same model. Enough confidence and insight was developed so as to be able to change the parameters within the model and incorporate the new concepts into the

computer program without changing its framework. This was thought to be a relatively simple step and the problem was at this stage assumed to be practically solved, yet we found that this was not so.

It was decided to drop the $\bar{\beta}_i$ parameters we have used so far and replace them with a $\bar{\gamma}_i$ set of parameters, each one associated with the stiffness of an individual element.

The frame is now assumed to have element stiffness characteristics as shown in Fig. 14.

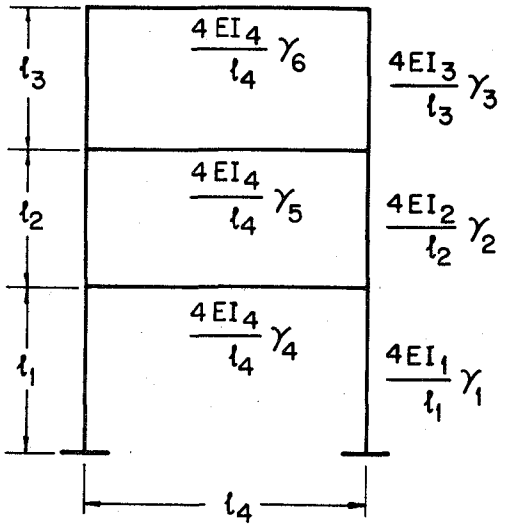

FIGURE 14 THE STRUCTURAL FRAME WITH THE SECOND SET OF PARAMETERS $\bar{\gamma}_i$

The damping coefficients are left unchanged and therefore γ_7 and γ_8 have the same meaning as β_7 and β_8.

Since the previous results were not of much help in assigning appropriate values to the $\bar{\gamma}_i$ coefficients, the problem had to be restarted with an initial guess as before.

$$\bar{\gamma}_i = < 1 \quad 1 \quad 1 \quad 1 \quad 1 \quad 1 \quad 1 \quad 1 >$$

The computer program is modified such that after an initial guess for $\bar{\gamma}$ is made, the 6 x 6 stiffness matrix and, through the same condensation procedure, the 3 x 3 translational stiffness matrix would automatically be set up. One major distinction of this phase of the work from the preceding phase is that now there is no way of obtaining the sensitivity coefficients directly by differentiating Eq. (1). Though symbolically one could obtain the 3 x 3 stiffness matrix from the complete 6 x 6 matrix, the dependence of each term of the reduced matrix on the $\bar{\gamma}$ coefficients is so complex that differentiation of each term of this matrix with respect to γ_1 through γ_6 is an almost impossible job. This is where it was decided to evaluate the sensitivity coefficients by finite differences. Once Eq. (1) is solved for a given set of coefficients, the same equation is solved once more with all coefficients kept constant except for one which is increased by $\Delta\gamma_j$. The difference between the two solutions divided by $\Delta\gamma_j$ would define the sensitivity coefficient for any response function with respect to this particular coefficient. This operation would have to be repeated eight times, once for each parameter within each iteration. The effectiveness of the finite difference approach is tested by taking values for $\Delta\gamma_j = \pm 0.001\,\gamma_j, \pm 0.0001\,\gamma_j, \ldots, \pm 0.000001\,\gamma_j$ using forward and backward differences and comparing the output. The differences in the sensitivity coefficients obtained from each operation were negligibly small as smaller and smaller increments were taken, while for values of $\Delta\gamma_j = \pm 0.01\,\gamma_j$ and $\Delta\gamma_j = \pm 0.1\,\gamma_j$ the differences were rather pronounced as expected.

As an additional check, before proceeding, we used finite differences to obtain the sensitivity coefficients for the previous eight parameter model (involving the $\bar{\beta}$ parameters) and agreement with those obtained by solving the differentiated equations was excellent.

After completion of those checks and comparisons it was decided that evaluation of the sensitivity coefficients by finite differences was a very acceptable procedure and had the advantage of introducing a lot of flexibility into the method. The increase in computer cost while changing to this new formulation was not significant.

The error function being constructed as before, using accelerations and displacements at all three floors, one would assume that convergence would be automatic as before since basically nothing much had changed. The first few trials were disastrous. There was no sign of convergence and the elements of the direction vector were wild. A large number of checks were performed in the hope of locating an error without much luck. Usually, the components of the direction vector related to the top girder and top floor column were the wildest, but it was noticed that they were always of the same order of magnitude and of opposite sign. Without optimism, we decided to fix the stiffness of the top girder to a preassigned value and let the process continue with the remaining seven parameters. To our surprise convergence was excellent. The 3 x 3 stiffness matrix obtained was exactly the same as the one previously obtained and all quantities did match extremely well. The stiffness of the top girder was then fixed to a different value and another run was performed. The results were an entirely different set of the $\bar{\gamma}$ coefficients compared to those from the first run, but an identical stiffness matrix as before resulted. A number of runs were then performed with values for γ_6 ranging

from a value of 0.75 up to values of the order of 5. The outcome was always the same. Excellent convergence in each case, the same final stiffness matrix, perfect match on the measured and predicted displacements and accelerations at all floors, but a different set of $\bar{\gamma}$'s in all cases.

This led us to the conclusion that there can be a family of structures whose stiffness characteristics bear no relationship to each other and yet would all produce the same displacement and acceleration time histories and the same 3 x 3 stiffness matrix when subjected to the same input. Table 13 shows a number of members of this family of frames and their output when the error function is constructed as before on accelerations and displacements at all floor levels.

We finally concluded that the error function is not properly formulated to identify the structure uniquely and that additional information would be required.

Now we start to look for different response quantities to set up the error function. One fact that was noticed in the previous phase of the work was that if the accelerations at floor levels were kept in the error function and displacements deleted or vice versa, the convergence was practically not affected at all and the final values of the parameters were identical. Thus, at least for the elastic case, those two sets of measurements could not be considered as independent constraints as far as the optimization process is concerned. If the match on one of these quantities is good, the match on the other is automatically as good.

The next step is to remove displacements from the error function and introduce a different set of responses closely related to the rotations of the joints. Since strain measurements were available at all ends of the columns and girders, by straight line extrapolation between the strain

TABLE 13 A SET OF FRAMES YIELDING SIMILAR OUTPUT

Trial No. 1	Starting Value	Final Value	Final Stiffness Matrix and Damping Coefficient
γ_1	0.95	1.177	$\begin{bmatrix} 27.44 & -38.90 & 13.67 \\ -38.90 & 77.67 & -50.91 \\ 13.67 & -50.91 & 71.21 \end{bmatrix}$
γ_2	1.00	0.827	
γ_3	1.25	1.452	$a_o = 0.149$
γ_4	0.95	0.866	$a_1 = 0.000125$
γ_5	1.00	0.858	$\lambda_1 = 0.58\%$
γ_6	1.25*	--	$\lambda_2 = 0.47\%$
γ_7	0.65	0.638	$\lambda_3 = 0.76\%$
γ_8	0.39	0.415	
Error	3743	867	
Slope	-5712	-0.018	

*fixed

Trial No. 2	Starting Value	Final Value	Final Stiffness Matrix and Damping Coefficients
γ_1	1.177	1.200	$\begin{bmatrix} 27.47 & -38.90 & 13.67 \\ -38.91 & 77.49 & -50.80 \\ 13.73 & -50.80 & 71.10 \end{bmatrix}$
γ_2	0.827	0.773	
γ_3	1.452	1.867	$a_o = 0.1482$
γ_4	0.866	0.834	$a_1 = 0.000133$
γ_5	0.858	0.952	$\lambda_1 = 0.59\%$
γ_6	1.000*	--	$\lambda_2 = 0.48\%$
γ_7	0.638	0.634	$\lambda_3 = 0.80\%$
γ_8	0.415	0.443	
Error	8228	891	
Slope	-14340	-0.047	

*fixed

TABLE 13 A SET OF FRAMES YIELDING SIMILAR OUTPUT (cont.)

Trial No. 3	Starting Value	Final Value	Final Stiffness Matrix and Damping Coefficient
γ_1	0.95	1.107	$\begin{bmatrix} 27.39 & -38.99 & 13.55 \\ -38.99 & 78.16 & -50.80 \\ 13.55 & -50.80 & 70.75 \end{bmatrix}$
γ_2	1.00	1.043	
γ_3	1.25	0.741	$a_0 = 0.1624$
γ_4	0.95	1.019	$a_1 = 0.0001$
γ_5	1.00	0.653	$\lambda_1 = 0.57\%$
γ_6	5.00*	--	$\lambda_2 = 0.44\%$
γ_7	0.65	0.694	$\lambda_3 = 0.83\%$
γ_8	0.39	0.327	
Error	6020	918	
Slope	-7230	-0.072	

*fixed

readings at both ends of the members, the moments at the ends of all members could be computed. Thus the displacements in the error function are replaced by moments at the ends of the girders and the procedure is restarted again with eight parameters. Unfortunately, there was no convergence in this case either. The problem turned out to be almost identical to the one previously described: fixing one parameter (usually the top girder stiffness) to preassigned value yields perfect convergence. By assigning different values to this parameter, again a family of structures which are far from each other (as far as stiffness characteristics are concerned) can be defined such that almost perfect agreement exists between the predicted versus measured accelerations and moments and also between the stiffness matrices obtained from different members of the family. But the problem of uniquely identifying the given frame still remained open. A thorough investigation of the obtained results reveals the fact that from one member of the family of structures to another the moments display very minor changes while the rotations of the joints in each case are different. So we thought it worthwhile to give one more try by replacing the moments at the ends of the girders in the error function by the rotations at the joints. Those rotations are not measured independently. They are obtained from the large amount of data available by assuming the base completely fixed and summing up the $1/\rho$ area where ρ is the radius of curvature from bottom to top. Thus

$$\bar{\omega}_x = \bar{\omega}_0 + \int_0^x \frac{1}{\rho}\, dx = \bar{\omega}_0 + \int_0^x \frac{\varepsilon(x)}{c}\, dx \qquad (27)$$

where $\varepsilon(x)$ is the maximum strain at any section along the column and is assumed to have a linear variation along the member and c is the distance from the neutral axis to the extreme fiber.

In this method of evaluating the rotations at the joints, the stiffness characteristics of the members do not come into the picture and thus the rotations can be considered to be independent measurements. The straight line extrapolation of the strain readings at two sections on the column to the centerlines of the limiting girders (or for the first floor, extrapolation to the centerline of the first floor girder and the centerline of the fixed base) is where a certain amount of error is necessarily built in, but is assumed to be rather minor.

The error function is now reconstructed with $\{y_j(t)\}_m$ such that $m = 1$ identifies accelerations and $m = 2$ identifies the rotations at the joints. It was thought proper to multiply all rotations by E which is taken to be 29600 K/in^2 so that $\{y_j(t)\}_1$ and $\{y_j(t)\}_2$ although of different units would be of the same order of magnitude.

The optimization program is tried again with all eight parameters free to float. The program converged in eight cycles and the error is reduced from an initial value of $\sim$ 12700 to a final value $\sim$ 9000 for $T = 12$ sec. We concluded from this that the accelerations and rotations are the necessary data to identify the system uniquely and the modifications introduced from then on always keep the error function constructed from accelerations and rotations records. Numerous checks are performed on response quantities like moments and displacements even though they are not included in the error function to see whether a good match on accelerations and rotations would be at the expense of other quantities such as displacements, moments, etc. The results were all very encouraging since the agreement on predicted versus measured displacements and moments (with the predicted response values obtained using the parameters previously defined by accelerations and rotations) is also perfect. With all of

those checks performed, we are now confident about the ability of the model to predict the response very accurately and also as to the type of information required that will impose a rich enough constraint on the method so as to identify the structure uniquely.

Figures 15, 16 and 17 show examples of the type of correlation obtained on all predicted quantities for the EC 400-II base motion when the $\bar{\gamma}$ coefficients are all taken to be equal to 1 and also when they are taken to be equal to the values given the following optimization.

In Tables 14 and 15 a summary of the convergence of this last run is given and a comparison of initial versus final values of the parameters is made.

Similar runs are performed with the EC 100-I base motion. The initial error which is extremely large, in this case of the order of 514000 for T = 12 sec., is reduced to approximately 22000. The larger errors in this case compared to the previous ones can be related to the weak panel zones, the distortions of which are not accounted for in the model. Agreement is, however, very good.

As observed from Table 15, the values of the final parameters vary considerably in using four or six seconds of data and some of the parameters such as the one for the top girder are far from realistic. The optimization technique although satisfactory from the point of view of curve fitting is rather unstable when we try to assign physical significance to the optimized values of the $\bar{\gamma}$ parameters. An explanation could be as follows.

In setting up the complete stiffness matrix, terms of the type k/L and k/L^2 are dealt with, where k is the stiffness of a typical member and L its corresponding length. Since during the optimization process

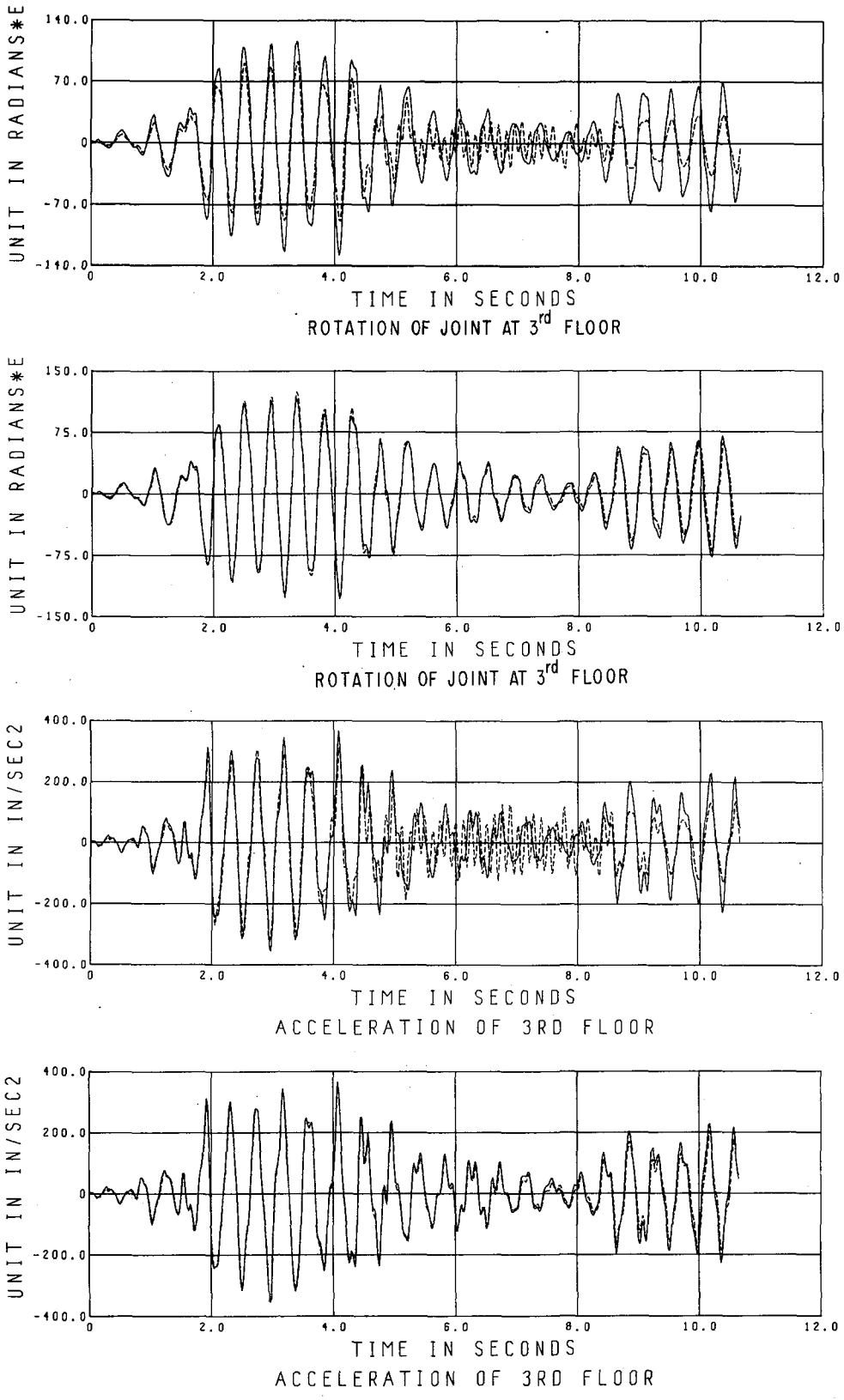

FIGURE 15 EC 400-II COMPARISON OF MEASURED AND COMPUTED RESPONSE TIME HISTORIES BEFORE AND AFTER OPTIMIZATION OF PARAMETERS (SECOND EIGHT PARAMETER MODEL)

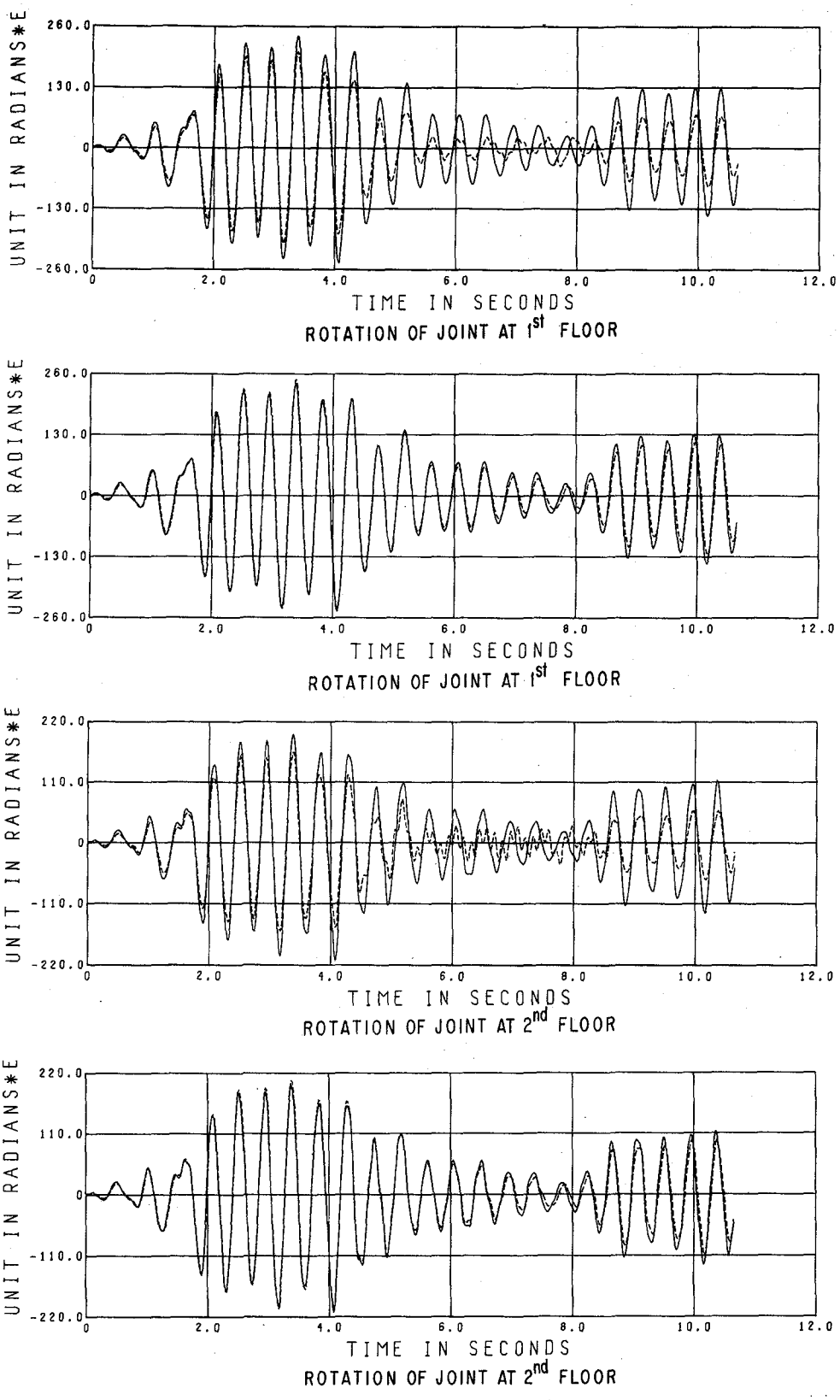

FIGURE 16 EC 400-II COMPARISON OF MEASURED AND COMPUTED RESPONSE TIME HISTORIES BEFORE AND AFTER OPTIMIZATION OF PARAMETERS (SECOND EIGHT PARAMETER MODEL)

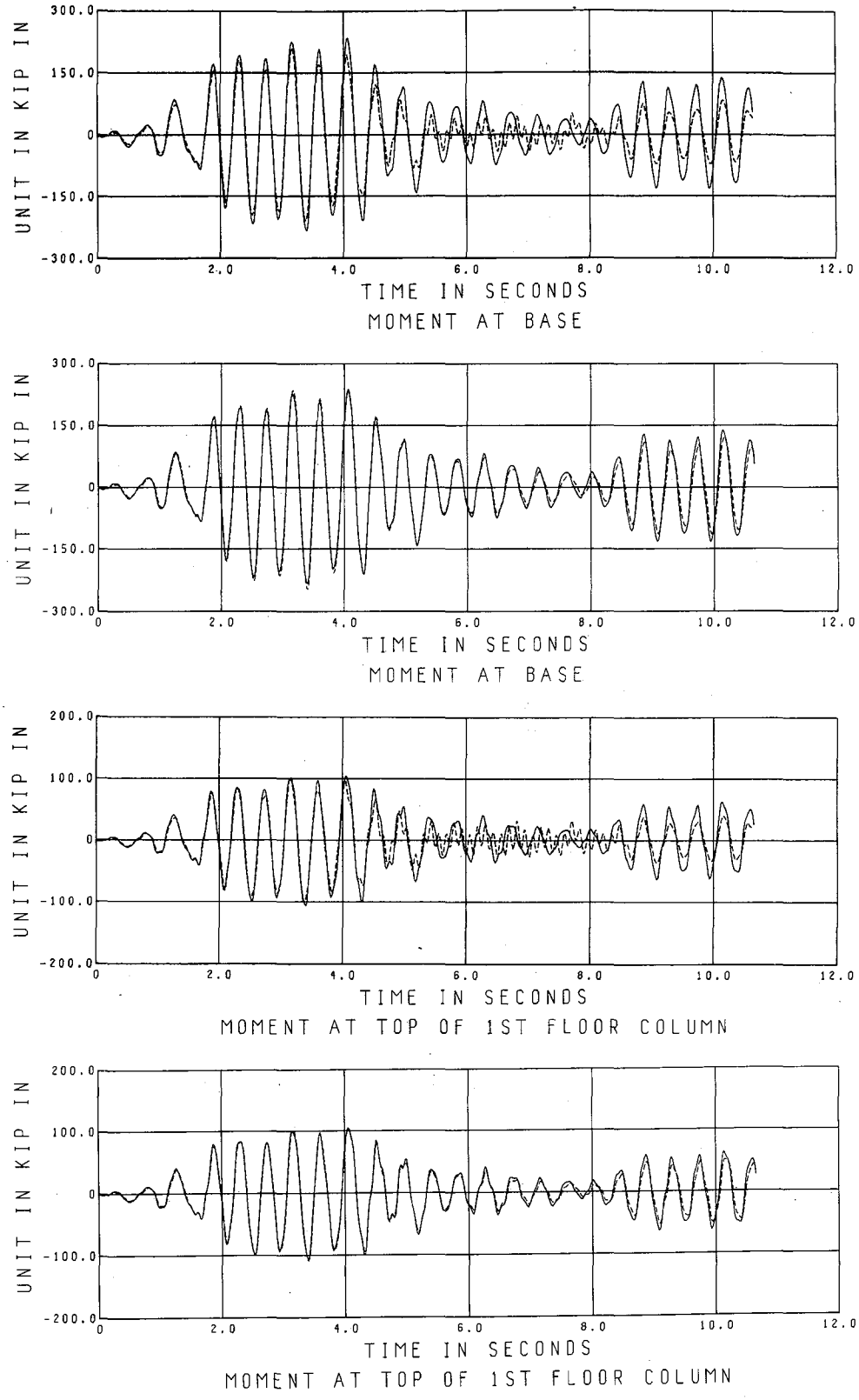

FIGURE 17 EC 400-II COMPARISON OF MEASURED AND COMPUTED RESPONSE TIME HISTORIES BEFORE AND AFTER OPTIMIZATION OF PARAMETERS (SECOND EIGHT PARAMETER MODEL)

TABLE 14 EC 400-II RESULTS OF A TYPICAL RUN WITH ERROR FUNCTION CONSTRUCTED FROM ACCELERATION AND ROTATION RECORDS (T = 4 sec.)

	Initial $\bar{\gamma}$ Value	Final $\bar{\gamma}$ Value	Final Stiffness Matrix and Damping Coefficients
γ_1	0.95	1.012	$\begin{bmatrix} 26.88 & -37.43 & 12.33 \\ -37.43 & 77.16 & -51.55 \\ 12.33 & -51.55 & 71.34 \end{bmatrix}$
γ_2	1.00	1.036	
γ_3	1.25	0.979	$a_o = 0.1813$
γ_4	0.95	0.855	$a_1 = 0.00012$
γ_5	1.00	1.054	$\lambda_1 = 0.67\%$
γ_6	1.25	1.621	$\lambda_2 = 0.40\%$
γ_7	0.650	0.775	$\lambda_3 = 0.57\%$
γ_8	0.396	0.293	
Error	4980	1500	
Slope	-6877	-0.0016	

TABLE 15 EC 400-II RESULTS OF A TYPICAL RUN WITH ERROR FUNCTION CONSTRUCTED FROM ACCELERATION AND ROTATION RECORDS (T = 6 sec.)

	Initial $\bar{\gamma}$ Value	Final $\bar{\gamma}$ Value	Final Stiffness Matrix and Damping Coefficients
γ_1	1.012	1.016	$\begin{bmatrix} 28.27 & -39.28 & 12.91 \\ -39.28 & 78.59 & -50.84 \\ 12.91 & -50.84 & 69.50 \end{bmatrix}$
γ_2	1.036	0.944	
γ_3	0.979	1.142	$a_o = 0.1472$
γ_4	0.855	0.869	$a_1 = 0.00016$
γ_5	1.054	0.999	$\lambda_1 = 0.61\%$
γ_6	1.621	1.614	$\lambda_2 = 0.57\%$
γ_7	0.775	0.629	$\lambda_3 = 0.99\%$
γ_8	0.293	0.554	
Error	5433	3838	
Slope	-3107	-0.0853	

only the k values of the members are modified, this automatically implies that L is kept constant (as a center-to-center distance) and as $k = 4EI/L$ and since E and L are constants the only variable is the moment of inertia I. In other words, we have so far been looking for a mathematical model which has the same geometry of the real frame, but the cross sectional properties modified to match the response of the real frame. It therefore appears that the moments of inertia of the members in the model have to take appreciably different values from those of the real structure to match the response properly.

We therefore concluded that the present model is not particularly realistic from a physical standpoint and is of little physical significance since it can always be argued that moments of inertia are accurately known and can be obtained from tables, while there are other quantities in k that are more questionable and require further investigation.

At this point in the research a major step has been taken in that we now have an eight parameter model which identifies uniquely the stiffness of each member. What we still do not have is an acceptable theory about which contribution to the stiffness (E, I or L) accounts for the significant change in k during optimization. The next section is devoted to this study.

V.2 The Eight Parameter Model with a Third Set of Parameters

Keeping the same physical model, we are now looking for a different set of parameters $\overline{\delta}_i$ that will replace the $\overline{\gamma}_i$ parameters previously used and that will give insight into which contribution to the stiffness changes during optimization.

The effective length of each member is the quantity that we choose

as the candidate as it is well known that within an analysis whether center-to-center measurements are used to define effective lengths or whether clear height distances are considered there is always an element of uncertainty involved. Therefore, if the effective length of each member is modified by a coefficient δ_i and the optimization process is carried out on those newly defined parameters it may very well be that some reasonable values may be obtained.

With this argument in mind, the eight parameter model is modified so as to deal with effective length factors of the members as free parameters. Since in the total stiffness matrix the girders only appear with terms of the type 4EI/L the $\bar{\gamma}_i$ and $1/\bar{\delta}_i$ coefficients for the girders have basically the same meaning. For the columns, however, they are essentially different. The damping coefficients do not require any modifications and still have the same meaning. We are now choosing a model which has identical cross sectional properties as the real frame, but geometrical dimensions modified by the optimization process in an effort to match the measured response quantities. Figure 18 shows the chosen model.

Replacing the $\bar{\gamma}_i$ parameters by the newly defined $\bar{\delta}_i$ parameters in the computer program, using data on the EC 400-II, and taking as the initial guess

$$\bar{\delta}_i = < 1 \quad 1 \quad 1 \quad 1 \quad 1 \quad 1 \quad 1 \quad 1 >$$

as before, another run was performed. Needless to say, convergence was as good and as rapid as before. The error with this initial guess for T = 12 sec. was ~ 127000, which was reduced to ~ 9000 for the same period of time when the optimized parameters on 6 sec. of data were used to predict the response quantities. This reduction in error is the same as for the γ parameters and this is to be expected since there is no change in the number of

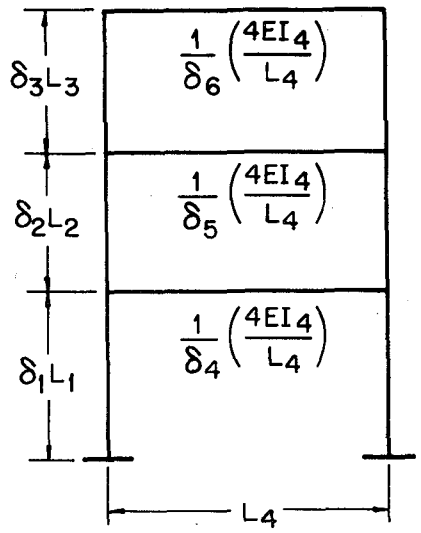

FIGURE 18 THE EIGHT PARAMETER MODEL WITH THE THIRD SET OF PARAMETERS $\overline{\delta}_i$

parameters; they are simply used in a different way. But the important difference between the two sets of coefficients is that the ones obtained for the effective lengths of the structural members are much more sensible than those obtained for the element stiffnesses of the same members. Tables 16 and 17 summarize the results of this final run. Note that the parameters for the effective lengths of the columns are all smaller but not too far from 1.0. The coefficients for the girders while all above 1.0 seem to be very close to one another, but the deviation from 1.0 although not as much as before is still in the range of 25%.

Figure 19 shows some additional correlation between predicted and measured response quantities at different locations.

TABLE 16 EC 400-II RESULTS OF A TYPICAL RUN
EFFECTIVE LENGTHS MODIFIED (T = 4 sec.)

	Initial $\overline{\delta}$ Value	Final $\overline{\delta}$ Value	Final Stiffness Matrix and Damping Coefficients
δ_1	0.96	0.954	$\begin{bmatrix} 24.33 & -37.40 & 15.32 \\ -37.40 & 82.49 & -59.01 \\ 15.32 & -59.01 & 78.19 \end{bmatrix}$
δ_2	0.93	0.961	
δ_3	0.91	0.904	$a_o = 0.308$
δ_4	1.25	1.258	$a_1 = 0.00015$
δ_5	1.25	1.269	$\lambda_1 = 1.14\%$
δ_6	1.25	1.283	$\lambda_2 = 0.69\%$
δ_7	0.538	0.680	$\lambda_3 = 0.99\%$
δ_8	0.669	0.318	
Error	12084	1228	
Slope	-21368	-0.064	

TABLE 17 EC 400-II RESULTS OF A TYPICAL RUN
EFFECTIVE LENGTHS MODIFIED (T = 6 sec.)

	Initial $\bar{\delta}$ Value	Final $\bar{\delta}$ Value	Final Stiffness Matrix and Damping Coefficients
δ_1	0.954	0.956	$\begin{bmatrix} 27.14 & -39.67 & 14.77 \\ -39.67 & 82.41 & -56.05 \\ 14.77 & -56.05 & 76.99 \end{bmatrix}$
δ_2	0.961	0.971	
δ_3	0.904	0.891	$a_o = 0.134$
δ_4	1.258	1.242	$a_1 = 0.00018$
δ_5	1.269	1.274	$\lambda_1 = 0.58\%$
δ_6	1.283	1.322	$\lambda_2 = 0.60\%$
δ_7	0.680	0.574	$\lambda_3 = 1.08\%$
δ_8	0.318	0.612	
Error	5153	3350	
Slope	-3572	-0.582	

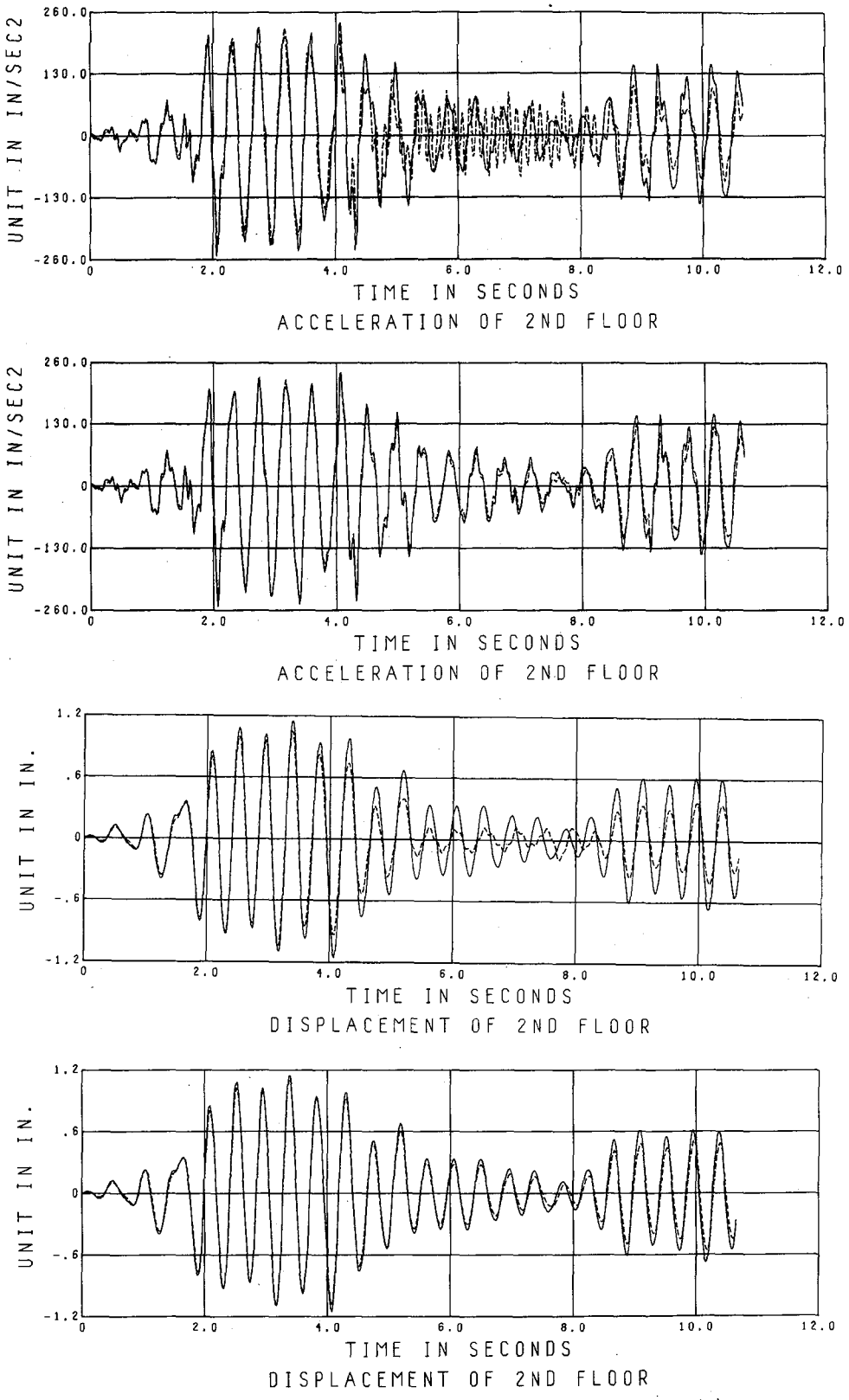

FIGURE 19 EC 400-II COMPARISON OF MEASURED AND COMPUTED RESPONSE TIME HISTORIES BEFORE AND AFTER OPTIMIZATION OF PARAMETERS (THIRD EIGHT PARAMETER MODEL)

Study of the effective length factors shows that when their difference from one is found and accounted for in the model the improvement in the model for predicting earthquake response is significant. If the continuity between columns and girders were perfect the factors would be 1.0, so we conclude that our optimized factors reflect lack of perfect continuity through the panels and that the larger the deformation of the panels, the more different from 1.0 would be the factors.

Fortunately, from the Clough and Tang experiments we have data to confirm these conclusions. We have responses for experimental Phase I with simple plates as panels, and responses from Phase II for the same frame except that the panels have been stiffened.

We have at this point the effective length factors for Phase II (EC 400-II), so we decided to derive the same set of factors from the data from Phase I (EC 100-I). If our conclusions were correct, the factors for this phase should differ more from 1.0 than those already obtained. Also, the total error should be greater.

For Phase I the error involved using $\overline{\delta}_i = < I >$, where $< I >$ is the identity vector, is much larger than before. The optimization process worked just as well as before and the parameters adjusted themselves to values that are summarized in Table 18. The 12 sec. period error was reduced during optimization from ~ 514000 to ~ 22000.

Comparison of the effective length factors in Table 18 with those in Tables 16 and 17 for Phase II confirms our conjecture. The factors for Phase I are farther from one than those for Phase II. We feel that confirmation of our conclusions gives us considerable insight into the engineering analysis of such a frame.

Figures 20 and 21 show correlation of the measured versus predicted

TABLE 18 EC 100-I RESULTS OF A TYPICAL RUN
EFFECTIVE LENGTHS MODIFIED (T = 6 sec.)

	Initial $\overline{\delta}$ Value	Final $\overline{\delta}$ Value	Final Stiffness Matrix and Damping Coefficients
δ_1	0.956	0.978	$\begin{bmatrix} 24.33 & -37.40 & 15.32 \\ -37.40 & 82.49 & -59.01 \\ 15.32 & -59.01 & 78.19 \end{bmatrix}$
δ_2	0.971	0.932	
δ_3	0.891	0.898	$a_o = 0.308$
δ_4	1.242	1.400	$a_1 = 0.00015$
δ_5	1.274	1.412	$\lambda_1 = 1.14\%$
δ_6	1.322	1.465	$\lambda_2 = 0.69\%$
δ_7	0.574	1.318	$\lambda_3 = 0.99\%$
δ_8	0.612	0.508	
Error	18842	13258	
Slope	-10907	-0.897	

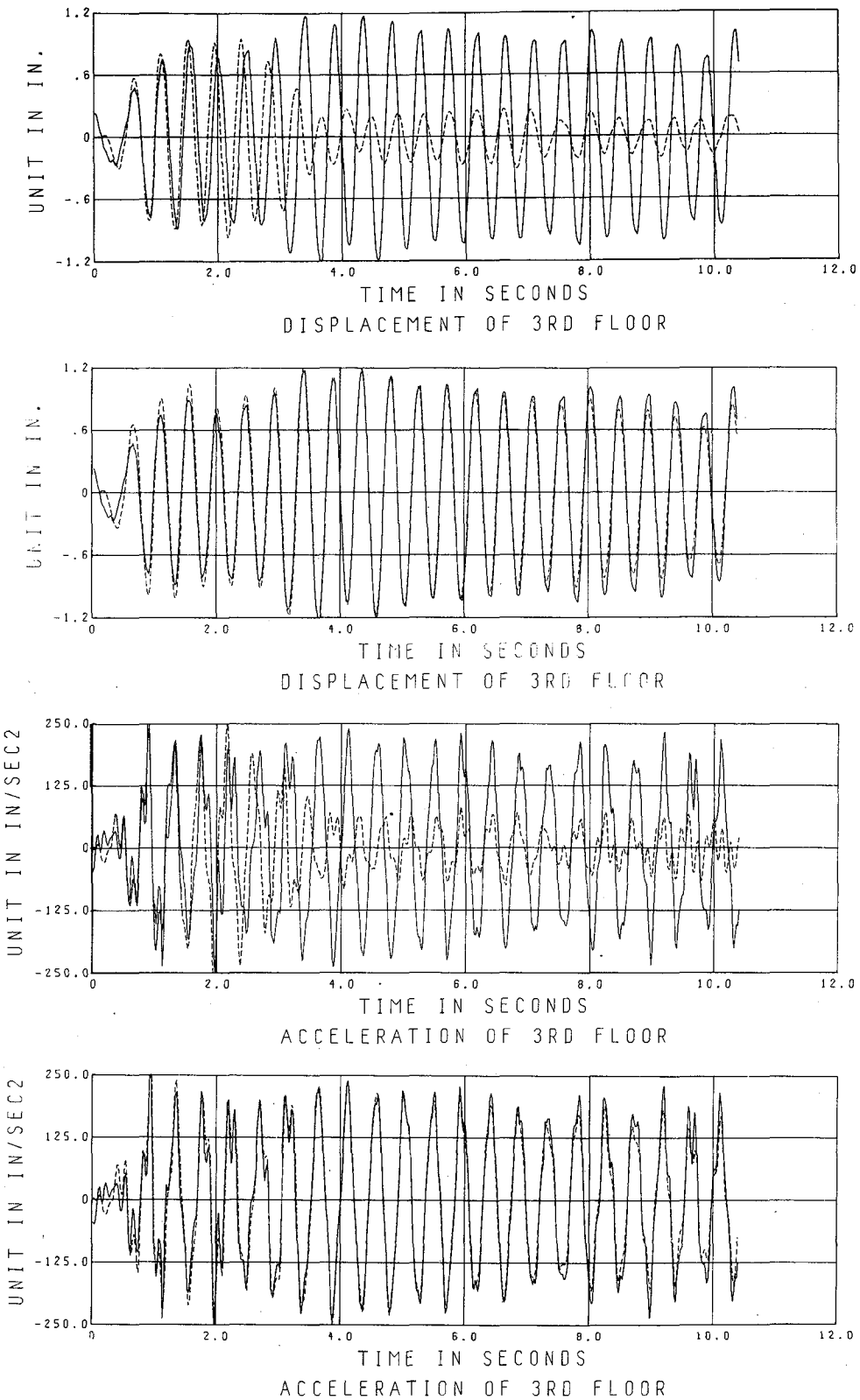

FIGURE 20 EC 100-I COMPARISON OF MEASURED AND COMPUTED RESPONSE TIME HISTORIES BEFORE AND AFTER OPTIMIZATION OF PARAMETERS (THIRD EIGHT PARAMETER MODEL)

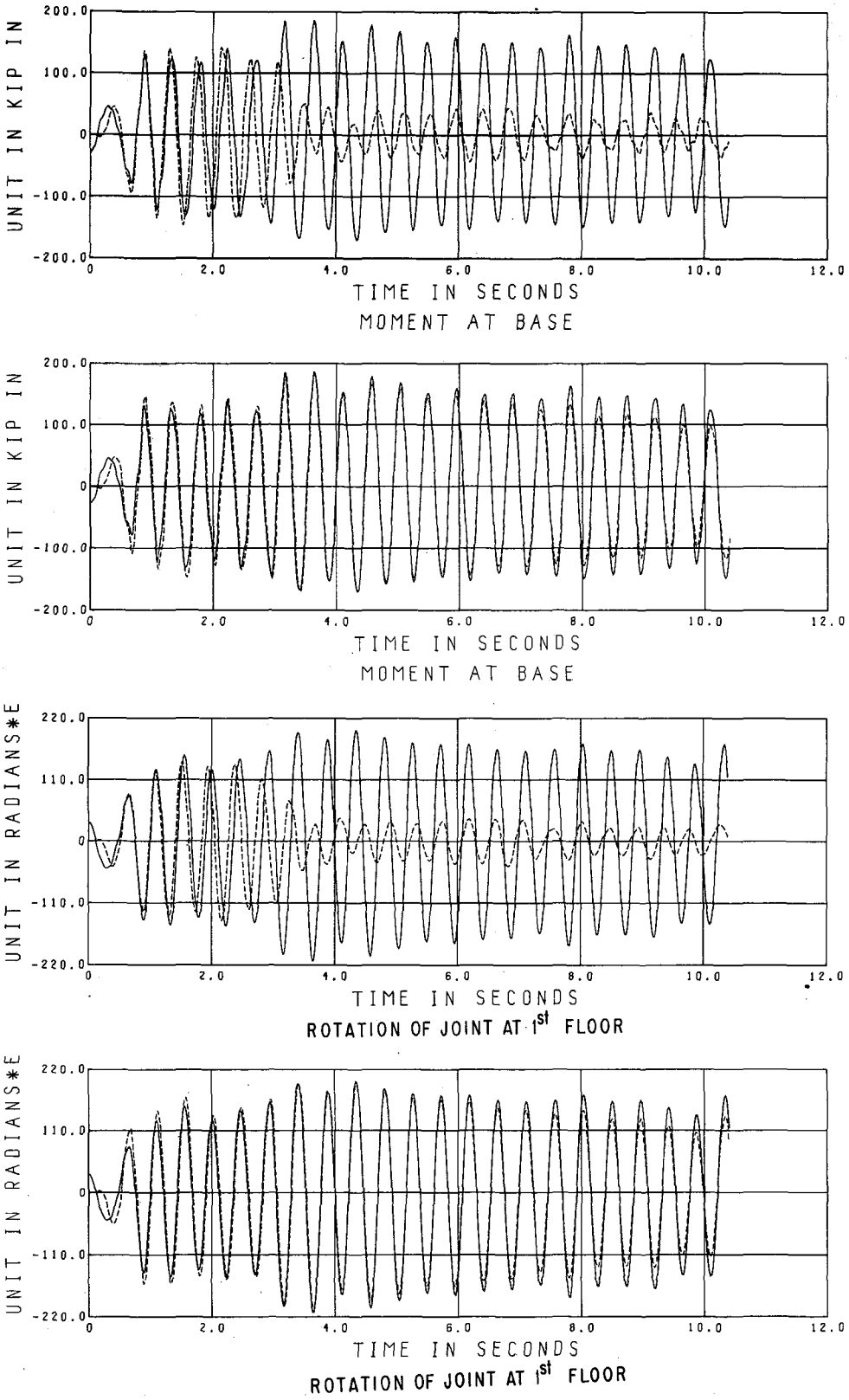

FIGURE 21 EC 100-I COMPARISON OF MEASURED AND COMPUTED RESPONSE TIME HISTORIES BEFORE AND AFTER OPTIMIZATION OF PARAMETERS (THIRD EIGHT PARAMETER MODEL)

response quantities with initial and final values of the parameters for EC 100-I.

One aspect of the model still bothered us. The effective length factors for the columns differ from 1.0 (for Phase II) from 4% to 9% while those of the girders differ from 24% to 32%. It appeared that an important degree of freedom affecting mainly the girders has not been accounted for in the model. The girders seem to behave more flexibly than they probably actually do to account for the missing degree of freedom. In our analysis thus far we have assumed that the shaking table has a purely translational motion. We now speculate that if there is a slight pitching motion of the table it would indeed affect the girders more than the columns and if this additional degree of freedom were accounted for, the model would be further improved. We were very much influenced in this conclusion by the work of Clough and Tang. They found that when the pitching of the table was accounted for, their model improved significantly.

Further study showed that this pitching of the table could be accounted for with the addition of only one parameter. We conclude our construction of mathematical models in the next chapter in which we present a nine parameter model.

CHAPTER VI THE NINE PARAMETER MODEL

In an effort to explain the rather large deviation from 1.0 of the coefficients for the effective lengths of the girders, an additional degree of freedom is introduced to account for possible pitching motion of the shaking table. The model is modified to include the additional degree of freedom shown in Fig. 22.

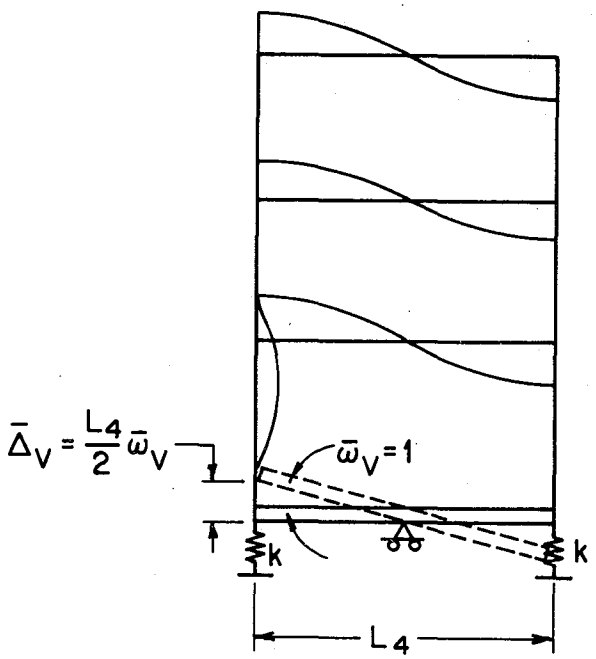

FIGURE 22 ADDITIONAL DEGREE OF FREEDOM: PITCHING MOTION OF THE SHAKING TABLE

The shaking table is considered to be infinitely rigid, immovable at its midpoint and supported on two symmetrical linear springs, one at each end. The complete stiffness matrix which is now 7 x 7 can still be reduced to a 3 x 3 matrix by condensing the 7 x 7 matrix as before and taking into account that $\overline{P}_V = -k\,\overline{\Delta}_V$ where $\overline{P}_V$ is the force in the spring and k is the stiffness of the spring in k/in (see Appendix A).

Since the eight parameter model is a special case of the present model with $k = \infty$, initially the same eight parameter model is used with a fixed value for k. Only subroutine TWO required some modification in setting up the [K] matrix; the rest remained unchanged. To get a feel for a reasonable value of k, a number of runs were performed, in each case keeping k constant, but reducing it gradually. For large values of k on the order of 500 k/in, the coefficients in the eight parameter model were affected little. As k is reduced to the range of 150 k/in its effect is felt in the girders and the coefficients related to the girders start being reduced significantly. Thus, instead of trying different fixed values for k, we now introduce it as a ninth parameter and leave it free to be adjusted by the optimization process as the other eight parameters are.

Thus the model is now increased to nine free parameters and k is chosen to be of the form

$$k = \delta_9 \times 100 \text{ k/in}$$

with δ_9 taken as 1.0 for the initial guess. The introduction of this ninth parameter, besides contributing to the cost of the computer time required (one cycle with an average of four iterations for the determination of a proper step size being in the range of 25 seconds), did in fact contribute to the further reduction of the error. But this reduction was not highly

significant since the introduction of this new parameter reduced the error for the period of time T = 12 sec. down to ~ 8500 as compared to the eight parameter model in which the error for the same amount of time is ~ 9000 . This is an indication that the eight parameter model is almost as effective as any other with more parameters so far as reduction of the total error is concerned. Introduction of additional degrees of freedom would probably not contribute significantly to the reduction of the error. The influence of this last parameter is on the values of the other eight. The new parameters are displayed in Table 19 for Phase II data and Table 20 for Phase I.

The parameters for all of the members are affected by the new degree of freedom, but the changes in the girder parameters are more dramatic. We note that all coefficients for the girders are reduced and brought much closer to 1.0. All effective length parameters for the girders now deviate from 1.0 on the order of 10 to 12% for EC 400-II.

Since the effective length parameters are now significantly changed, again we feel it is worthwhile to check on nodal displacements and moments using this final set of parameters. These response quantities are not included in the error function. The agreement again is extremely good. Figures 23 and 24 provide the evidence.

With the establishment of the parameters, the construction of the nine parameter model is complete. It also means that this study of linear models is complete. We are convinced that the introduction of a model of higher order would improve this model little and would not add to our understanding of the physical behavior of the structure.

TABLE 19 EC 400-II COMPARISON OF PARAMETERS FROM EIGHT AND NINE PARAMETER MODELS (T = 6 sec.)

	Final Parameter Values 8 Parameter Model	Final Parameter Values 9 Parameter Model
δ_1	0.956	0.953
δ_2	0.971	0.919
δ_3	0.891	0.955
δ_4	1.242	1.126
δ_5	1.274	1.130
δ_6	1.322	1.056
δ_7	0.574	0.629
δ_8	0.612	0.568
δ_9	∞	1.416

TABLE 20 EC 100-I COMPARISON OF PARAMETERS FROM EIGHT AND NINE PARAMETER MODELS (T = 6 sec.)

	Final Parameter Values 8 Parameter Model	Final Parameter Values 9 Parameter Model
δ_1	0.978	0.945
δ_2	0.932	0.935
δ_3	0.898	0.955
δ_4	1.400	1.230
δ_5	1.412	1.151
δ_6	1.465	1.128
δ_7	1.318	1.235
δ_8	0.508	0.705
δ_9	∞	1.845

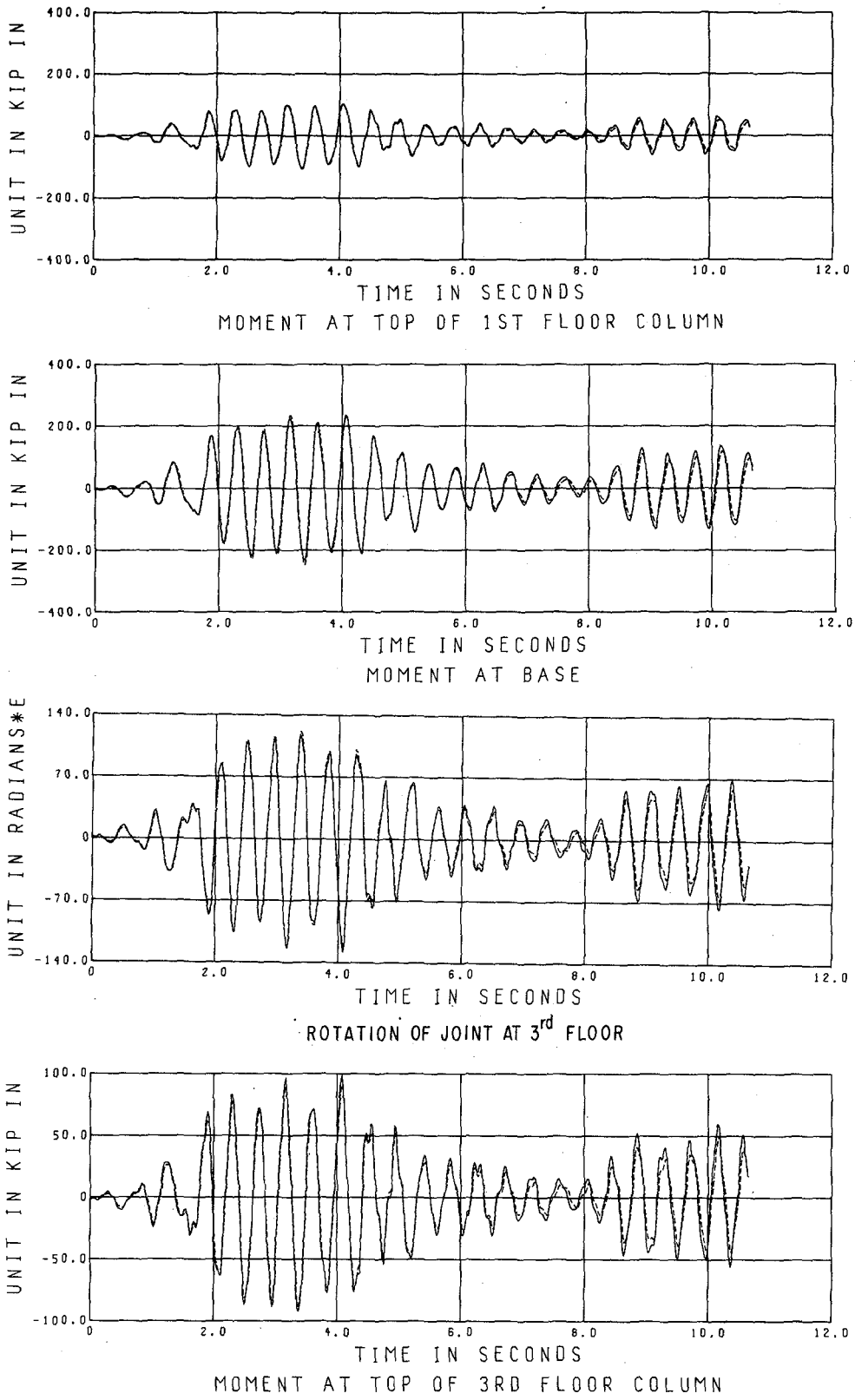

FIGURE 23 EC 400-II COMPARISON OF MEASURED AND COMPUTED RESPONSE TIME HISTORIES (NINE PARAMETER MODEL)

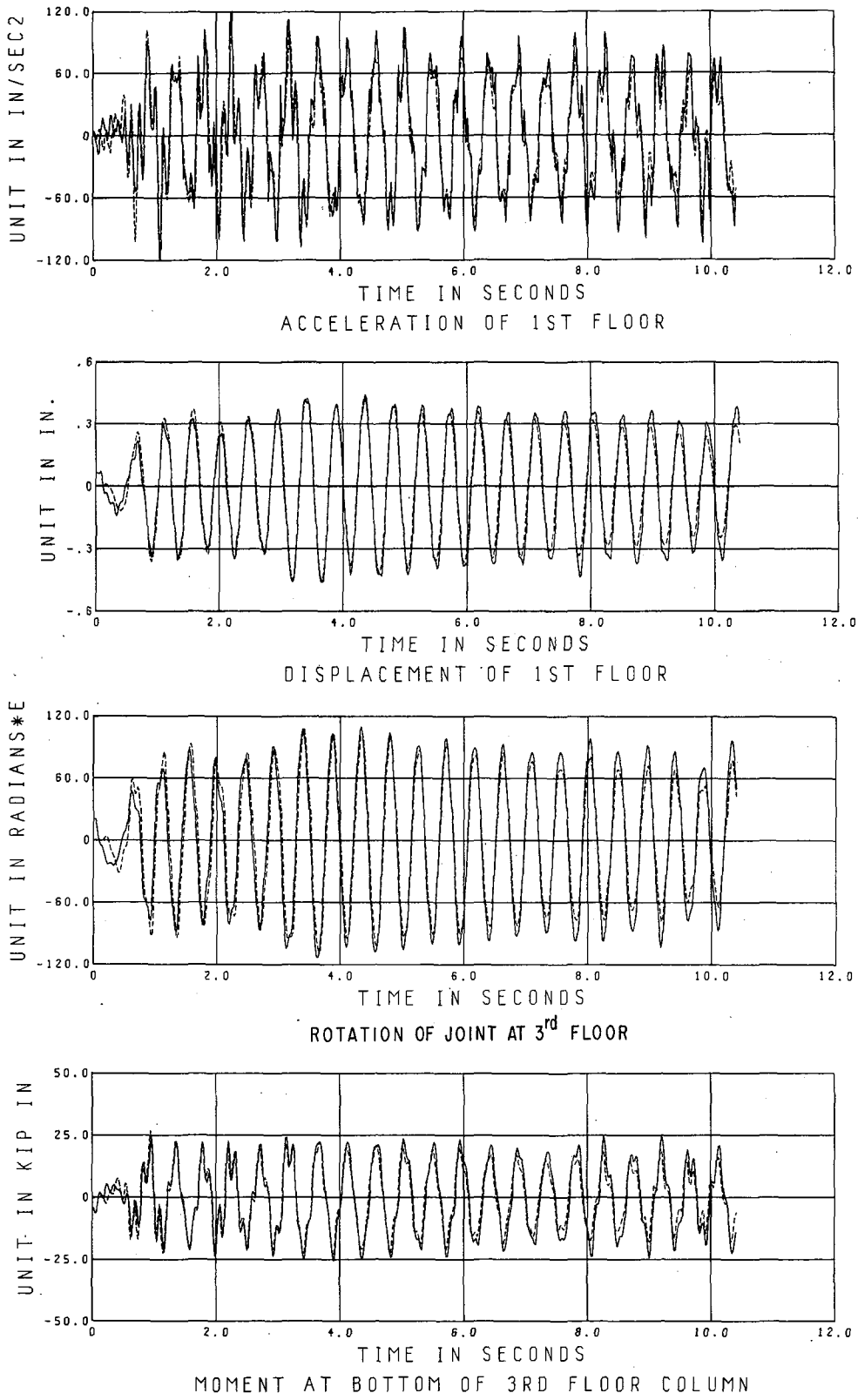

FIGURE 24 EC 100-I COMPARISON OF MEASURED AND COMPUTED RESPONSE TIME HISTORIES (NINE PARAMETER MODEL)

CHAPTER VII CONCLUSIONS

Three models in increasing order of complexity have been constructed to predict the dynamic response of a three story steel frame which was constructed and tested at the Earthquake Engineering Research Center of the University of California, Berkeley. The frame had been subjected to base motion excitations such that the response remained within the linear range.

The five parameter model gives a modest fit for floor accelerations and displacements. The model is, however, inadequate for frames whose lateral displacement involves rotations of the joints.

Three eight parameter models are constructed, the first of which is little improvement on the five parameter model, but the second and third account for joint rotations. The third eight parameter model, similar to the models used in practice, yields excellent results when the parameters in the model are optimized by a modified Gauss-Newton algorithm.

The nine parameter model improves slightly on the fit between measured and predicted local and global response quantities, but is useful in throwing some light on the physical aspects of the model.

The eight parameter model contains six coefficients related to the stiffness characteristics of the system. Those parameters were originally chosen to be the elements of the symmetric 3 x 3 stiffness matrix. This approach yielded extremely good results for displacements and accelerations,

but offered no way of identifying other response quantities such as moments and rotations.

Next, the stiffness characteristics of each member are considered separately as the parameters of the system. This modification proved to be very fruitful in precisely determining the set of data required to identify the system uniquely and in providing means of matching global as well as local response quantities. It is shown that accelerations and displacements are not independent response quantities, within the linear range. Also, it is shown that displacements (or accelerations) and moments are not a sufficiently independent set of constraints to identify the system uniquely. The set of measurements that are required to construct the error function properly are shown to be acceleration (or displacement) and rotation time histories of the nodal points. With this particular type of information used in forming the error function, the stiffness characteristics of each member could be uniquely determined.

Within the same model, the parameters were varied for this third model once to identify the effective lengths of each member. We assume E and I for each member to be constant and well known. The same set of response quantities within the error function was sufficient to obtain reasonable values for the effective lengths of the members to give a perfect match of measured versus predicted response quantities.

In the final eight parameter model we have used as stiffness parameters the effective length factors for each column and girder. During optimization, these factors change from 1.0 to factors close to but different from 1.0. The model with the optimized parameters predicts responses much closer to the experimental response than the model in which the stiffnesses are based on the physical lengths. This leads us to the

conclusion that perfect continuity between columns and girders cannot be assumed and that distortion of the panels connecting these members must be accounted for.

This conclusion is supported by further study of our final eight parameter model. For the frame identified as Phase I, the panels were unreinforced, whereas for Phase II the frame was the same except that the panels were stiffened. Using the response for these two phases the effective length factors were found and compared. Those for Phase II were different than, but closer to, 1.0 than those for Phase I.

In all of the eight parameter models, damping is assumed of the Rayleigh type, i.e. a damping matrix proportional to the mass and stiffness matrices. This seems to give a very reasonable idea as to the amount of viscous damping present in the steel frame, especially for the first two modal damping ratios, but the third modal damping ratio shows variations of a slightly larger order of magnitude from test to test.

The parameters entering the analysis were optimized using four to six seconds of data. With those optimized coefficients the rest of the signal matched reasonably closely. Using more data to identify the parameters involved would certainly introduce additional improvements, but at the expense of higher computer cost and higher storage requirements in the computer. In setting up the approximate Hessian matrix, which is the key step in improving on the parameters, the first derivatives of all response quantities at all time steps and at all floor levels need to be present in the memory simultaneously and this restricts the amount of data that can be used to optimize the parameters unless special measures are taken.

In the nine parameter model the pitching motion of the table is introduced as an additional degree of freedom. This additional parameter

brought slight improvements on the match between measured versus predicted response quantities. But its importance is mainly in yielding a set of effective lengths which were much more realistic than the ones predicted with the eight parameter model. The pitching motion of the table affected particularly the coefficients related to the girders, as expected.

In the final model, the nine parameter, the effective length factors are all sensible, that is they are realistically close to 1.0. The factors for the columns are all less than 1.0, and are greater than 1.0 for the girders. We will not at this time speculate on the reasons for this.

With the development of the nine parameter model, the study of models to predict the linear response of the three story frame ends. We feel that from models of higher order, we would learn little more of physical frame, or of system identification and little improvement could be made on the model's ability to predict responses.

The method for constructing a linear model, described in this report, can be extended to a model for predicting nonlinear behavior. This nonlinear model has been completed and will be described in a subsequent report.

REFERENCES

1. Hugh D. McNiven and Vernon C. Matzen, "A Mathematical Model to Predict the Inelastic Response of a Steel Frame: Formulation of the Model," Earthquake Engineering and Structural Dynamics, Vol. 6, 189-202 (1978).

2. R. W. Clough and D. T. Tang, "Earthquake Simulator Study of a Steel Frame Structure, Vol. I: Experimental Results," Report No. EERC 75-6, Earthquake Engineering Research Center, University of California, Berkeley (1975).

3. D. T. Tang, "Earthquake Simulator Study of a Steel Frame Structure, Vol. II: Analytical Results," Report No. EERC 75-36, Earthquake Engineering Research Center, University of California, Berkeley (1975).

4. N. Distefano and B. Peña-Pardo, "System Identification of Frames Under Seismic Loads," Journal of the Engineering Mechanics Division, ASCE, Vol. 102, No. EM2, Proc. Paper 12047, 313-330 (1976).

APPENDIX A

The degrees of freedom of the nine parameter model are shown in Fig. 25. The 7 x 7 stiffness matrix is obtained from Fig. 25 and is given in Table 21.

The condensation procedure can be summarized as follows. From Table 21 we can write:

$$\begin{Bmatrix} \{\bar{M}\} \\ \{\bar{P}\} \\ \bar{P}_V \end{Bmatrix} = \begin{bmatrix} [K_{11}] & [K_{12}] & \{K_{13}\} \\ [K_{21}] & [K_{22}] & \{K_{23}\} \\ < K_{31} > & < K_{32} > & K_{33} \end{bmatrix} \begin{Bmatrix} \{\bar{\omega}\} \\ \{\bar{\Delta}\} \\ \bar{\Delta}_V \end{Bmatrix} \tag{28}$$

Taking

$$\{\bar{M}\} = \{\bar{0}\}$$

and

$$\bar{P}_V = -k\,\bar{\Delta}_V$$

we have, from the last equation in (28),

$$\bar{P}_V = -k\,\bar{\Delta}_V = < K_{31} > \{\bar{\omega}\} + < K_{32} > \{\bar{\Delta}\} + K_{33}\,\bar{\Delta}_V$$

from which

$$\bar{\Delta}_V = -\frac{1}{k + K_{33}} \left[< K_{31} > \{\bar{\omega}\} + < K_{32} > \{\bar{\Delta}\} \right] \tag{29}$$

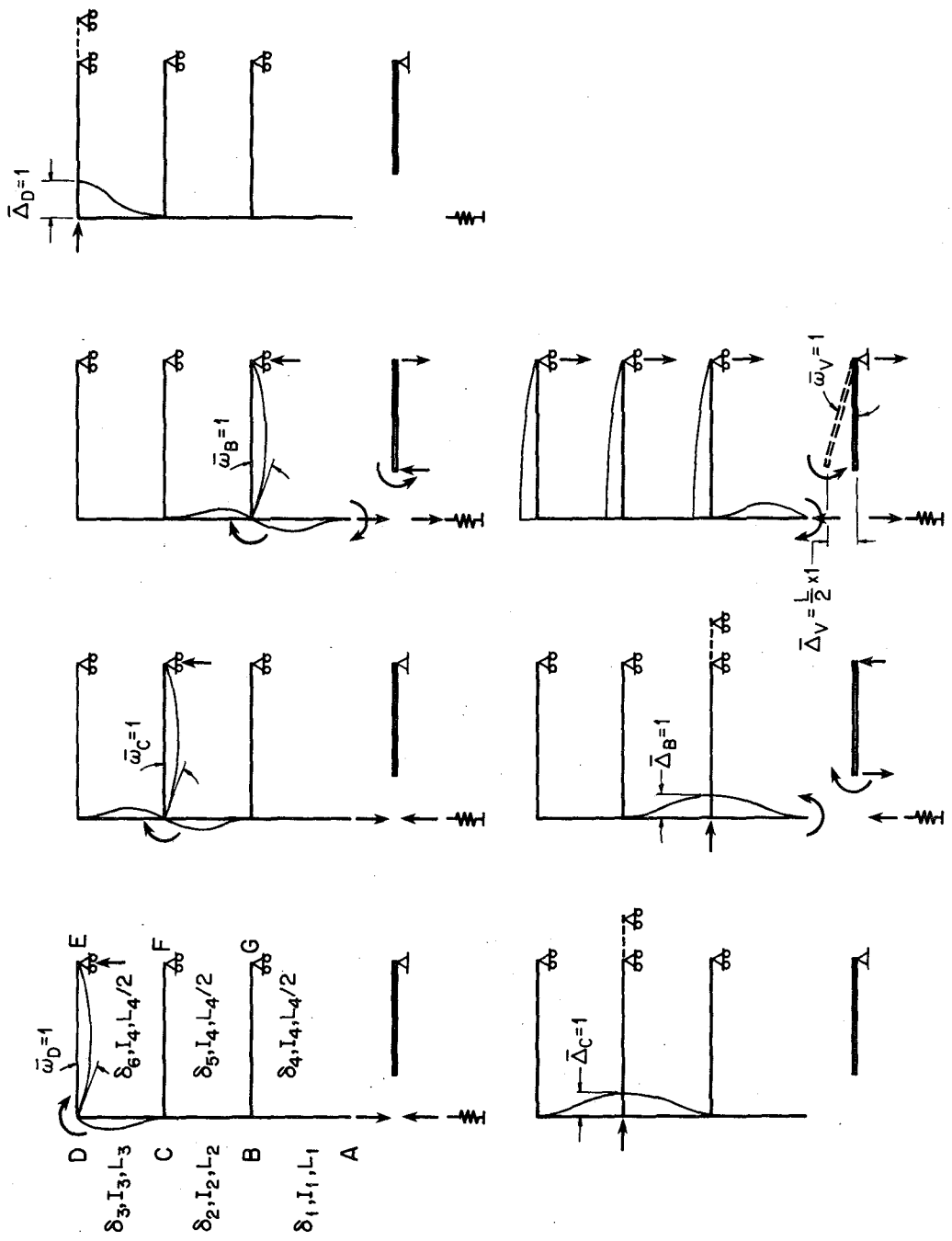

FIGURE 25 DEGREES OF FREEDOM IN THE NINE PARAMETER MODEL

$$
\begin{Bmatrix} \bar{M}_D \\ \bar{M}_C \\ \bar{M}_B \\ \bar{P}_D \\ \bar{P}_C \\ \bar{P}_B \\ \bar{P}_V \end{Bmatrix} =
\begin{bmatrix}
\frac{4EI_3}{\delta_3 L_3} + \frac{3}{2}\left(\frac{4EI_4}{\delta_6 L_4}\right) & \frac{2EI_3}{\delta_3 L_3} & 0 & -\frac{6EI_3}{(\delta_3 L_3)^2} & \frac{6EI_3}{(\delta_3 L_3)^2} & 0 & -\frac{1}{2}\frac{6EI_4}{(\delta_4 L_4/2)^2} \\
\frac{2EI_3}{\delta_3 L_3} & \frac{4EI_3}{\delta_3 L_3} + \frac{4EI_2}{\delta_2 L_2} + \frac{3}{2}\left(\frac{4EI_4}{\delta_5 L_4}\right) & \frac{2EI_2}{\delta_2 L_2} & -\frac{6EI_3}{(\delta_3 L_3)^2} & \frac{6EI_3}{(\delta_3 L_3)^2} - \frac{6EI_3}{(\delta_2 L_2)^2} & \frac{6EI_2}{(\delta_2 L_2)^2} & -\frac{1}{2}\frac{6EI_4}{(\delta_5 L_4/2)^2} \\
0 & \frac{2EI_2}{\delta_2 L_2} & \frac{4EI_2}{\delta_2 L_2} + \frac{4EI_1}{\delta_1 L_1} + \frac{3}{2}\left(\frac{4EI_4}{\delta_4 L_4}\right) & 0 & -\frac{6EI_2}{(\delta_2 L_2)^2} & \frac{6EI_2}{(\delta_2 L_2)^2} - \frac{6EI_1}{(\delta_1 L_1)^2} & -\frac{1}{2}\frac{6EI_4}{(\delta_6 L_4/2)^2} + \frac{2EI_1}{\delta_1 L_1} \times \left(\frac{1}{L_4/2}\right) \\
-\frac{6EI_3}{(\delta_3 L_3)^2} & -\frac{6EI_3}{(\delta_3 L_3)^2} & 0 & \frac{12EI_3}{(\delta_3 L_3)^3} & -\frac{12EI_3}{(\delta_3 L_3)^3} & 0 & 0 \\
\frac{6EI_3}{(\delta_3 L_3)^2} & \frac{6EI_3}{(\delta_3 L_3)^2} - \frac{6EI_2}{(\delta_2 L_2)^2} & -\frac{6EI_2}{(\delta_2 L_2)^2} & -\frac{12EI_3}{(\delta_3 L_3)^3} & \frac{12EI_3}{(\delta_3 L_3)^3} + \frac{12EI_2}{(\delta_2 L_2)^3} & -\frac{12EI_2}{(\delta_2 L_2)^3} & 0 \\
0 & \frac{6EI_2}{(\delta_2 L_2)^2} & \frac{6EI_2}{(\delta_2 L_2)^2} - \frac{6EI_1}{(\delta_1 L_1)^2} & 0 & -\frac{12EI_2}{(\delta_2 L_2)^3} & \frac{12EI_2}{(\delta_2 L_2)^3} + \frac{12EI_1}{(\delta_1 L_1)^3} & -\frac{6EI_1}{(\delta_1 L_1)^2} \times \left(\frac{1}{L_4/2}\right) \\
-\frac{3}{2}\left(\frac{4EI_4}{\delta_6 L_4}\right) \times \frac{1}{(\delta_6 L_4/2)} & -\frac{3}{2}\left(\frac{4EI_4}{\delta_5 L_4}\right) \times \frac{1}{(\delta_5 L_4/2)} & \left(\frac{2EI_1}{\delta_1 L_1}\right) \times \left(\frac{1}{L_4/2}\right) - \frac{3}{2}\left(\frac{4EI_4}{\delta_4 L_4}\right)\left(\frac{1}{\delta_4 L_4/2}\right) & 0 & 0 & -\frac{6EI_1}{(\delta_1 L_1)^2} \times \left(\frac{1}{L_4/2}\right) & \frac{1}{2} \times \frac{6EI_4}{(\delta_4 L_4/2)^3} + \frac{1}{2} \times \frac{6EI_4}{(\delta_5 L_4/2)^3} + \frac{1}{2} \times \frac{6EI_4}{(\delta_6 L_4/2)^3} + \frac{4EI_1}{\delta_1 L_1}\left(\frac{1}{L_4/2}\right)^2
\end{bmatrix}
\begin{Bmatrix} \bar{\omega}_D \\ \bar{\omega}_C \\ \bar{\omega}_B \\ \bar{\Delta}_D \\ \bar{\Delta}_C \\ \bar{\Delta}_B \\ \bar{\Delta}_V \end{Bmatrix}
$$

TABLE 21 7 x 7 STIFFNESS MATRIX FOR THE NINE PARAMETER MODEL

From the first equation in (28)

$$\{\bar{M}\} = \{\bar{0}\} = [K_{11}]\{\bar{\omega}\} + [K_{12}]\{\bar{\Delta}\} + \{K_{13}\}\Delta_V$$

By substituting from Eq. (29) for $\bar{\Delta}_V$ and isolating $\{\bar{\omega}\}$, we obtain

$$\{\bar{\omega}\} = -\left[[K_{11}] - \frac{\{K_{13}\}<K_{31}>}{k+K_{33}}\right]^{-1}\left[[K_{12}] - \frac{\{K_{13}\}<K_{32}>}{k+K_{33}}\right]\{\bar{\Delta}\} \quad (30)$$

Using the second equation in (28) and substituting for $\bar{\Delta}_V$ from Eq. (29) and for $\{\bar{\omega}\}$ from Eq. (30), we obtain

$$\{\bar{P}\} = [K_{21}]\{\bar{\omega}\} + [K_{22}]\{\bar{\Delta}\} + \{K_{23}\}\bar{\Delta}_4$$

or

$$\{\bar{P}\} = \left[-\left[[K_{21}] - \frac{\{K_{23}\}<K_{31}>}{k+K_{33}}\right]\left[[K_{11}] - \frac{\{K_{13}\}<K_{31}>}{k+K_{33}}\right]^{-1} \cdot \left[[K_{12}] - \frac{\{K_{13}\}<K_{32}>}{k+K_{33}}\right] + \left[[K_{22}] - \frac{\{K_{23}\}<K_{32}>}{k+K_{33}}\right]\right]\{\bar{\Delta}\} \quad (31)$$

from which

$$\{\bar{P}\} = [-[\tilde{K}_{21}][\tilde{K}_{11}]^{-1}[\tilde{K}_{12}] + [\tilde{K}_{22}]]\{\bar{\Delta}\} \quad (32)$$

or

$$\{\bar{P}\} = [K]\{\bar{\Delta}\} \quad (33)$$

For $k = \infty$, we have

$$[\tilde{K}_{21}] = [K_{21}] \quad ; \quad [\tilde{K}_{11}] = [K_{11}]$$

$$[\tilde{K}_{12}] = [K_{12}] \quad ; \quad [\tilde{K}_{22}] = [K_{22}]$$

The same equations hold for the eight parameter model.

Since Eq. (33) has been derived for half of the frame, from symmetry, the total lateral load on the entire frame can be obtained simply by using

$$\{\overline{P}_T\} = 2 \cdot [\tilde{K}]\{\overline{\Delta}\} \tag{34}$$

EARTHQUAKE ENGINEERING RESEARCH CENTER REPORTS

NOTE: Numbers in parenthesis are Accession Numbers assigned by the National Technical Information Service; these are followed by a price code. Copies of the reports may be ordered from the National Technical Information Service, 5285 Port Royal Road, Springfield, Virginia, 22161. Accession Numbers should be quoted on orders for reports (PB --- ---) and remittance must accompany each order. Reports without this information were not available at time of printing. Upon request, EERC will mail inquirers this information when it becomes available.

EERC 67-1 "Feasibility Study Large-Scale Earthquake Simulator Facility," by J. Penzien, J.G. Bouwkamp, R.W. Clough and D. Rea - 1967 (PB 187 905)A07

EERC 68-1 Unassigned

EERC 68-2 "Inelastic Behavior of Beam-to-Column Subassemblages Under Repeated Loading," by V.V. Bertero - 1968 (PB 184 888)A05

EERC 68-3 "A Graphical Method for Solving the Wave Reflection-Refraction Problem," by H.D. McNiven and Y. Mengi - 1968 (PB 187 943)A03

EERC 68-4 "Dynamic Properties of McKinley School Buildings," by D. Rea, J.G. Bouwkamp and R.W. Clough - 1968 (PB 187 902)A07

EERC 68-5 "Characteristics of Rock Motions During Earthquakes," by H.B. Seed, I.M. Idriss and F.W. Kiefer - 1968 (PB 188 338)A03

EERC 69-1 "Earthquake Engineering Research at Berkeley," - 1969 (PB 187 906)A11

EERC 69-2 "Nonlinear Seismic Response of Earth Structures," by M. Dibaj and J. Penzien - 1969 (PB 187 904)A08

EERC 69-3 "Probabilistic Study of the Behavior of Structures During Earthquakes," by R. Ruiz and J. Penzien - 1969 (PB 187 886)A06

EERC 69-4 "Numerical Solution of Boundary Value Problems in Structural Mechanics by Reduction to an Initial Value Formulation," by N. Distefano and J. Schujman - 1969 (PB 187 942)A02

EERC 69-5 "Dynamic Programming and the Solution of the Biharmonic Equation," by N. Distefano - 1969 (PB 187 941)A03

EERC 69-6 "Stochastic Analysis of Offshore Tower Structures," by A.K. Malhotra and J. Penzien - 1969 (PB 187 903)A09

EERC 69-7 "Rock Motion Accelerograms for High Magnitude Earthquakes," by H.B. Seed and I.M. Idriss - 1969 (PB 187 940)A02

EERC 69-8 "Structural Dynamics Testing Facilities at the University of California, Berkeley," by R.M. Stephen, J.G. Bouwkamp, R.W. Clough and J. Penzien - 1969 (PB 189 111)A04

EERC 69-9 "Seismic Response of Soil Deposits Underlain by Sloping Rock Boundaries," by H. Dezfulian and H.B. Seed 1969 (PB 189 114)A03

EERC 69-10 "Dynamic Stress Analysis of Axisymmetric Structures Under Arbitrary Loading," by S. Ghosh and E.L. Wilson 1969 (PB 189 026)A10

EERC 69-11 "Seismic Behavior of Multistory Frames Designed by Different Philosophies," by J.C. Anderson and V. V. Bertero - 1969 (PB 190 662)A10

EERC 69-12 "Stiffness Degradation of Reinforcing Concrete Members Subjected to Cyclic Flexural Moments," by V.V. Bertero, B. Bresler and H. Ming Liao - 1969 (PB 202 942)A07

EERC 69-13 "Response of Non-Uniform Soil Deposits to Travelling Seismic Waves," by H. Dezfulian and H.B. Seed - 1969 (PB 191 023)A03

EERC 69-14 "Damping Capacity of a Model Steel Structure," by D. Rea, R.W. Clough and J.G. Bouwkamp - 1969 (PB 190 663)A06

EERC 69-15 "Influence of Local Soil Conditions on Building Damage Potential during Earthquakes," by H.B. Seed and I.M. Idriss - 1969 (PB 191 036)A03

EERC 69-16 "The Behavior of Sands Under Seismic Loading Conditions," by M.L. Silver and H.B. Seed - 1969 (AD 714 982)A07

EERC 70-1 "Earthquake Response of Gravity Dams," by A.K. Chopra - 1970 (AD 709 640)A03

EERC 70-2 "Relationships between Soil Conditions and Building Damage in the Caracas Earthquake of July 29, 1967," by H.B. Seed, I.M. Idriss and H. Dezfulian - 1970 (PB 195 762)A05

EERC 70-3 "Cyclic Loading of Full Size Steel Connections," by E.P. Popov and R.M. Stephen - 1970 (PB 213 545)A04

EERC 70-4 "Seismic Analysis of the Charaima Building, Caraballeda, Venezuela," by Subcommittee of the SEAONC Research Committee: V.V. Bertero, P.F. Fratessa, S.A. Mahin, J.H. Sexton, A.C. Scordelis, E.L. Wilson, L.A. Wyllie, H.B. Seed and J. Penzien, Chairman - 1970 (PB 201 455)A06

EERC 70-5 "A Computer Program for Earthquake Analysis of Dams," by A.K. Chopra and P. Chakrabarti - 1970 (AD 723 994)A05

EERC 70-6 "The Propagation of Love Waves Across Non-Horizontally Layered Structures," by J. Lysmer and L.A. Drake 1970 (PB 197 896)A03

EERC 70-7 "Influence of Base Rock Characteristics on Ground Response," by J. Lysmer, H.B. Seed and P.B. Schnabel 1970 (PB 197 897)A03

EERC 70-8 "Applicability of Laboratory Test Procedures for Measuring Soil Liquefaction Characteristics under Cyclic Loading," by H.B. Seed and W.H. Peacock - 1970 (PB 198 016)A03

EERC 70-9 "A Simplified Procedure for Evaluating Soil Liquefaction Potential," by H.B. Seed and I.M. Idriss - 1970 (PB 198 009)A03

EERC 70-10 "Soil Moduli and Damping Factors for Dynamic Response Analysis," by H.B. Seed and I.M. Idriss - 1970 (PB 197 869)A03

EERC 71-1 "Koyna Earthquake of December 11, 1967 and the Performance of Koyna Dam," by A.K. Chopra and P. Chakrabarti 1971 (AD 731 496)A06

EERC 71-2 "Preliminary In-Situ Measurements of Anelastic Absorption in Soils Using a Prototype Earthquake Simulator," by R.D. Borcherdt and P.W. Rodgers - 1971 (PB 201 454)A03

EERC 71-3 "Static and Dynamic Analysis of Inelastic Frame Structures," by F.L. Porter and G.H. Powell - 1971 (PB 210 135)A06

EERC 71-4 "Research Needs in Limit Design of Reinforced Concrete Structures," by V.V. Bertero - 1971 (PB 202 943)A04

EERC 71-5 "Dynamic Behavior of a High-Rise Diagonally Braced Steel Building," by D. Rea, A.A. Shah and J.G. Bouwkamp 1971 (PB 203 584)A06

EERC 71-6 "Dynamic Stress Analysis of Porous Elastic Solids Saturated with Compressible Fluids," by J. Ghaboussi and E. L. Wilson - 1971 (PB 211 396)A06

EERC 71-7 "Inelastic Behavior of Steel Beam-to-Column Subassemblages," by H. Krawinkler, V.V. Bertero and E.P. Popov 1971 (PB 211 335)A14

EERC 71-8 "Modification of Seismograph Records for Effects of Local Soil Conditions," by P. Schnabel, H.B. Seed and J. Lysmer - 1971 (PB 214 450)A03

EERC 72-1 "Static and Earthquake Analysis of Three Dimensional Frame and Shear Wall Buildings," by E.L. Wilson and H.H. Dovey - 1972 (PB 212 904)A05

EERC 72-2 "Accelerations in Rock for Earthquakes in the Western United States," by P.B. Schnabel and H.B. Seed - 1972 (PB 213 100)A03

EERC 72-3 "Elastic-Plastic Earthquake Response of Soil-Building Systems," by T. Minami - 1972 (PB 214 868)A08

EERC 72-4 "Stochastic Inelastic Response of Offshore Towers to Strong Motion Earthquakes," by M.K. Kaul - 1972 (PB 215 713)A05

EERC 72-5 "Cyclic Behavior of Three Reinforced Concrete Flexural Members with High Shear," by E.P. Popov, V.V. Bertero and H. Krawinkler - 1972 (PB 214 555)A05

EERC 72-6 "Earthquake Response of Gravity Dams Including Reservoir Interaction Effects," by P. Chakrabarti and A.K. Chopra - 1972 (AD 762 330)A08

EERC 72-7 "Dynamic Properties of Pine Flat Dam," by D. Rea, C.Y. Liaw and A.K. Chopra - 1972 (AD 763 928)A05

EERC 72-8 "Three Dimensional Analysis of Building Systems," by E.L. Wilson and H.H. Dovey - 1972 (PB 222 438)A06

EERC 72-9 "Rate of Loading Effects on Uncracked and Repaired Reinforced Concrete Members," by S. Mahin, V.V. Bertero, D. Rea and M. Atalay - 1972 (PB 224 520)A08

EERC 72-10 "Computer Program for Static and Dynamic Analysis of Linear Structural Systems," by E.L. Wilson, K.-J. Bathe, J.E. Peterson and H.H.Dovey - 1972 (PB 220 437)A04

EERC 72-11 "Literature Survey - Seismic Effects on Highway Bridges," by T. Iwasaki, J. Penzien and R.W. Clough - 1972 (PB 215 613)A19

EERC 72-12 "SHAKE-A Computer Program for Earthquake Response Analysis of Horizontally Layered Sites," by P.B. Schnabel and J. Lysmer - 1972 (PB 220 207)A06

EERC 73-1 "Optimal Seismic Design of Multistory Frames," by V.V. Bertero and H. Kamil - 1973

EERC 73-2 "Analysis of the Slides in the San Fernando Dams During the Earthquake of February 9, 1971," by H.B. Seed, K.L. Lee, I.M. Idriss and F. Makdisi - 1973 (PB 223 402)A14

EERC 73-3 "Computer Aided Ultimate Load Design of Unbraced Multistory Steel Frames," by M.B. El-Hafez and G.H. Powell 1973 (PB 248 315)A09

EERC 73-4 "Experimental Investigation into the Seismic Behavior of Critical Regions of Reinforced Concrete Components as Influenced by Moment and Shear," by M. Celebi and J. Penzien - 1973 (PB 215 884)A09

EERC 73-5 "Hysteretic Behavior of Epoxy-Repaired Reinforced Concrete Beams," by M. Celebi and J. Penzien - 1973 (PB 239 568)A03

EERC 73-6 "General Purpose Computer Program for Inelastic Dynamic Response of Plane Structures," by A. Kanaan and G.H. Powell - 1973 (PB 221 260)A08

EERC 73-7 "A Computer Program for Earthquake Analysis of Gravity Dams Including Reservoir Interaction," by P. Chakrabarti and A.K. Chopra - 1973 (AD 766 271)A04

EERC 73-8 "Behavior of Reinforced Concrete Deep Beam-Column Subassemblages Under Cyclic Loads," by O. Küstü and J.G. Bouwkamp - 1973 (PB 246 117)A12

EERC 73-9 "Earthquake Analysis of Structure-Foundation Systems," by A.K. Vaish and A.K. Chopra - 1973 (AD 766 272)A07

EERC 73-10 "Deconvolution of Seismic Response for Linear Systems," by R.B. Reimer - 1973 (PB 227 179)A08

EERC 73-11 "SAP IV: A Structural Analysis Program for Static and Dynamic Response of Linear Systems," by K.-J. Bathe, E.L. Wilson and F.E. Peterson - 1973 (PB 221 967)A09

EERC 73-12 "Analytical Investigations of the Seismic Response of Long, Multiple Span Highway Bridges," by W.S. Tseng and J. Penzien - 1973 (PB 227 816)A10

EERC 73-13 "Earthquake Analysis of Multi-Story Buildings Including Foundation Interaction," by A.K. Chopra and J.A. Gutierrez - 1973 (PB 222 970)A03

EERC 73-14 "ADAP: A Computer Program for Static and Dynamic Analysis of Arch Dams," by R.W. Clough, J.M. Raphael and S. Mojtahedi - 1973 (PB 223 763)A09

EERC 73-15 "Cyclic Plastic Analysis of Structural Steel Joints," by R.B. Pinkney and R.W. Clough - 1973 (PB 226 843)A08

EERC 73-16 "QUAD-4: A Computer Program for Evaluating the Seismic Response of Soil Structures by Variable Damping Finite Element Procedures," by I.M. Idriss, J. Lysmer, R. Hwang and H.B. Seed - 1973 (PB 229 424)A05

EERC 73-17 "Dynamic Behavior of a Multi-Story Pyramid Shaped Building," by R.M. Stephen, J.P. Hollings and J.G. Bouwkamp - 1973 (PB 240 718)A06

EERC 73-18 "Effect of Different Types of Reinforcing on Seismic Behavior of Short Concrete Columns," by V.V. Bertero, J. Hollings, O. Küstü, R.M. Stephen and J.G. Bouwkamp - 1973

EERC 73-19 "Olive View Medical Center Materials Studies, Phase I," by B. Bresler and V.V. Bertero - 1973 (PB 235 986)A06

EERC 73-20 "Linear and Nonlinear Seismic Analysis Computer Programs for Long Multiple-Span Highway Bridges," by W.S. Tseng and J. Penzien - 1973

EERC 73-21 "Constitutive Models for Cyclic Plastic Deformation of Engineering Materials," by J.M. Kelly and P.P. Gillis 1973 (PB 226 024)A03

EERC 73-22 "DRAIN - 2D User's Guide," by G.H. Powell - 1973 (PB 227 016)A05

EERC 73-23 "Earthquake Engineering at Berkeley - 1973," (PB 226 033)A11

EERC 73-24 Unassigned

EERC 73-25 "Earthquake Response of Axisymmetric Tower Structures Surrounded by Water," by C.Y. Liaw and A.K. Chopra 1973 (AD 773 052)A09

EERC 73-26 "Investigation of the Failures of the Olive View Stairtowers During the San Fernando Earthquake and Their Implications on Seismic Design," by V.V. Bertero and R.G. Collins - 1973 (PB 235 106)A13

EERC 73-27 "Further Studies on Seismic Behavior of Steel Beam-Column Subassemblages," by V.V. Bertero, H. Krawinkler and E.P. Popov - 1973 (PB 234 172)A06

EERC 74-1 "Seismic Risk Analysis," by C.S. Oliveira - 1974 (PB 235 920)A06

EERC 74-2 "Settlement and Liquefaction of Sands Under Multi-Directional Shaking," by R. Pyke, C.K. Chan and H.B. Seed 1974

EERC 74-3 "Optimum Design of Earthquake Resistant Shear Buildings," by D. Ray, K.S. Pister and A.K. Chopra - 1974 (PB 231 172)A06

EERC 74-4 "LUSH - A Computer Program for Complex Response Analysis of Soil-Structure Systems," by J. Lysmer, T. Udaka, H.B. Seed and R. Hwang - 1974 (PB 236 796)A05

EERC 74-5 "Sensitivity Analysis for Hysteretic Dynamic Systems: Applications to Earthquake Engineering," by D. Ray 1974 (PB 233 213)A06

EERC 74-6 "Soil Structure Interaction Analyses for Evaluating Seismic Response," by H.B. Seed, J. Lysmer and R. Hwang 1974 (PB 236 519)A04

EERC 74-7 Unassigned

EERC 74-8 "Shaking Table Tests of a Steel Frame - A Progress Report," by R.W. Clough and D. Tang - 1974 (PB 240 869)A03

EERC 74-9 "Hysteretic Behavior of Reinforced Concrete Flexural Members with Special Web Reinforcement," by V.V. Bertero, E.P. Popov and T.Y. Wang - 1974 (PB 236 797)A07

EERC 74-10 "Applications of Reliability-Based, Global Cost Optimization to Design of Earthquake Resistant Structures," by E. Vitiello and K.S. Pister - 1974 (PB 237 231)A06

EERC 74-11 "Liquefaction of Gravelly Soils Under Cyclic Loading Conditions," by R.T. Wong, H.B. Seed and C.K. Chan 1974 (PB 242 042)A03

EERC 74-12 "Site-Dependent Spectra for Earthquake-Resistant Design," by H.B. Seed, C. Ugas and J. Lysmer - 1974 (PB 240 953)A03

EERC 74-13 "Earthquake Simulator Study of a Reinforced Concrete Frame," by P. Hidalgo and R.W. Clough - 1974 (PB 241 944)A13

EERC 74-14 "Nonlinear Earthquake Response of Concrete Gravity Dams," by N. Pal - 1974 (AD/A 006 583)A06

EERC 74-15 "Modeling and Identification in Nonlinear Structural Dynamics - I. One Degree of Freedom Models," by N. Distefano and A. Rath - 1974 (PB 241 548)A06

EERC 75-1 "Determination of Seismic Design Criteria for the Dumbarton Bridge Replacement Structure, Vol. I: Description, Theory and Analytical Modeling of Bridge and Parameters," by F. Baron and S.-H. Pang - 1975 (PB 259 407)A15

EERC 75-2 "Determination of Seismic Design Criteria for the Dumbarton Bridge Replacement Structure, Vol. II: Numerical Studies and Establishment of Seismic Design Criteria," by F. Baron and S.-H. Pang - 1975 (PB 259 408)A11 (For set of EERC 75-1 and 75-2 (PB 259 406))

EERC 75-3 "Seismic Risk Analysis for a Site and a Metropolitan Area," by C.S. Oliveira - 1975 (PB 248 134)A09

EERC 75-4 "Analytical Investigations of Seismic Response of Short, Single or Multiple-Span Highway Bridges," by M.-C. Chen and J. Penzien - 1975 (PB 241 454)A09

EERC 75-5 "An Evaluation of Some Methods for Predicting Seismic Behavior of Reinforced Concrete Buildings," by S.A. Mahin and V.V. Bertero - 1975 (PB 246 306)A16

EERC 75-6 "Earthquake Simulator Study of a Steel Frame Structure, Vol. I: Experimental Results," by R.W. Clough and D.T. Tang - 1975 (PB 243 981)A13

EERC 75-7 "Dynamic Properties of San Bernardino Intake Tower," by D. Rea, C.-Y. Liaw and A.K. Chopra - 1975 (AD/A008 406) A05

EERC 75-8 "Seismic Studies of the Articulation for the Dumbarton Bridge Replacement Structure, Vol. I: Description, Theory and Analytical Modeling of Bridge Components," by F. Baron and R.E. Hamati - 1975 (PB 251 539)A07

EERC 75-9 "Seismic Studies of the Articulation for the Dumbarton Bridge Replacement Structure, Vol. 2: Numerical Studies of Steel and Concrete Girder Alternates," by F. Baron and R.E. Hamati - 1975 (PB 251 540)A10

EERC 75-10 "Static and Dynamic Analysis of Nonlinear Structures," by D.P. Mondkar and G.H. Powell - 1975 (PB 242 434)A08

EERC 75-11 "Hysteretic Behavior of Steel Columns," by E.P. Popov, V.V. Bertero and S. Chandramouli - 1975 (PB 252 365)A11

EERC 75-12 "Earthquake Engineering Research Center Library Printed Catalog," - 1975 (PB 243 711)A26

EERC 75-13 "Three Dimensional Analysis of Building Systems (Extended Version)," by E.L. Wilson, J.P. Hollings and H.H. Dovey - 1975 (PB 243 989)A07

EERC 75-14 "Determination of Soil Liquefaction Characteristics by Large-Scale Laboratory Tests," by P. De Alba, C.K. Chan and H.B. Seed - 1975 (NUREG 0027)A08

EERC 75-15 "A Literature Survey - Compressive, Tensile, Bond and Shear Strength of Masonry," by R.L. Mayes and R.W. Clough - 1975 (PB 246 292)A10

EERC 75-16 "Hysteretic Behavior of Ductile Moment Resisting Reinforced Concrete Frame Components," by V.V. Bertero and E.P. Popov - 1975 (PB 246 388)A05

EERC 75-17 "Relationships Between Maximum Acceleration, Maximum Velocity, Distance from Source, Local Site Conditions for Moderately Strong Earthquakes," by H.B. Seed, R. Murarka, J. Lysmer and I.M. Idriss - 1975 (PB 248 172)A03

EERC 75-18 "The Effects of Method of Sample Preparation on the Cyclic Stress-Strain Behavior of Sands," by J. Mulilis, C.K. Chan and H.B. Seed - 1975 (Summarized in EERC 75-28)

EERC 75-19 "The Seismic Behavior of Critical Regions of Reinforced Concrete Components as Influenced by Moment, Shear and Axial Force," by M.B. Atalay and J. Penzien - 1975 (PB 258 842)A11

EERC 75-20 "Dynamic Properties of an Eleven Story Masonry Building," by R.M. Stephen, J.P. Hollings, J.G. Bouwkamp and D. Jurukovski - 1975 (PB 246 945)A04

EERC 75-21 "State-of-the-Art in Seismic Strength of Masonry - An Evaluation and Review," by R.L. Mayes and R.W. Clough 1975 (PB 249 040)A07

EERC 75-22 "Frequency Dependent Stiffness Matrices for Viscoelastic Half-Plane Foundations," by A.K. Chopra, P. Chakrabarti and G. Dasgupta - 1975 (PB 248 121)A07

EERC 75-23 "Hysteretic Behavior of Reinforced Concrete Framed Walls," by T.Y. Wong, V.V. Bertero and E.P. Popov - 1975

EERC 75-24 "Testing Facility for Subassemblages of Frame-Wall Structural Systems," by V.V. Bertero, E.P. Popov and T. Endo - 1975

EERC 75-25 "Influence of Seismic History on the Liquefaction Characteristics of Sands," by H.B. Seed, K. Mori and C.K. Chan - 1975 (Summarized in EERC 75-28)

EERC 75-26 "The Generation and Dissipation of Pore Water Pressures during Soil Liquefaction," by H.B. Seed, P.P. Martin and J. Lysmer - 1975 (PB 252 648)A03

EERC 75-27 "Identification of Research Needs for Improving Aseismic Design of Building Structures," by V.V. Bertero 1975 (PB 248 136)A05

EERC 75-28 "Evaluation of Soil Liquefaction Potential during Earthquakes," by H.B. Seed, I. Arango and C.K. Chan - 1975 (NUREG 0026)A13

EERC 75-29 "Representation of Irregular Stress Time Histories by Equivalent Uniform Stress Series in Liquefaction Analyses," by H.B. Seed, I.M. Idriss, F. Makdisi and N. Banerjee - 1975 (PB 252 635)A03

EERC 75-30 "FLUSH - A Computer Program for Approximate 3-D Analysis of Soil-Structure Interaction Problems," by J. Lysmer, T. Udaka, C.-F. Tsai and H.B. Seed - 1975 (PB 259 332)A07

EERC 75-31 "ALUSH - A Computer Program for Seismic Response Analysis of Axisymmetric Soil-Structure Systems," by E. Berger, J. Lysmer and H.B. Seed - 1975

EERC 75-32 "TRIP and TRAVEL - Computer Programs for Soil-Structure Interaction Analysis with Horizontally Travelling Waves," by T. Udaka, J. Lysmer and H.B. Seed - 1975

EERC 75-33 "Predicting the Performance of Structures in Regions of High Seismicity," by J. Penzien - 1975 (PB 248 130)A03

EERC 75-34 "Efficient Finite Element Analysis of Seismic Structure - Soil - Direction," by J. Lysmer, H.B. Seed, T. Udaka, R.N. Hwang and C.-F. Tsai - 1975 (PB 253 570)A03

EERC 75-35 "The Dynamic Behavior of a First Story Girder of a Three-Story Steel Frame Subjected to Earthquake Loading," by R.W. Clough and L.-Y. Li - 1975 (PB 248 841)A05

EERC 75-36 "Earthquake Simulator Study of a Steel Frame Structure, Volume II - Analytical Results," by D.T. Tang - 1975 (PB 252 926)A10

EERC 75-37 "ANSR-I General Purpose Computer Program for Analysis of Non-Linear Structural Response," by D.P. Mondkar and G.H. Powell - 1975 (PB 252 386)A08

EERC 75-38 "Nonlinear Response Spectra for Probabilistic Seismic Design and Damage Assessment of Reinforced Concrete Structures," by M. Murakami and J. Penzien - 1975 (PB 259 530)A05

EERC 75-39 "Study of a Method of Feasible Directions for Optimal Elastic Design of Frame Structures Subjected to Earthquake Loading," by N.D. Walker and K.S. Pister - 1975 (PB 257 781)A06

EERC 75-40 "An Alternative Representation of the Elastic-Viscoelastic Analogy," by G. Dasgupta and J.L. Sackman - 1975 (PB 252 173)A03

EERC 75-41 "Effect of Multi-Directional Shaking on Liquefaction of Sands," by H.B. Seed, R. Pyke and G.R. Martin - 1975 (PB 258 781)A03

EERC 76-1 "Strength and Ductility Evaluation of Existing Low-Rise Reinforced Concrete Buildings - Screening Method," by T. Okada and B. Bresler - 1976 (PB 257 906)A11

EERC 76-2 "Experimental and Analytical Studies on the Hysteretic Behavior of Reinforced Concrete Rectangular and T-Beams," by S.-Y.M. Ma, E.P. Popov and V.V. Bertero - 1976 (PB 260 843)A12

EERC 76-3 "Dynamic Behavior of a Multistory Triangular-Shaped Building," by J. Petrovski, R.M. Stephen, E. Gartenbaum and J.G. Bouwkamp - 1976

EERC 76-4 "Earthquake Induced Deformations of Earth Dams," by N. Serff and H.B. Seed - 1976

EERC 76-5 "Analysis and Design of Tube-Type Tall Building Structures," by H. de Clercq and G.H. Powell - 1976 (PB 252 220) A10

EERC 76-6 "Time and Frequency Domain Analysis of Three-Dimensional Ground Motions, San Fernando Earthquake," by T. Kubo and J. Penzien (PB 260 556)A11

EERC 76-7 "Expected Performance of Uniform Building Code Design Masonry Structures," by R.L. Mayes, Y. Omote, S.W. Chen and R.W. Clough - 1976

EERC 76-8 "Cyclic Shear Tests on Concrete Masonry Piers," Part I - Test Results," by R.L. Mayes, Y. Omote and R.W. Clough - 1976 (PB 264 424)A06

EERC 76-9 "A Substructure Method for Earthquake Analysis of Structure - Soil Interaction," by J.A. Gutierrez and A.K. Chopra - 1976 (PB 257 783)A08

EERC 76-10 "Stabilization of Potentially Liquefiable Sand Deposits using Gravel Drain Systems," by H.B. Seed and J.R. Booker - 1976 (PB 258 820)A04

EERC 76-11 "Influence of Design and Analysis Assumptions on Computed Inelastic Response of Moderately Tall Frames," by G.H. Powell and D.G. Row - 1976

EERC 76-12 "Sensitivity Analysis for Hysteretic Dynamic Systems: Theory and Applications," by D. Ray, K.S. Pister and E. Polak - 1976 (PB 262 859)A04

EERC 76-13 "Coupled Lateral Torsional Response of Buildings to Ground Shaking," by C.L. Kan and A.K. Chopra - 1976 (PB 257 907)A09

EERC 76-14 "Seismic Analyses of the Banco de America," by V.V. Bertero, S.A. Mahin and J.A. Hollings - 1976

EERC 76-15 "Reinforced Concrete Frame 2: Seismic Testing and Analytical Correlation," by R.W. Clough and J. Gidwani - 1976 (PB 261 323)A08

EERC 76-16 "Cyclic Shear Tests on Masonry Piers, Part II - Analysis of Test Results," by R.L. Mayes, Y. Omote and R.W. Clough - 1976

EERC 76-17 "Structural Steel Bracing Systems: Behavior Under Cyclic Loading," by E.P. Popov, K. Takanashi and C.W. Roeder - 1976 (PB 260 715)A05

EERC 76-18 "Experimental Model Studies on Seismic Response of High Curved Overcrossings," by D. Williams and W.G. Godden - 1976

EERC 76-19 "Effects of Non-Uniform Seismic Disturbances on the Dumbarton Bridge Replacement Structure," by F. Baron and R.E. Hamati - 1976

EERC 76-20 "Investigation of the Inelastic Characteristics of a Single Story Steel Structure Using System Identification and Shaking Table Experiments," by V.C. Matzen and H.D. McNiven - 1976 (PB 258 453)A07

EERC 76-21 "Capacity of Columns with Splice Imperfections," by E.P. Popov, R.M. Stephen and R. Philbrick - 1976 (PB 260 378)A04

EERC 76-22 "Response of the Olive View Hospital Main Building during the San Fernando Earthquake," by S. A. Mahin, R. Collins, A.K. Chopra and V.V. Bertero - 1976

EERC 76-23 "A Study on the Major Factors Influencing the Strength of Masonry Prisms," by N.M. Mostaghel, R.L. Mayes, R. W. Clough and S.W. Chen - 1976

EERC 76-24 "GADFLEA - A Computer Program for the Analysis of Pore Pressure Generation and Dissipation during Cyclic or Earthquake Loading," by J.R. Booker, M.S. Rahman and H.B. Seed - 1976 (PB 263 947)A04

EERC 76-25 "Rehabilitation of an Existing Building: A Case Study," by B. Bresler and J. Axley - 1976

EERC 76-26 "Correlative Investigations on Theoretical and Experimental Dynamic Behavior of a Model Bridge Structure," by K. Kawashima and J. Penzien - 1976 (PB 263 388)A11

EERC 76-27 "Earthquake Response of Coupled Shear Wall Buildings," by T. Srichatrapimuk - 1976 (PB 265 157)A07

EERC 76-28 "Tensile Capacity of Partial Penetration Welds," by E.P. Popov and R.M. Stephen - 1976 (PB 262 899)A03

EERC 76-29 "Analysis and Design of Numerical Integration Methods in Structural Dynamics," by H.M. Hilber - 1976 (PB 264 410)A06

EERC 76-30 "Contribution of a Floor System to the Dynamic Characteristics of Reinforced Concrete Buildings," by L.J. Edgar and V.V. Bertero - 1976

EERC 76-31 "The Effects of Seismic Disturbances on the Golden Gate Bridge," by F. Baron, M. Arikan and R.E. Hamati - 1976

EERC 76-32 "Infilled Frames in Earthquake Resistant Construction," by R.E. Klingner and V.V. Bertero - 1976 (PB 265 892)A13

UCB/EERC-77/01 "PLUSH - A Computer Program for Probabilistic Finite Element Analysis of Seismic Soil-Structure Interaction," by M.P. Romo Organista, J. Lysmer and H.B. Seed - 1977

UCB/EERC-77/02 "Soil-Structure Interaction Effects at the Humboldt Bay Power Plant in the Ferndale Earthquake of June 7, 1975," by J.E. Valera, H.B. Seed, C.F. Tsai and J. Lysmer - 1977 (PB 265 795)A04

UCB/EERC-77/03 "Influence of Sample Disturbance on Sand Response to Cyclic Loading," by K. Mori, H.B. Seed and C.K. Chan - 1977 (PB 267 352)A04

UCB/EERC-77/04 "Seismological Studies of Strong Motion Records," by J. Shoja-Taheri - 1977 (PB 269 655)A10

UCB/EERC-77/05 "Testing Facility for Coupled-Shear Walls," by L. Li-Hyung, V.V. Bertero and E.P. Popov - 1977

UCB/EERC-77/06 "Developing Methodologies for Evaluating the Earthquake Safety of Existing Buildings," by No. 1 - B. Bresler; No. 2 - B. Bresler, T. Okada and D. Zisling; No. 3 - T. Okada and B. Bresler; No. 4 - V.V. Bertero and B. Bresler - 1977 (PB 267 354)A08

UCB/EERC-77/07 "A Literature Survey - Transverse Strength of Masonry Walls," by Y. Omote, R.L. Mayes, S.W. Chen and R.W. Clough - 1977 (PB 277 933)A07

UCB/EERC-77/08 "DRAIN-TABS: A Computer Program for Inelastic Earthquake Response of Three Dimensional Buildings," by R. Guendelman-Israel and G.H. Powell - 1977 (PB 270 693)A07

UCB/EERC-77/09 "SUBWALL: A Special Purpose Finite Element Computer Program for Practical Elastic Analysis and Design of Structural Walls with Substructure Option," by D.Q. Le, H. Peterson and E.P. Popov - 1977 (PB 270 567)A05

UCB/EERC-77/10 "Experimental Evaluation of Seismic Design Methods for Broad Cylindrical Tanks," by D.P. Clough (PB 272 280)A13

UCB/EERC-77/11 "Earthquake Engineering Research at Berkeley - 1976," - 1977 (PB 273 507)A09

UCB/EERC-77/12 "Automated Design of Earthquake Resistant Multistory Steel Building Frames," by N.D. Walker, Jr. - 1977 (PB 276 526)A09

UCB/EERC-77/13 "Concrete Confined by Rectangular Hoops Subjected to Axial Loads," by J. Vallenas, V.V. Bertero and E.P. Popov - 1977 (PB 275 165)A06

UCB/EERC-77/14 "Seismic Strain Induced in the Ground During Earthquakes," by Y. Sugimura - 1977 (PB 284 201)A04

UCB/EERC-77/15 "Bond Deterioration under Generalized Loading," by V.V. Bertero, E.P. Popov and S. Viwathanatepa - 1977

UCB/EERC-77/16 "Computer Aided Optimum Design of Ductile Reinforced Concrete Moment Resisting Frames," by S.W. Zagajeski and V.V. Bertero - 1977 (PB 280 137)A07

UCB/EERC-77/17 "Earthquake Simulation Testing of a Stepping Frame with Energy-Absorbing Devices," by J.M. Kelly and D.F. Tsztoo - 1977 (PB 273 506)A04

UCB/EERC-77/18 "Inelastic Behavior of Eccentrically Braced Steel Frames under Cyclic Loadings," by C.W. Roeder and E.P. Popov - 1977 (PB 275 526)A15

UCB/EERC-77/19 "A Symplified Procedure for Estimating Earthquake-Induced Deformations in Dams and Embankments," by F.I. Makdisi and H.B. Seed - 1977 (PB 276 820) A04

UCB/EERC-77/20 "The Performance of Earth Dams during Earthquakes," by H.B. Seed, F.I. Makdisi and P. de Alba - 1977 (PB 276 821)A04

UCB/EERC-77/21 "Dynamic Plastic Analysis Using Stress Resultant Finite Element Formulation," by P. Lukkunapvasit and J.M. Kelly - 1977 (PB 275 453)A04

UCB/EERC-77/22 "Preliminary Experimental Study of Seismic Uplift of a Steel Frame," by R.W. Clough and A.A. Huckelbridge 1977 (PB 278 769)A08

UCB/EERC-77/23 "Earthquake Simulator Tests of a Nine-Story Steel Frame with Columns Allowed to Uplift," by A.A. Huckelbridge - 1977 (PB 277 944)A09

UCB/EERC-77/24 "Nonlinear Soil-Structure Interaction of Skew Highway Bridges," by M.-C. Chen and J. Penzien - 1977 (PB 276 176)A07

UCB/EERC-77/25 "Seismic Analysis of an Offshore Structure Supported on Pile Foundations," by D.D.-N. Liou and J. Penzien 1977 (PB 283 180)A06

UCB/EERC-77/26 "Dynamic Stiffness Matrices for Homogeneous Viscoelastic Half-Planes," by G. Dasgupta and A.K. Chopra - 1977 (PB 279 654)A06

UCB/EERC-77/27 "A Practical Soft Story Earthquake Isolation System," by J.M. Kelly and J.M. Eidinger - 1977 (PB 276 814)A07

UCB/EERC-77/28 "Seismic Safety of Existing Buildings and Incentives for Hazard Mitigation in San Francisco: An Exploratory Study," by A.J. Meltsner - 1977 (PB 281 970)A05

UCB/EERC-77/29 "Dynamic Analysis of Electrohydraulic Shaking Tables," by D. Rea, S. Abedi-Hayati and Y. Takahashi 1977 (PB 282 569)A04

UCB/EERC-77/30 "An Approach for Improving Seismic - Resistant Behavior of Reinforced Concrete Interior Joints," by B. Galunic, V.V. Bertero and E.P. Popov - 1977

UCB/EERC-78/01 "The Development of Energy-Absorbing Devices for Aseismic Base Isolation Systems," by J.M. Kelly and D.F. Tsztoo 1978 (PB 284 978)A04

UCB/EERC-78/02 "Effect of Tensile Prestrain on the Cyclic Response of Structural Steel Connections," by J.G. Bouwkamp and A. Mukhopadhyay - 1978

UCB/EERC-78/03 "Experimental Results of an Earthquake Isolation System using Natural Rubber Bearings," by J.M. Eidinger and J.M. Kelly - 1978

UCB/EERC-78/04 "Seismic Behavior of Tall Liquid Storage Tanks," by A. Niwa 1978

UCB/EERC-78/05 "Hysteretic Behavior of Reinforced Concrete Columns Subjected to High Axial and Cyclic Shear Forces," by S.W. Zagajeski, V.V. Bertero and J.G. Bouwkamp - 1978

UCB/EERC-78/06 "Inelastic Beam-Column Elements for the ANSR-I Program," by A. Riahi, D.G. Row and G.H. Powell - 1978

UCB/EERC-78/07 "Studies of Structural Response to Earthquake Ground Motion," by O.A. Lopez and A.K. Chopra - 1978

UCB/EERC-78/08 "A Laboratory Study of the Fluid-Structure Interaction of Submerged Tanks and Caissons in Earthquakes," by R.C. Byrd - 1978 (PB 284 957)A08

UCB/EERC-78/09 "Models for Evaluating Damageability of Structures," by I. Sakamoto and B. Bresler - 1978

UCB/EERC-78/10 "Seismic Performance of Secondary Structural Elements," by I. Sakamoto - 1978

UCB/EERC-78/11 Case Study--Seismic Safety Evaluation of a Reinforced Concrete School Building," by J. Axley and B. Bresler 1978

UCB/EERC-78/12 "Potential Damageability in Existing Buildings," by T. Blejwas and B. Bresler - 1978

UCB/EERC-78/13 "Dynamic Behavior of a Pedestal Base Multistory Building," by R. M. Stephen, E. L. Wilson, J. G. Bouwkamp and M. Button - 1978

UCB/EERC-78/14 "Seismic Response of Bridges - Case Studies," by R.A. Imbsen, V. Nutt and J. Penzien - 1978

UCB/EERC-78/15 "A Substructure Technique for Nonlinear Static and Dynamic Analysis," by D.G. Row and G.H. Powell - 1978

UCB/EERC-78/16 "Seismic Performance of Nonstructural and Secondary Structural Elements," by Isao Sakamoto - 1978

UCB/EERC-78/17 "Model for Evaluating Damageability of Structures," by Isao Sakamoto and B. Bresler - 1978

UCB/EERC-78/18 "Response of K-Braced Steel Frame Models to Lateral Loads," by J.G. Bouwkamp, R.M. Stephen and E.P. Popov - 1978

UCB/EERC-78/19 "Rational Design Methods for Light Equipment in Structures Subjected to Ground Motion," by Jerome L. Sackman and James M. Kelly - 1978

UCB/EERC-78/20 "Testing of a Wind Restraint for Aseismic Base Isolation," by James M. Kelly and Daniel E. Chitty - 1978

UCB/EERC-78/21 "APOLLO A Computer Program for the Analysis of Pore Pressure Generation and Dissipation in Horizontal Sand Layers During Cyclic or Earthquake Loading," by Philippe P. Martin and H. Bolton Seed - 1978

UCB/EERC-78/22 "Optimal Design of an Earthquake Isolation System," by M.A. Bhatti, K.S. Pister and E. Polak - 1978

UCB/EERC-78/23 "MASH A Computer Program for the Non-Linear Analysis of Vertically Propagating Shear Waves in Horizontally Layered Deposits," by Philippe P. Martin and H. Bolton Seed - 1978

UCB/EERC-78/24 "Investigation of the Elastic Characteristics of a Three Story Steel Frame Using System Identification," by Izak Kaya and Hugh D. McNiven - 1978